An exploratory study evaluating the effectiveness of a data driven approach to identifying coordinative features that are associated with sprint velocity

Chris L. Vellucci, Bachelor of Science in Kinesiology (Honours)

Applied Health Science (Kinesiology)

Submitted in partial fulfillment

of the requirements for the degree of

Master of Science

Faculty of Applied Health Science

Brock University

St. Catharines, Ontario, Canada

Abstract

Sprint performance is multifactorial in nature and is dependent on a variety of coordination and motor control features. During the sequential phases of a sprint, the athlete completes a series of spatiotemporal coordination strategies to achieve the fastest possible velocity. The overall aim of the study was to leverage wearable sensor technology and data-driven tools to objectively assess the kinematic and neuromuscular determinants of optimal sprint velocity from a large dataset of university-aged sprinters. To achieve this, we recruited participants to run three 60 m sprints as fast as possible, while being outfitted with wireless electromyography (EMG) and a full-body inertial measurement unit (IMU) suit to obtain full-body 3D kinematics. Five strides about peak sprint velocity were selected and used for inputs into a principal components analysis (PCA). Significant stepwise multivariable regression models were generated for both kinematic and EMG features identified using PCA, with the kinematic model outperforming the EMG model as the kinematic model displayed a higher R^2 value. This suggests that the kinematic dataset used in this study is a better predictor of sprint performance when compared to the EMG dataset, and that both may be viable options in the development of data-driven objective sprint coaching tools.

Keywords: Biomechanics, Sprint Performance, Coordination, Machine Learning, Wearable Sensors

Acknowledgements

I would like to thank the following people and groups for there contributions for this project.

First, I would like to thank and express my sincerest gratitude to my supervisor Dr. Shawn Beaudette who has provided me with unrelenting support over the past two years. Your guidance and support has greatly influenced who I am as a person, researcher, and entrepreneur. I'm grateful for the opportunity to work alongside you and am beyond exited to continue our work together over next four years!

Second, I would like to thank my family and friends. Specifically, my parents Patti and Louie Vellucci and my sister Kristiana (our parents lacked originality), and my friends Brian Neff, Sunny Gahunia, Nick Sbrocchi and Parth Patel. The support you have provided me with throughout this process has helped keep me level-headed and focused. I am grateful for your support and would not have been able to do it without you guys!

Third, I'd like to thank my M.Sc advisory committee, Dr. Kelly Lockwood, and Dr. Gabriel. The insight that each of you has provided throughout my degree has been helped me become a better researcher.

Lastly, I'd like to thank my colleagues in the Spine Lab for each of your contributions to the project. Specifically, I would like to thank my undergraduate research assistants Robin Mackenzie and Nick Eck for their assistance with data collection. I'm very excited to see you see what your futures holds

TABLE OF CONTENTS

LIST OF TABLES

LIST OF FIGURES

Figure 11. A) Displays the distribution of peak sprint velocities for both males and females. **B)** Displays the mean sprint velocity for male, female, and all participants.

Figure 12. A) Scree Plot for PCs from kinematic PCA, **B)** Scree Plot for PCs from EMG PCA.

Figure 13. MCR for PC 1, 3, 9, 11, 12 and 6 **A**) Sagittal plane view **B)** Frontal plane view **C**) Transverse plane view. The blue avatar represents the 5^{th} percentile (slow), black represents the mean and red represents the 95th percentile (fast).

Figure 14. MCR for PC 1, 5, 21 and 22 for **A**) GAS, **B)** BF, **C)** GMAX, **D)** GMED, **E)** LES, **F)** LD, **G)** EO, **H)** VLO, **I)** RF. Blue represents the 95%tile sprinter (fast), Red represents the 5%tile sprinter, and grey represents the stance

Figure 15. Extracted knowledge and future directions building the work presented in this Thesis

LIST OF APPENDIXES

CHAPTER I – INTRODUCTION

1.1 Data Driven Coaching

The analysis of sprint performance using biomechanical tools has traditionally been limited to well-funded performance institutes and research laboratories. Recently, with advancements in technology, sophisticated biomechanical technologies are now more affordable and accessible to practitioners. Specifically, wearable sensors have provided practitioners with the ability to easily capture three-dimensional (i.e., 3D) movement kinematics and muscle activation in ecologically relevant scenarios. Despite this, there is a lack of information regarding patterns of coordination that define optimal sport technique. Current coaching standards rely on anecdotal evidence, and visual appraisal of movement, which can be subjective, and lack the sensitivity needed to optimize performance and avoid injury. Further, these methods fail to capture the coordinative dynamics of a movement, as traditional methods often rely on selecting a single data point at extreme points in the movement (Glazier, 2021). This results in poor feedback to the athlete and practitioner as it provides no insight into how an individual can improve their movement strategy to change their movement outcome.

The coordinative strategy used by an individual to during sprinting to achieve a maximal sprint velocity is likely to differ based on the individual's demographics and skill level (Newell & Vaillancourt, 2001). This makes it challenging to identify key features using traditional biomechanical methods of data analysis because of the natural variation that is likely to occur (Riley & Turvey, 2002). However, using techniques borrowed from computer science such as machine learning and artificial intelligence, we can begin to define coordinative patterns that exist. One particularly useful technique is Principal Component Analysis (PCA). PCA works to identify key modes of variation in a data set, these modes of variation are called principal

components (PCs). Principal components can then be used to inform other machine learning methods such as regression, clustering, or classification to identify patterns in a data set. In the study of coordination, PCA has been used to identify differences in skill level (Gløersen et al., 2018; Ross et al., 2018a) and injury history (Astephen & Deluzio, 2004).

The importance of objectively quantifying the coordinative strategy utilized by individuals during a complex movement is vital to improving skill acquisition (Newell & Vaillancourt, 2001). The feedback can be used to inform coaches and athletes on how to optimize task outcomes. Previous work with PCA has been able to objectively identify differences between novice and advanced athletes (Gløersen et al., 2018; Ross et al., 2018a) but have failed to (1) understand the impact different coordinative strategies have on objective movement outcomes (such as sprint velocity) and (2) objectively identify the biomechanical meaning of principal components. Both present large limitations to the practical applications of data-driven analyses in applied settings.

1.2 Biomechanical Determinants of Sprint Velocity

The objective of sprinting is to cover a set amount of distance in the shortest time. Given this, a key determinant to sprint performance is horizontal running velocity. To achieve maximal running velocity, a sprinter leverages three phases: the start, acceleration phase, and the maximal speed phase. As the athlete progresses from acceleration to maximal speed, the athlete will increase their stride length and decrease their ground contact time (Hunter et al., 2004; Mattes et al., 2021). This therefore suggests that during the peak speed phase, maximum sprinting velocity is the by-product of stride length and stride rate (Coh et al., 2018; Hay, 2002; Hunter et al., 2004; Krzysztof & Mero, 2013). Previous work has suggested that stride length and stride rate are mutually dependent variables with a negative interaction (Hunter et al., 2004). In essence, this

means when stride length increases, stride rate decreases and vice versa (Debaere, Jonkers, et al., 2013; Hunter et al., 2004). Throughout the literature, conflicting findings have been reported when trying to determine whether stride rate or stride length is the rate limiting parameter affecting sprint performance. Some authors have shown a strong correlation between stride length and peak sprint velocity (Hunter et al., 2004; Mattes et al., 2021), while others have suggested that stride rate is better correlated with peak sprint velocity (Morin et al., 2012). Despite these conflicting findings, there is agreement that both parameters are important to consider when optimizing sprint performance. Further it is clear is that both parameters rely on conflicting requirements. Stride rate is favourably influenced by low moments of inertia of the leg and therefore low masses and short limb length. Meanwhile, stride length is positively influenced by explosive strength and muscle mass (Babić et al., 2007; Hunter et al., 2005).

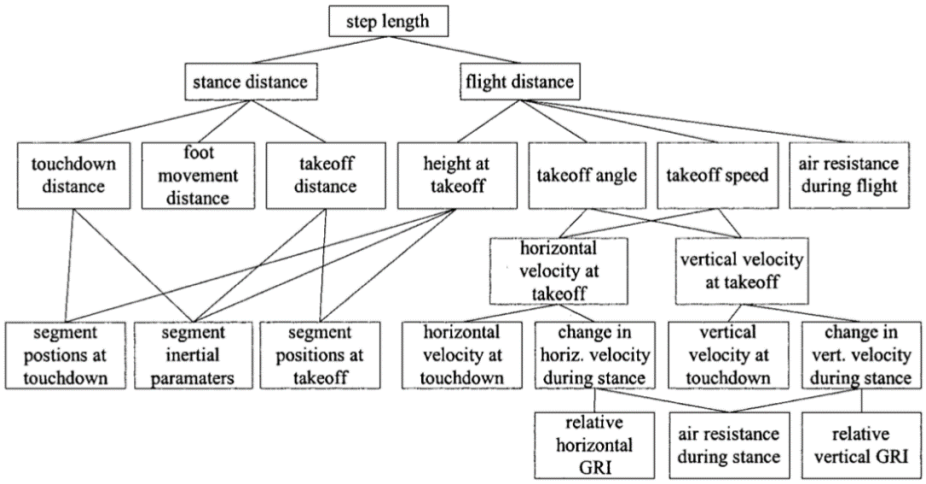

Figure 1. A summary of the deterministic model of sprinting stride length. Retrieved from Hunter et al (2004).

1.2.1 Stride Length

Stride length increases with each step of sprinting, with peak values occurring between 50-80 m during a straight-line sprinting bout (Salo et al., 2011). The deterministic model of sprinting originally published by Hay, (1994) shows that stride length is determined by stance distance and flight time (Figure 1). Stance distance is the horizontal distance of the centre of mass (COM) traveled during the stance phase and flight time is the duration of the flight (i.e., non-contact) phase. In a study conducted by Hunter and colleagues (2004), regression analysis was used to understand which determinants appeared to influence the stride characteristics the most. Specifically, stride length was shown to have a stronger correlation to sprint velocity than stride rate (Hunter et al., 2004). For stride length they found that stride length and flight distance showed a strong correlation ($r \geq 0.89$) while showing no correlation in stance distance ($r \leq 0.10$). Furthermore, it was determined that 88% of the variance in flight distance was explained by height of take-off, vertical velocity at take-off, and horizontal velocity at takeoff. Vertical velocity influenced flight distance the most and horizontal velocity of take-off affecting it the least.

Other studies have shown complimentary associations between stride length and various other biomechanical and neuromuscular variables. For instance stride length appears to be favourably influenced by explosive strength and muscle mass (Debaere, Jonkers, et al., 2013). This is consistent with other findings which suggested that the body mass and height of a sprinter may be important in producing greater ground support forces. This could be used to achieve greater flight distance (Hunter et al., 2004; Weyand & Davis, 2005). Other factors that influence stride length are the length of the lower extremity, biological sex, reaction force, the duration of

the contact phase, and the dynamic flexibility of the hips (Coh et al., 2010; Debaere, Jonkers, et al., 2013; Mattes et al., 2021).

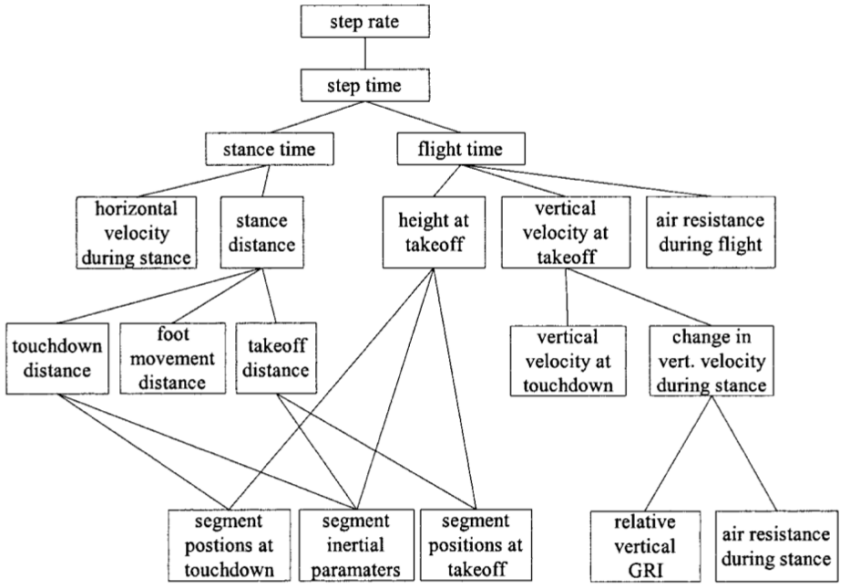

Figure 2. A summary of the deterministic model of sprinting stride rate. Retrieved from Hunter et al (2004)

1.2.2 Stride Rate

Unlike stride length, stride rate does not significantly increase across the duration of a race. During the final stages of initial acceleration 95% of the maximal stride rate that is achieved during the maximal velocity phase has already been achieved (Debaere, Jonkers, et al., 2013). Hay's (1994) deterministic model of sprinting also addresses the critical determinants of stride rate (Figure 2). Previous work assessing the validity of this model found a strong negative correlation of stride rate with flight time ($r = -0.81$) and no correlation with stance time (Hunter et al., 2004). Factors such as height at takeoff, vertical velocity at take-off, and air resistance during flight are thought to influence flight time (Hunter et al., 2004). The findings of the

regression analysis revealed that flight time is strongly influenced by the vertical velocity at take-off (Hunter et al., 2004).

Findings by Morin and colleagues (2012) conflicted with evidence provide by Hunter et al. Specifically, these authors noted that a strong relationship exists between stride rate and sprint velocity and suggest that stance time is a key determinant in stride rate. Stance time appears to display a more complex interaction of various biomechanical and neuromuscular parameters. Specifically, Morin and colleagues (2012) found that a velocity-oriented force-velocity profile allowed for shorter stance times, as this allowed sprinters to apply more force quicker during the stance phase. Rate of force development is also heavily influenced by a variety of neuromuscular factors including muscle motor unit subtype, motor neuron excitability, inter and intramuscular coordination and central and peripheral fatigue (Coh et al., 2010). Along with these differences in neuromuscular factors, kinematic factors of horizontal velocity of the COM during stance, leg angle at touch down, leg angle at take-off and leg length have all been shown to influence the stance time (Hunter et al., 2004).

Many different factors influence the correlation of stride length and stride rate to sprint velocity. Differences in methodology such as overground sprinting (Debaere, Jonkers, et al., 2013; Hunter et al., 2004; Mattes et al., 2021; Salo et al., 2011) versus treadmill sprinting (e.g., Morin et al., 2012) may influence the step characteristics used to achieve maximal velocity. However, other factors such as the kinematic system used, sprinter anthropometrics, and neuromuscular characteristics of the sprinter influence the contribution of stride rate and stride length to maximal sprinting velocity. Individual differences in the sprinters morphological and neuromuscular make up could explain some of the variance in the literature. Salo and colleagues (2011) analyzed 11 athletes who performed 10 or more races. They found that different athletes

had different reliance on stride rate and stride length to achieve their fastest sprint times. The result of these individual differences could result in different coordinative strategies used to achieve maximal sprint velocity (Hunter et al., 2004; Salo et al., 2011).

1.3 An Overview of the Kinematics of Sprinting and Running

The trunk and pelvis are require specific coordination strategies during running (Preece et al., 2016b; Schache et al., 1999; Seay et al., 2011). Previous literature on the kinematics and coordination of the trunk and pelvis during running is limited. Even more limited is the study of the trunk and pelvis axial rotation during sprinting. Currently, the role of the trunk and pelvis during running is not clear. It has been suggested that the anti-phase coordination of the pelvis and thorax may play an important role in controlling the centre of mass displacement during running (Preece et al., 2016b). This next section provides a detailed overview of the kinematics of the thoracic spine, lumbar spine, pelvis, and hip during running and sprinting (Figure 3).

1.3.1 Sagittal plane

1.3.1.1 Trunk and Pelvis

The pelvis and trunk undergo a biphasic movement pattern in the sagittal plane, this pattern occurs in both running and sprinting (Novacheck, 1998). During running the pelvis operates in a anterior tilt relative to neutral, while the thoracic and lumbar spine operate in flexion relative to neutral (Preece et al., 2016a). The lumbar spine, thoracic spine, and pelvis reach peak flexion during the early swing phase. The pelvis reaches a secondary peak of anterior tilt during the late swing phase while the lumbar and thoracic spine both reach a secondary peak of flexion during the mid-swing phase. The pelvis and thorax kinematic trajectories suggest an anti-phase movement (Preece et al., 2016a; Schache et al., 2002).

The mean magnitude of pelvic tilting motion is within the range of 5-7°, which appears to stay relatively consistent with increases in running velocity (Schache et al., 1999). Interestingly, during sprinting the pelvis and trunk move into greater relative forward flexion, this is especially apparent in the acceleration phase. By using greater relative forward flexion the sprinter lowers their centre of mass which allows them to maximize horizontal force during the propulsion phase (Novacheck, 1998).

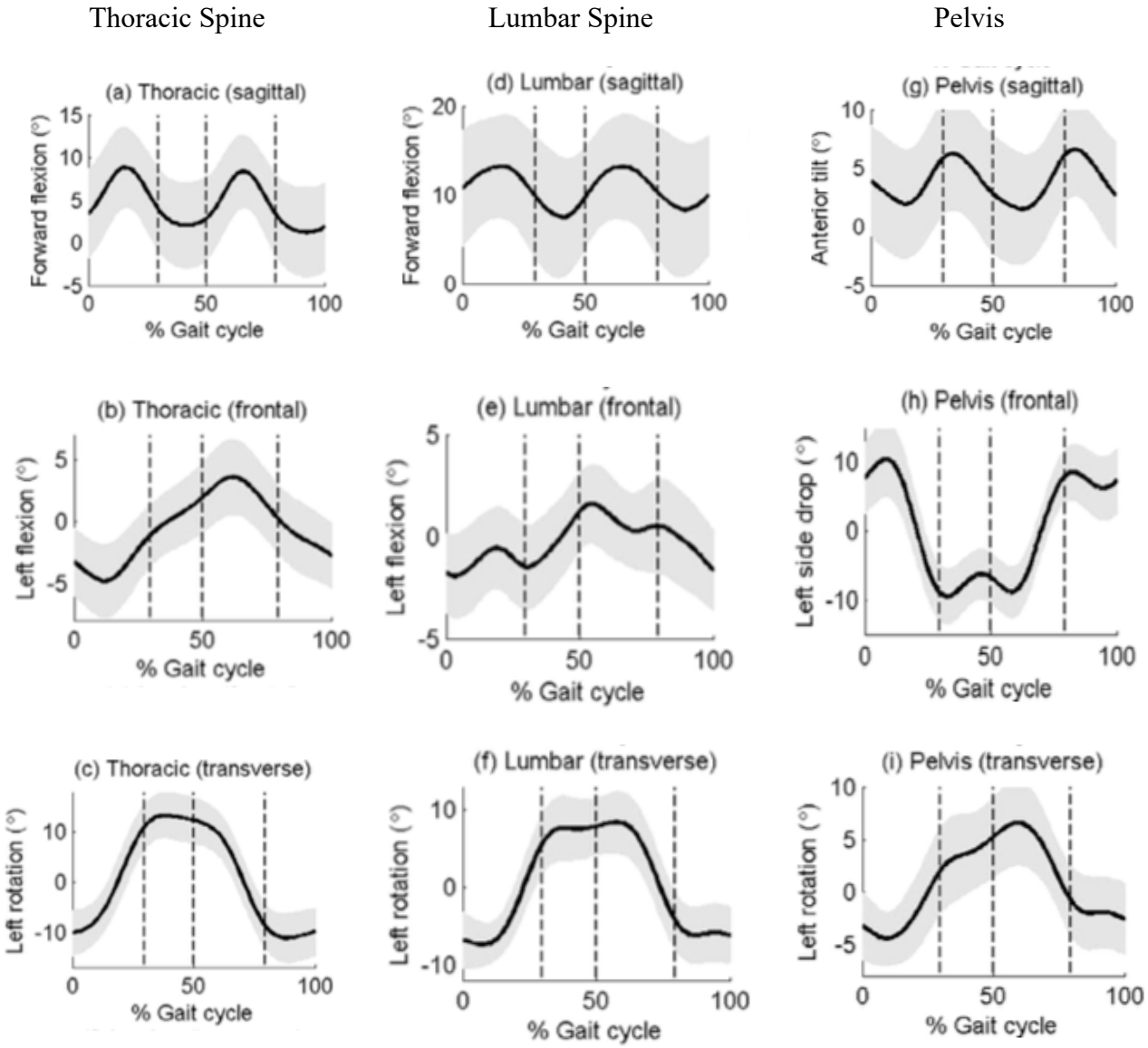

Figure 3. Time series data for the thoracic spine, lumbar spine and pelvis during running gait with averages represented as the solid black line and standard deviation represented in grey. Data is plotted from right initial contact to the following right initial contact. The three dotted vertical lines represent right toe off, left initial contact and left toe off from left to right, respectively (Preece et al., 2016a).

Table 1. Summary of sagittal plane movement of the Trunk and Pelvis

Study	Type of Running	Sample Population	Motion Capture Method	Region	Speed (m/s)	*Magnitude (°)
(Schache et al., 2002)	Treadmill running	Male runners	Optoelectric	Lumbar Pelvis	4.2 m/s	8.1 4.8
(Preece et al., 2016a)	Overground running	Healthy males and females	Optoelectric	Thoracic Lumbar Pelvis	3.9 m/s	6.0 5.0 3.0
(Debaere et al., 2013)	Acceleration phase of sprinting	Male and female sprinters	Optoelectric	Pelvis	10 m sprint	10.0
(Nagahara et al., 2018)	Acceleration phase of sprinting	Male sprinters	Optoelectric	Trunk Pelvis	60 m sprint	5.0-12.0 5.0-10.0

**Note: Magnitudes are calculated as max-min range of motion (ROM)*

1.3.1.2 Hip

During the initial swing phase after maximal extension has occurred near toe off, the hip reverses direction and begins to flex rapidly. The onset of hip extension begins at contralateral leg foot strike or slightly after (Schache et al., 1999). Hip flexion continues through the first 2/3 of swing phase until a maximal position is reached. In the last 1/3 of the swing phase the hip reverses direction and begins to extend prior to foot strike. As running speed increases the relative duration of hip flexion increases while hip extension of the running cycle decreases (Schache et al., 1999). Interestingly, hip flexion during the first half of the swing phase seems to play an important role in increasing running speed. Specifically, Kunz and Kaufmann (1981) found that elite sprinters display greater peak hip flexion during the swing phase. Greater hip flexion during this swing phase has been shown to be associated with longer stride lengths.

Peak hip flexion and extension occur at the same time as peak pelvis posterior tilt and peak anterior tilt. Peak hip extension is reached immediately after take-off (Schache et al., 2002). The hip continues to extend during the second half of the swing phase, this is done to prevent excessive deceleration that would occur at the time of initial contact (Novacheck, 1998). This may also increase the stiffness of the leg upon ground contact. Increases in the degree of hip extension at toe off have been shown to be one of the variables associated with longer stride lengths (Schache et al., 1999). Kunz and Kaufmann (1981) found that elite sprinters have less extension at toe off which would decrease contact time.

Table 2. Summary of sagittal plane movement of the hip

Study	Type of Running	Sample Population	Motion Capture Method	Region	Speed (m/s)	*Magnitude (°)
(Schache et al., 2002)	Treadmill running	Male runners	Optoelectric	Lumbar	4.2 m/s	73.0
(Debaere et al., 2013)	Acceleration phase of sprinting	Male and female sprinters	Optoelectric	Pelvis	10 m sprint	10.0

**Note: Magnitudes are calculated as max-min range of motion (ROM)*

1.3.1.3 Limbs

In the sagittal plane the limbs undergo flexion, extension, dorsiflexion and plantarflexion. The range of motion experienced by these shoulder, elbow and knee increase as running velocity increases (Novacheck, 1998). During sprinting the knee undergoes two peaks, with one peak occurring in the stance phase and a greater peak occurring during the swing phase. The range of motion of this can differ greatly depending on the skill level of the sprinter, with elite sprinters exhibiting up to 130 degree of maximum knee flexion (Novacheck, 1998). A summary of the kinematics of the upper and lower limbs can be found in Table 3 and 4.

In the sagittal plane the limbs undergo flexion, extension, dorsiflexion and plantarflexion. The range of motion experienced by these shoulder, elbow and knee increase as running velocity increases (Novacheck, 1998). During sprinting the knee undergoes two peaks, with one peak occurring in the stance phase and a greater peak occurring during the swing phase. The range of motion of this can differ greatly depending on the skill level of the sprinter, with elite sprinters exhibiting up to 130 degree of maximum knee flexion (Novacheck, 1998). A summary of the kinematics of the upper and lower limbs can be found in Table 3 and 4.

Table 3. Overview of the Lower Limb Range of Motions

Study	Joint	Type of Running	Sample Population	Motion Capture Method	Speed (m/s)	*Magnitude (°)
Novacheck (1998)	Ankle	Maximal Velocity Sprinting	Sprinters	Optoelectic	Max	50.0
	Knee		Sprinters	Optoelectric	Max	125.0
Sides (2015)	Ankle	Maximal Velocity sprinting	Sub elite and elite	Optolectric	Max	44.0
	Knee				Max	119.0

**Note: Magnitudes are calculated as max-min range of motion (ROM)*

Table 4. Overview of the Upper Limb Range of Motions

Study	Joint	Type of Running	Sample Population	Motion Capture Method	Speed (m/s)	*Magnitude (°)
Mann and Herman (1985)	Shoulder	200 m Sprinting	200 m sprinters	2D Photometric	Max	118-135
	Elbow	200 m Sprinting	200 m sprinters	2D Photometric	Max	67-84

**Note: Magnitudes are calculated as max-min range of motion (ROM)*

1.3.2 Frontal Plane

1.3.2.1 Trunk and Pelvis

The magnitude of movement in the frontal plane is more subtle than the sagittal plane of motion. Despite the smaller magnitude of movement, this motion plays an important role in stabilizing the upper body. Frontal plane motion of the trunk during running is not well studied. Thortenson et al (1984) and Carlson et al (1988) placed kinematic markers over the L3 and C7 to evaluate the angular displacement of the trunk during running. They both found that the maximal displacement of the trunk in the frontal plane occurred just prior to the mid to early stance phase. Maximal displacement occurred on the stance leg side.

Frontal plane range of motion of the trunk during running appears to range between 3-15 degrees of absolute movement. Thorstenson et al (1984) found that the net amplitudes of the angular displacement ranged from 4 to 14 degrees. Carlson et al (1988) found that at running speeds of 2.5 m/s the net amplitude of frontal plane deviation had a magnitude of 7 degrees. These ranges are similar to more recent studies were magnitudes of lateral movement to range from 3 degrees to 11 degrees of motion (Preece et al., 2016a).

Currently, Nagahara et al (2018) is the only study that evaluated the frontal plane kinematics of the trunk during the acceleration phase of sprinting. They found that the magnitude of lateral tilting decreased as the athlete reached the maximal velocity phase. During the first five strides the mean peak magnitude of thorax lateral tilting was found to be 20 degrees by the time the athlete reached there 25th step the athlete had decreased the magnitude of lateral tilting down to five degrees. Interestingly, they also found that small stance side thorax lateral tilting was correlated with increased running speed during steps 15-25 during the acceleration phase of sprinting.

The motion that the pelvis goes through in the frontal plane is called lateral tilting, pelvic obliquity or pelvic list (Debaere, Jonkers, et al., 2013; Novacheck, 1998; Preece et al., 2016a; Schache et al., 1999). Like the thorax the magnitude of motion is relatively small compared to movements occurring concurrently in the sagittal plane. This motion serves an important function in shock absorption and controlling smooth decent and ascent of the body's centre of gravity (Novacheck, 1998). Pelvic obliquity operates out of phase with thorax obliquity, with thorax obliquity preceding pelvic obliquity (Nagahara et al., 2018; Preece et al., 2016a).

At foot strike the stance side pelvic bone is slightly higher than the horizontal, while on the swing leg the pelvic bone sits slightly lower than the horizontal (Preece et al., 2016a; Schache et al., 1999). Once the sprinter reaches mid stance, the pelvic girdle is horizontal. As the sprinter continues to elevate on the swing side the pelvis reaches a maximal downward obliquity on the stance side around toe off (Preece et al., 2016a; Schache et al., 1999). During the flight the pelvis then begins to rise on the initial swing side and lower on the terminal swing side as it approached foot strike. This stops once the opposite side foot contacts the ground. During the flight phase there is minimal frontal plane movement.

Overall, the magnitude of frontal plane trunk and pelvis motion in this is very small compared to other anatomically relevant planes of motion. Novacheck (1998) found that the magnitude of pelvis motion in this plane was 7-12 degrees while running at a velocity of 3.2-3.8 m/s. This was consistent with other studies that found mean magnitudes to range between 10-20 degrees of movement at similar running speeds (Preece et al., 2016; Schache et al., 2002). The magnitude of frontal plane pelvic motion does not appear to differ substantially in running vs sprinting with slightly greater magnitudes displayed during sprinting (Debaere et al., 2013; Nagahara et al., 2018; Novacheck, 1998). Nagahara (2018) found a mean magnitude of 5 degrees during the 4^{th}-15^{th} step of acceleration suggesting that pelvic obliquity is tightly regulated at higher velocity sprinting. They also found that small upward obliquity of the stance side pelvis was associated with effective 4^{th}-15^{th} step of acceleration.

Table 3. Summary of frontal plane movement of the trunk and pelvis

Study	Type of Running	Sample Population	Motion Capture Method	Region	Speed (m/s)	*Magnitude (°)
(Schache et al., 2002)	Treadmill running	Male runners	Optoelectric	Lumbar Pelvis	4.2 m/s	18.0 12
(Debaere et al., 2013)	Acceleration phase of sprinting	Male and female sprinters	Optoelectric	Pelvis	10 m sprint	20.0
(Preece et al., 2016a)	Overground running	Healthy males and females	Optoelectric	Thoracic Lumbar Pelvis	3.9 m/s	8.0 10.0 20.0
(Nagahara et al., 2018)	Acceleration phase of sprinting	Male sprinters	Optoelectric	Trunk Pelvis	60 m sprint	7.0-22.0 12.0-25.0

**Note: Magnitudes are calculated as max-min range of motion (ROM)*

1.3.2.2 Hip

The hip in the frontal plane undergoes abduction and adduction. Hip adduction and abduction occurs relative to the pelvis (Novacheck, 1998). Hip adduction during the initial contact acts as a shock absorption mechanism. This is an important mechanism in decoupling the lower extremity motion from the trunk and head. The result of the decoupling allows for minimal head and trunk motion, allowing for balance to be maintained.

The kinematic pattern between running and sprinting is similar. At foot strike the hip is adducted, during the initial stance phase adduction increases slightly. From midstance until toe off, during the propulsive period of stance the hip abducts until toe off. This hip abduction may

serve to generate space to allow the contralateral swing leg to clear during its swing phase. During the mid-swing phase, the hip continues abducting. At terminal swing phase the hip begins to adduct again in preparation for initial contact.

The frontal plane motion of the hip has the largest magnitude of motion compared to other frontal plane rotations in the lumbo-pelvic hip complex. Mann and Hagy (1980) were amongst the first to look at the frontal plane motion of the hip. Using 2D analysis they found that the amplitude of movement was 16-22 degrees while running at 3.3-5.4 m/s. In sprinting the magnitudes of frontal plane motion appear to be larger in comparisons to running. Deborare (2012) reported magnitudes of 21-22 degrees of frontal plane hip motion in sprinters during 10 m accelerations. Interestingly, Deborare et al (2012) showed a large amount of abduction during the propulsion phase. They suggested that hip abduction range of motion and minimal mediolateral velocity was an indicator of a compensatory mechanism that occurred in well trained athletes. This compensatory mechanism allowed for the athlete to minimize the effect of the lateral foot position during acceleration on the mediolateral velocity of the centre of mass.

Table 4. Summary of frontal plane movement of the hip

Study	Type of Running	Sample Population	Motion Capture Method	Speed (m/s)	*Magnitude (°)
Mann and Hagy (1980)	Overground	Sprinters and runners	Photometric	3.3-5.4	16.0-22.0
(Debaere et al., 2013)	Acceleration phase of sprinting	Male and female sprinters	Optoelectric	10 m sprint	11.0
(Preece et al., 2016a)	Acceleration phase of sprinting	Healthy males and females	Optoelectric	4.2 m/s	20.0

**Note: Magnitudes are calculated as max-min range of motion (ROM)*

1.3.3 Transverse Plane

1.1.3.1 Trunk and Pelvis

Few studies have successfully quantified rotation of the lumbar and/or thoracic spine in the transverse plane. The thoracic and lumbar spine were found to have a monophasic kinematic pattern (Nagahara et al., 2018; Preece et al., 2016a; Schache et al., 1999). During the stance phase the lumbar spine rotates towards the stance side leg. The lumbar spine continues this rotation to the stance side leg until reaching peak axial rotation immediately preceding the contralateral side toe off. During the swing phase the lumbar spine rotates towards the ipsilateral leg until reaching a peak at 86.4% of the running cycle (Schache et al., 2002). The lumbar spine then begins to rotate to the left preceding initial contact of the foot (Preece et al., 2016a; Schache et al., 2002).

From mid-swing to early stance the thorax moves from rotated to a neutral position. This period of motion seems to be driven by stored elastic energy of the abdominal muscles, as they have been shown to be inactive during this period (Mann et al., 1986). During initial contact, the thorax begins to rotate towards the stance leg. This motion continues until mid-stance. At this point the abdominal wall actively engages to rotate the thorax relative to the pelvis.

Using skin markers during 3D motion capture, mean magnitudes were found to be between 23-30° (Preece et al., 2016a; Schache et al., 2002). However, MacWilliams (2013) used bone pins to analysis lumbar spine rotation during walking and found a much smaller magnitude 4.5 degrees. Despite differences in locomotive modalities (running vs walking) it appears that Schache et al (2002) and Preece et al (2016) experienced a degree of measurement error likely due to skin artifact and some other factors as typical ROM in this region is much smaller (Shin et al., 2013; Sung et al., 2012). Further to this, it appears that sprinting has a significantly higher

range of motion at the thorax then running or walking. MacWilliams (2013) found a magnitude of 8.9 degrees for thorax rotation, this was similar with Schache et al (2002) and Preece et al (2016). While evaluating the acceleration phase of sprinting Nagahara et al (2018) found that during sprint acceleration the thorax demonstrates a magnitude of 23 degrees.

Pelvis movement in the transverse plane is commonly known as axial rotation or internal and external rotation (Schache et al., 1999). Transverse plane pelvis motion in running displays a monophasic kinematic pattern. At foot strike the pelvis externally rotates to the side of the lower limb preparing for foot strike. The pelvis is externally rotated on the stance side, which continues to around mid-stance where the maximal position of external rotation occurs. During terminal stance the pelvis begins to internally rotate on the stance side such that by toe off the pelvis is in a neutral position. Internal rotation of the pelvis on the swing leg continues through early swing and reaches maximal position of internal rotation around mid-swing. The magnitude of pelvic rotation and running speed does not appear to display a consistent pattern. At a running speed of 3.2-4.2 m/s amplitude of pelvis axial rotation ranged between 10-18 degrees (Novacheck, 1998; Preece et al., 2016a; Schache et al., 2002). During sprinting magnitudes ranged between 12-20 degrees of motion (Debaere, Delecluse, et al., 2013; Nagahara et al., 2018). It is unclear if this variation in the data is a result of measurement error or differences in running technique.

Table 5. Summary of Transverse plane movement of the trunk and pelvis

Study	Type of Running	Sample Population	Motion Capture Method	Region	Speed (m/s)	Magnitude (°)
(Schache et al., 2002)	Treadmill running	Male runners	Optoelectric	Lumbar Pelvis	3.9	23.0 23.0
(MacWilliams et al., 2013)	Walking	Healthy males and females	Optoelectric, with bone pin markers (L1, L2, L3, L4, L5 ,S1)	Thorax Lumbar Pelvis	1.29	8.9 4.5 10.7
(Debaere, Delecluse, et al., 2013)	Acceleration phase of sprinting	Male and female sprinters	Optoelectric	Pelvis	10 m sprint	10.0
(Preece et al., 2016a)	Overground running	Healthy males and females	Optoelectric	Thorax Lumbar Pelvis	4.2	20.0 19.0 11.0
(Nagahara et al., 2018)	Acceleration phase of sprinting	Male sprinters	Optoelectric	Thorax Pelvis	60 m sprint	20-22 10.0-12.0

1.1.3.2 Hip

Transverse plane of movement of the hip is commonly known as internal and external rotation. During the absorption period of stance the hip internally rotates before returning to a neutral position by toe off (Novacheck, 1998). During the swing phase internal rotation increases during mid swing before returning to a neutrally rotated position by terminal swing.

Table 6. Summary of Transverse plane movement of the hip

Study	Type of Running	Sample Population	Motion Capture Method	Speed (m/s)	Magnitude (°)
(Debaere, Delecluse, et al., 2013)	Acceleration phase of sprinting	Male and female sprinters	Optoelectric	10 m sprint	12.0-15.0

1.1.3.3 Limbs

Transverse movement of the upper and lower extremity include internal, external rotation, pronation, supination, inversion, and eversion. Pronation occurs during the absorption phase of the movement. While supination usually occurs during the generation phase of a movement (Novacheck, 1998). There are currently no papers that report transverse plane movements for the upper and lower limb in sprinting

1.4 Optoelectrical Motion Capture Systems vs Inertial Measurement Units (IMU)

The gold standard for motion capture is an optoelectrical system. These systems facilitate the 3D tracking of passive or active infrared markers placed on the body of a human participant during a dynamic movement. However, due to the extensive set up data collection with these systems are typically limited to laboratory settings. Recently, inertial measurement units (IMUs) have started to overcome some of the practical limitations of optoelectrical systems. IMUs include a variety microelectromechanical system (MEMS) often including triaxial accelerometers, gyroscopes, magnetometers, and in some cases global positioning systems (GPS). In some practical cases IMUs are utilized in place of gold-standard optoelectronical systems since they are small sensors that are highly transportable and can be directly placed on

the skin of an athlete or participant. Further, these wireless sensors do not require direct line of sight, and therefore can be used for athletic or workplace-related movements where line of sight may be compromised. Finally, IMUs can be used to dramatically increase a 3D capture volume allowing for the wireless capture of movements spanning 10-250m, dramatically exceeding the capture volume of most optical systems. As noted previously, IMUs track motion via the fusion of three different sensors that are imbedded in the IMU. Typically the sensor fusion process implements some type of Kalman filter and computational anthropometric mode (Schepers et al., 2018).

With recent interest in IMUs a growing number of validation studies have aimed to assess the accuracy of many kinematic outputs obtained using these wearable sensors. It has typically been shown that error during gait analysis for lower limb sagittal plane angles show good correlation coefficients with optically derived angles. While errors may increase in frontal and axial plane angles (Ohtaki et al., 2001; Schepers et al., 2018; Seel et al., 2014; Weygers et al., 2020). In the sprint literature there is also a growing interest in IMUs. Traditionally, optoelectrical system have been the preferred assessment tool. However, the extensive set up and limited collection volume has typically prevented researchers from being able to capture longer sprinting bouts. With the growing interest a growing number of validation studies have aimed to assess the viability of IMUs as an alternative to optoelectrical systems for the motion capture of sprinting. IMUs have been shown to be accurate in estimating spatiotemporal parameters (de Ruiter & van Dieën, 2019), stance duration (Schmidt et al., 2016), sprint velocity (Gurchiek et al., 2018), sprint power (Slawinski et al., 2020) and trunk inclination (Bergamini et al., 2012), among others.

1.6 An Overview of Neuromuscular Control During Sprinting

Sprint velocity is a multifactorial motor ability which is dependent on many different features of the motor system. A component that often limits sprint velocity is the ability to coordinate the neuromuscular system. Coordination of the neuromuscular system requires the proper sequencing and timing of various muscles to effectively optimize sprint technique. Sprinting belongs to a classification of movements called terminal movements (Latash, 1994). Terminal movements have a precise set structure with a defined beginning and end of movement. Every terminal movement requires an adequate motor program. A motor program is a pre-set group of commands that sequence the order in which muscles fire. A key component of locomotion is the initial motor pattern generated by the central pattern generator (Golubitsky et al., 1999). A central pattern generator is a neural circuit that produces rhythmic patterns of motor activity without the need for sensory input. The effect of central patterns on locomotion have been well studied in animal models. The basic stepping behaviour can be entirely generated by central pattern generators at the spinal cord level (Kandel et al., 2012). These patterns become further refined by higher regions of the central nervous system, particularly the cerebellum, motor cortex, and the brain stem which integrate afferent feedback and assist in movement coordination. Specifically, various systems such as the visual, proprioceptive, and vestibular system provide information to these regions of the brain. For instance, proprioceptive systems appear to influence the timing and amplitude of the stepping behaviour (Kandel et al., 2012) While the visual system provides information to the motor cortex. The motor cortex then provides control over stepping movement and planning of coordination (Kandel et al., 2012).

Central patterns are a highly adaptive behaviour which are intertwined with various reflexes. These reflexes include reciprocal inhibition, recurrent inhibition, parallel

excitation/inhibition and mutual excitation (Kandel et al., 2012). Although all these reflexes are likely to influence sprint performance, one that is particularly important is reciprocal inhibition. Reciprocal inhibition describes the reflexive behaviour of the neuromuscular system which causes the relaxation of the antagonist muscle to accommodate the agonist muscle. The importance of quickly activating muscles is well documented (Coh et al., 2010; Morin et al., 2012). While, the ability to quickly relax muscles may also play an important role in the performance of high velocity movements (Pinto & McGill, 2020; Verkhoshansky & Siff, 2009).

Sprinting is an inherently unstable activity which requires the central nervous system to stabilize compressive buckling forces and shearing forces as the centre of mass displaces horizontally and vertically. As previously discussed the displacement of the COM appears to be functionally associated with the coordinative behaviour of the trunk and pelvis (Preece et al., 2016a). By adapting an anti-phase coordination strategy of the thorax and pelvis the system is inherently more stable because the displacement of the COM is minimized. This is critical in an activity like sprinting where athletes are required to accept forces up to 5x their body weight with each stride (Weyand et al., 2000). The result of this is the need for muscles to dynamically shift between different levels of activation. Traditionally, the literature has focused primarily on activation of the upper and lower extremities with minimal focus on muscles of the trunk. A summary of the activation patterns of both peripheral and axial muscles can be seen in Figure 4.

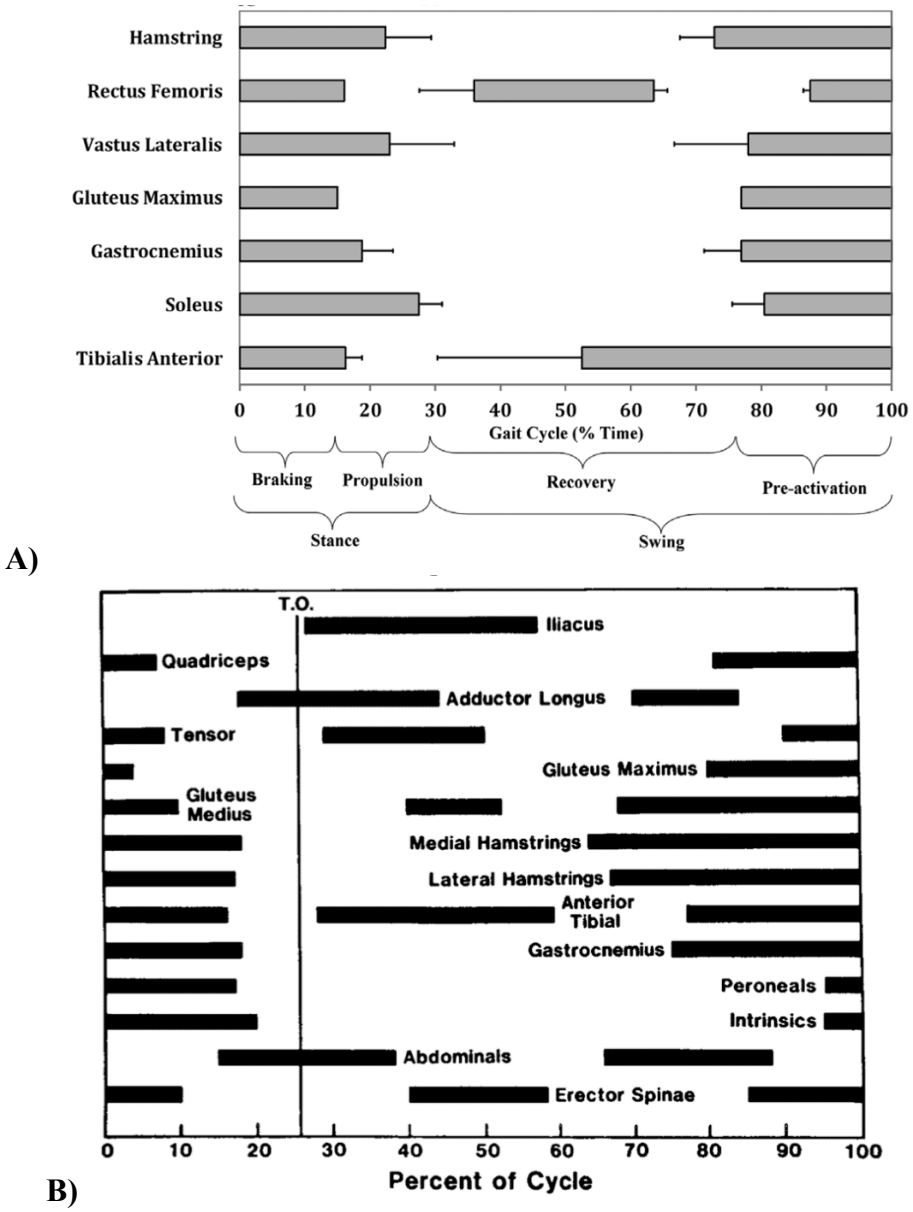

Figure 4. The muscle activation and timings of lower limb during the gait cycle. A) Timing was gathered from Chumanov et al. (2007), Higashihara et al. (2010), Kuitunen et al. (2002), Kyröläinen et al. (2005) Mero & Komi.(1987), Novacheck. (1998), Pinniger et al. (2000), (Thelen et al., 2005), (Yu et al., 2008) B) Muscle activation timing gathered from (Mann et al., 1986) indwelling electrodes were used for the iliacus, adductor longus and peroneus longus muscles. All other muscles were captured using surface electrodes.

1.6 An Overview of Coordination and Performance

Sprint performance is manifested through the complex interaction of many different joints and segments. Each of these joints and segments can undergo different actions which results in many movement degrees of freedom (i.e., the capacity for linear and rotational movement about specific joints). The movement apparatus (i.e., motor cortex) coordinates these structures to interact with the environment through a process known as *motor control*. Motor control can be modelled with two different types of measurements, namely a control parameter and/or an order parameter. Control parameters aim to quantify the result of a movement, with a classic example being movement velocity. Order parameters characterize the organisation of a movement to facilitate a control parameter outcome. For example, if an order parameter is movement velocity, an order parameter would characterize the differences in coordination between a walk, jog, run, or sprint. In summary, this means that any control parameter is dictated by the underlying order parameters, to accomplish a given movement (Kelso, 1997).

The formation of coordinative strategies is thought to form through self-organization. The strategy displayed is dependent on variety of factors including specific task, organism, and environmental constraints. When learning a task Bernstein (1967) noted that redundant degrees of freedom need to be mastered in order to reach task mastering, he coined this the degrees of freedom problem in his seminal text *The Co-ordination and Regulation of Movements*. In this he hypothesized that during motor learning the central nervous system (CNS) searchers for an appropriate coordinative pattern once this is identified the CNS freezes degrees of freedom to achieve greater control. The adaptation of the CNS is thought to increase the repeatability of the motor output at the cost of creating a less adaptable system. Further to this, Bernstein (1967) proposed that coordination is the "organisation of the control of the movement apparatus"

(p.127). Where control is the effect of coordination. To illustrate this point, consider a sprinter accelerating where the primary aim is cover as much distance in the shortest amount of time. The velocity of the centre of mass is governed by the coordination of the entire body. The formation and self-organization of coordinative structures is thus dependent on a variety of factors including task, organism, and environmental constraints.

The formation and self-organization of coordinative structures has been explored through the degrees of freedom problem proposed by Bernstein (1967). He proposed that joints, segments, and muscles give rise to redundant degrees of freedom. The highly intricate and co-dependent nature of these features is thought to give rise to the movement systems result in non-linearity and variability of most biological systems. The motor control system optimizes its variability by reaching functionally preferred states called attractor states. An order parameter (i.e., velocity of movement) can be manipulated to change a systems attractor state by walking the system to a non-equilibrium phase transition. As an order parameter reaches a phase transition, variability of the behaviour of the system will increase. Once variability becomes too much the system will destabilize the attractor state and either behave chaotically or find a new attractor state. Attractor states represent the ideal set of order parameters to accomplish a given control parameter outcomes. In some instances, a single motor strategy (or attractor state) is optimal, in other cases many optimal motor solutions to accomplish a given motor task within a set of control parameter constraints.

Movement variability can either be functional or non-functional. Functional variability increases the systems complexity and allows for the system to become more adaptable (Lipsitz, 2002). While non-functional variability is variability that produces noise in the system. Thus, the structure of variability is vital to the understanding of coordination of movement. In Bernstein's

degree of freedom problem, he attempted to explain the structure of variability as an individual reached mastery. He hypothesized that during motor learning the CNS searches for an appropriate coordinative pattern, once this is identified the CNS will freeze degrees of freedom to achieve greater control. This adaptation of the CNS is thought to increase the repeatability of the motor output at the cost of creating a less adaptable system. Bernstein's hypothesis went on to state that as the individual reach's mastery, the degrees of freedom become unfrozen, and the variability of the coordinative dynamics will increase. This results in a U-shaped relationship between coordinative variability and skill level.

The U-shaped pattern of variability has been seen on several occasions in the literature (Robins et al., 2006; Vereijken et al., 1992; Wilson et al., 2008). For instance, Wilson and colleagues found this pattern emerge in a group of five competitive triple jumpers. Wilson and colleagues evaluated three intra-limb couplings using vector coding (Coupling 1= stance leg ankle plantar/dorsi flexion-knee flexion/extension, coupling 2=stance leg knee flexion/extension-hip flexion/extension and coupling 3=swing leg knee flexion/extension-hip flexion/extension) during the hip-step transition phase in the triple jump. Mean coordinative variability for coupling three showed the strongest correlation with a U-shaped model (R^2=0.9868) while coupling one (R^2=0.3659) and two (R^2=0.6931) showed weaker correlations. Despite the weaker correlations in coupling one and two, it was still evident that the novice and advanced triple jumpers displayed higher coordinative variability then the intermediates. The findings suggest that even highly trained performers undergo a U-shaped change in coordinative variability as skill develop. As a result, it seems likely that the variability of the coordinative dynamics of an athlete fluctuate through one's career towards the development of mastery for any particular motor skill.

Unlike triple jump, sprinting is cyclical activity that lacks a discrete spatial target. Rather, sprinting requires the optimization of spatiotemporal factors with the goal of increasing running velocity (Hamill et al., 2012). Sides and colleagues used CRP and coordinative variability to identify differences in between sub-elite and elite sprinters. CRP has previously been used to quantify differences in running mechanics (Hamill et al., 2012). CRP works by taking the differences in the phase angle between two oscillators. The phase angle is calculated by calculating the arctangent function of the normalized position and velocity of a time-series data (Hamill et al., 2012). In Sides (2015) analysis of sub-elite and elite sprinters, they found that elite sprinters demonstrated subtle differences in the coordination of the hip-knee coupling and knee-ankle sagittal plane coupling. For instance, at the point of mid-stance, the sub-elite group had a significantly more out-off phase HK coupling than the elite sample While this difference converged towards a similar in-phase HK coupling between sub-elite and elite groups at TO. Another difference identified occurred in the early swing phase, the sub-elite group exhibited a more in-phase motion for both he HK and KA coupling compared to the elite group; however, this was not statically significant. While the main difference that occurred appeared to be in the timing of in-phase coordination and magnitude of out-phase coordination for the KA for during the swing phase. Sub-elite sprinters displayed a greater out-of-phase CRP value and did not reach an in-phase KA coupling until later in the gait cycle (Figure 5). This demonstrates that differences in the coordination of the lower limb may play a role in sprint performance.

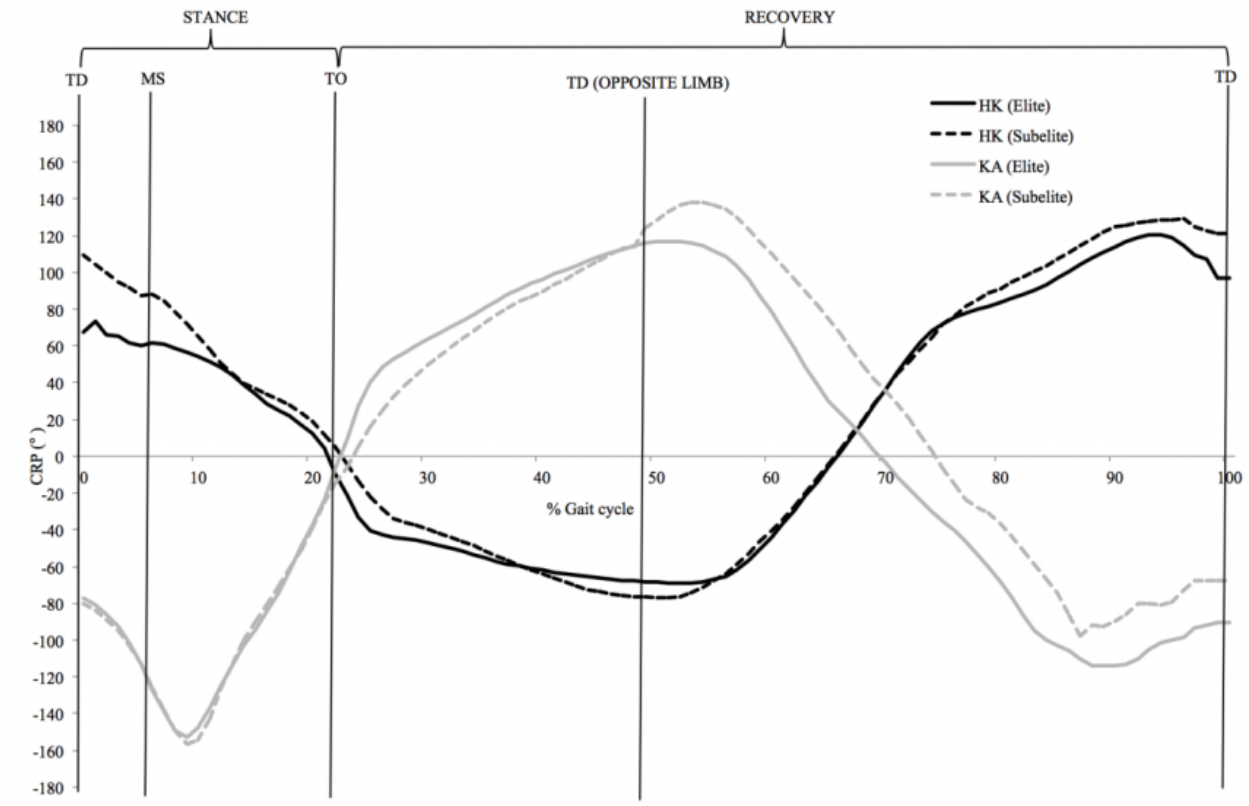

Figure 5. HK and KA coupling ensemble CRP time series differences between elite and sub-elite sprinters (Retrieved from Sides, 2015)

As previously mentioned, the variability is a key component of movement analysis. The role of it during sprint performance is not well understood. Several studies have aimed to provide insight into the temporal variation that occurs across the gait cycle (Sides, 2015; Wdowski & Gittoes, 2013). Sides (2015) demonstrated that sub-elite sprinters display more variability in the HK coupling at touchdown and toe off, less variability in the KA at touch down and toe off, more variability in the KA during opposite leg touch down, more variability in the HK during early swing, less variability in the KA during late swing. This suggests that the variability associated with sprint performance is likely to vary dependent on the skill level and time in the gait cycle.

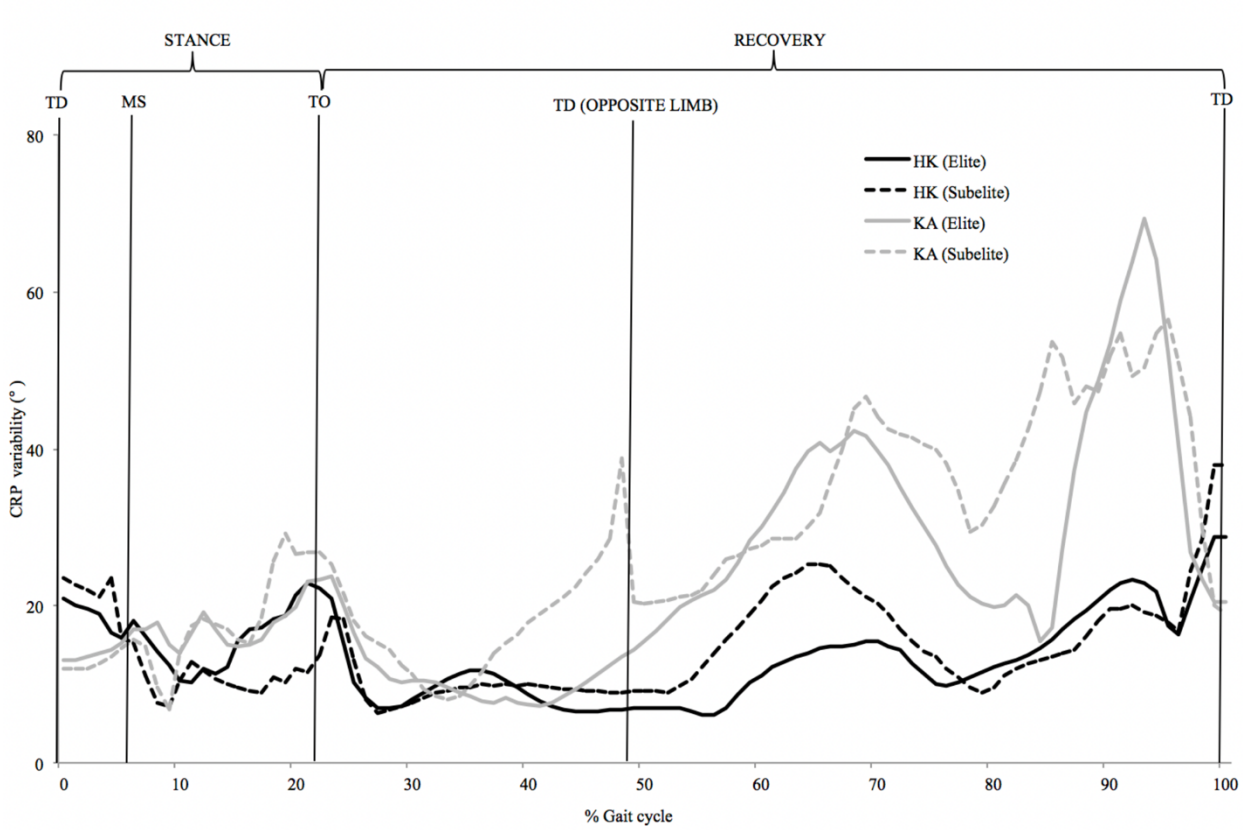

Figure 6. HK and KA coordinative variability time series differences between elite and sub-elite sprinters (Retrieved from Sides, 2015)

While initial work provide by Slides (2015) provides insights into the importance of coordination in sprint performance more work is needed to understand the role it plays. Future work should expand our understanding by using 3D kinematics, upper and lower body segments, and the analysis of both inter- and intra-limb coordination measures.

1.7 An Overview of Data Driven Approaches to Feature Identification in Human Movement

From autonomous cars and natural language processing to predictive sport modelling and skill classification models, machine learning systems are increasingly prevalent in society. These models can be used to solve a variety of different complex numerical problems, two common classes of problems are classification and regression. A classification problem aims to categorize a set of data into classes (i.e., skilled and unskilled). In biomechanics machine learning

algorithms such as Linear Discriminant Analysis can be used to classify athletes based on movement technique as novice or advanced (Ross et al., 2018a). While a regression problem aims to predict a continuous set of outcomes (i.e., sprint velocity). These models can often outperform humans or at the very least improve human performance. The deployment of machine learning models in biomechanics is a relatively recent phenomenon and has great potential.

The data collected in biomechanics is often of high spatiotemporal dimensionality, and also often highly redundant due to time-varying long-range spatiotemporal correlations between timeseries parameters (Riley & Turvey, 2002). Principal component analysis (PCA) can be used to reduce high volumes of high dimensional data to a smaller set of lower dimensional orthogonal modes of variation. PCA works by identifying orthogonal modes of variation in the data set and representing these as principal components (PC). The algorithm works by maximizing first PC so that it captures the largest mode of variation present in the data set, the subsequent PCs follow the same optimization rule but explain less variance in the data set. PCA has large clinical and research applications due to both reduce highly complex datasets, and to facilitate the re-construction of any raw data following analysis. For example, a single principal component score can be used to reconduct a representative waveform using single component reconstruction (SCR) (Brandon et al., 2013), further an entire set of principal components can reconstruct the original input data matrix.

PCA has large clinical and research application as it helps reduce high dimensional data sets to a set of orthogonal modes of variation. These partitions of the data can represent primary modes of variation without the need for *a priori* hypotheses. This facilitates a data-driven or hypothesis-generating approach to research. However, one challenge with the use of PCA in

biomechanics is the interpretation of the biomechanical meaning of these PCs. Two common approaches to aid with the interpretability of a PC is a biplot and SCR.

Biplots work by plotting the feature vectors present in a PCA against two or three PCs. From these plots we're able to understand several things, including the features magnitude of loading on each PC, the contribution of a feature to a PC and the correlation between two or more feature vectors. For example, how strongly a feature loads on a PC are represented by the length of the vector along the PC axis. To determine how much a feature contributes to a PC relative to other features, can be determined based on the relative angle between the feature vector and the PC axis. The smaller the relative angle between a feature vector and a PC axis the more that feature contributes to that PC. Lastly, the correlation between features can be determined based on the relative angle between feature vectors. A small relative angle, between feature vectors determines that the features display a strong positive correlation. On the other hand, if the angles are opposite to one another, this signifies a strong negative correlation. Lastly, if the feature vectors are perpendicular to one another then the two features are not correlated.

SCR is used to reconstruct a single PC to identify how the PC scales a biomechanical feature. Using the PC loading vector and the percentile of the PC score to reconstruct an upper band (i.e., 95^{th} percentile) and a lower band (i.e., 5^{th} percentile) for each PC. This allows for us to understand how the PC is influencing the behaviour of a biomechanical waveform. Brandon and colleagues recommended three types of classifications for a PC. These include a magnitude, difference and a phase shift feature. An example of these features can be seen in Figure 7.

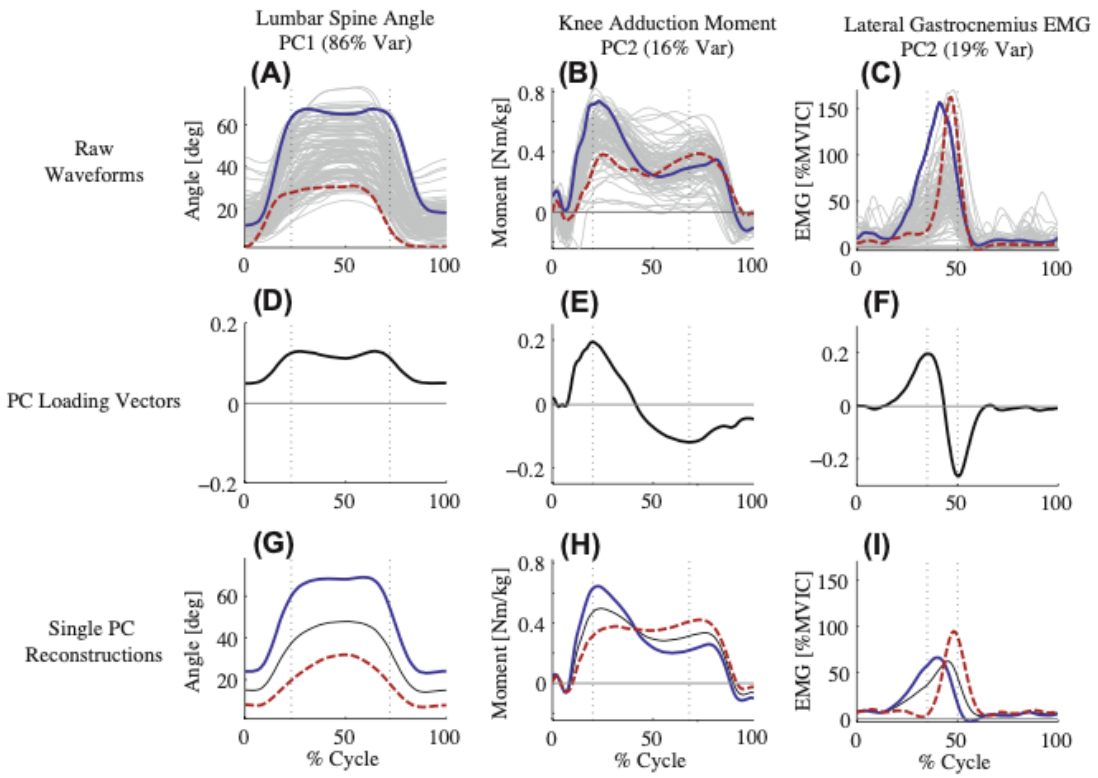

Figure 7. An example of representative of extremes, loading vectors and single component reconstruction on various biomechanical waveforms. Lumbar spine angle (A, D, G), knee adduction (B, E, H) and lateral gastrocnemius EMG (C, F, I). A, D, G represent magnitude features, B, E, H represents a difference feature and C, F, I represent a phase shift. Retrieved from (Brandon et al., 2013)

PCA has been used in a variety of applications in biomechanics with one of the early applications being the work of Troje (2002). Troje's work serves as a foundation for the application of PCA in the objective assessment movement technique. Troje initially set out to understand how biologically and psychologically relevant information is encoded in visual motion patterns. To understand this Troje used 40 participants (20 males and 20 females) to determine kinematic differences in gait features based on age, sex, and emotion. To discriminate these differences Troje used PCA. He found that four PCs accounted for 98% of the variance in whole-body kinematics dataset. Using PC scores Troje was able to model the spatiotemporal behaviour of the gait pattern across classifiers related to age, sex, and emotional state.

PCA can be used to assess sport technique and has been used to assess inter-athlete variability and intra-athlete variability of a sport technique. Gløersen et al (2018) showed that by condensing all participants into a single PCA it was possible to determine technical differences between athletes. To do this, the authors took the full body kinematics using an optoelectrical motion capture system to assess 12 consecutive strides of treadmill roller skiing on six internationally ranked cross-country skiers. Gløersen et al found that five PCs represented 96.1% of the variance in the dataset and found that they correlated to differences in the international ranking of their skiers. Through reconstruction of their data, they were able to determine the biomechanical significance of their PC scores. For example, PC2 suggested that the highest ranked skier flexed the hip approximately 29 ms earlier compared to the lowest ranked skier. This study shows the power of a PCA to provide sport biomechanist and coaches to objectively analyze and benchmark their athlete's technique to inform training interventions.

1.8 Thesis Overview & Bridge Summary

Traditional research studies in the areas of sport biomechanics rely on the development of *a priori* hypotheses, and the acquisition of human movement data from a small representative sample of athletes. This can result in non-trivial statistical and theoretical biases in the development and testing of specific hypotheses from small datasets. For instance, in the sprint literature there has been an emphasis on the analysis of the lower limb despite strong theoretical and anecdotal evidence that the spine and upper body may also be important to optimize performance. This thesis aims to use a holistic data-driven (i.e., hypothesis generating) approach to objectively identify key coordinative features are associated with optimal sprint velocity. The experiment conducted in this thesis was designed to identify kinematic and neuromuscular features using full-body kinematic and a nine channel surface EMG data set that could predict

sprint velocity using a data-driven framework. The findings of this thesis have implications concerning the role coordination plays in sprint performance and can be used to inform coaching practice. It was hypothesized that several distinct kinematic and neuromuscular features would be present as significant contributors to predicting sprint performance. These included distinct differences in the coordinative strategy of the thorax and pelvis, smaller range of motion of the pelvis, and differences in the timing of the activation of the muscles that attached to the thoracolumbar fascia. Although expected, these kinematic and neuromuscular differences did not inform the selection of specific outcomes, or the statistical testing of said outcomes following the acquisition of experimental data. Rather, a large sample of high-dimensional neuromechanical data was obtained from >40 sprinters varying in ability, and the data were analyzed holistically to assess if the hypothesized parameters had any apparent influence on sprint performance. The following chapters detail a draft of a manuscript which is in preparation for submission to a special edition of *Frontiers in Sports and Active Living*, titled *Rising Stars in Biomechanics and Control of Human Movement: 2022*. This special edition will showcase the high-quality work of both emerging talents and internationally recognized researchers in the early stages of their careers. The following sections of this thesis have been designed to align with the formatting requirements for this special edition to facilitate the rapid dissemination of this research.

CHAPTER II – AN EXPLORATORY STUDY EVALUATING THE EFFECTIVENESS OF A DATA DRIVEN APPROACH TO IDENTIFY COORDINATIVE FEATURES THAT ARE ASSOCIATED WITH PEAK SPRINT VELOCITY

Prepared for submission to *Frontiers in Sports and Active Living*, titled *Rising Stars in Biomechanics and Control of Human Movement: 2022*.

2.1 Introduction

The objective of sprinting is to cover a set amount of distance in the shortest amount of time. To do this the sprinter leverages three different phases: the start, acceleration phase and the maximal speed phase to achieve the fastest possible sprinting velocity. During each of these sequential phases the athlete undergoes a series of coordination strategies to achieve the fastest possible velocity. Although sprint performance is a popular topic in biomechanics, many of these studies have assessed specific sub-regions of the body and have selected discrete parameters *a priori* for statistical analysis. These approaches have led to a bias in the sprint biomechanics literature where many of the studies have focused on the kinematics of the lower limb, which has resulted in the failure to assess the relationship between sprint velocity and the upper body kinematics. While it would be simpler to evaluate the upper body in isolation to fill this gap in the literature, doing so would fail to accurately quantify the complexity of a whole-body movement such as sprinting. As it's believed that coordination of whole-body movements is highly intricate and co-dependent in nature (Kelso, 1997). Thus, the approach used in this work aims to use a data-driven approach to understand whole-body coordinative strategies associated with peak sprint velocity. This work constitutes as hypothesis generating research, which aims to inform future research and coaching practices.

Sprint velocity is multifactorial and is defined by a variety of kinematic, kinetic, and neuromuscular features. At its simplest sprint velocity is the by-product of stride length and stride rate (Hunter et al., 2004). Stride length and stride rate are mutually dependent variables

with an inverse relationship (Hunter et al., 2004). To accomplish a faster sprint velocity, an athlete must either increase stride length or stride rate while maintaining the other. These features have been reported to be influenced by different factors. For instance, stride length appears to be positively influenced by explosive strength, muscle mass, lower extremity length, biological sex, ground reaction force, ground contact duration, and dynamic flexibility of the hips (Coh et al., 2010; Debaere, Delecluse, et al., 2013; Hunter et al., 2004; Mattes et al., 2021; Weyand & Davis, 2005). In contrast stride rate appears to be influenced by rate of force development which can be affected by motor neuron excitability, inter and intramuscular coordination, fatigue, horizontal velocity of the COM during stance, leg angle touch down, leg angle at take-off, and leg length (Coh et al., 2010; Hunter et al., 2004).

During high velocity sprinting the neuromuscular system is required to activate and relax many muscles quickly and rhythmically. Previous work in the field has focused largely on the lower extremity and can provide insights into the complexity of neuromuscular coordination during sprinting. For instance, a shift in control strategy of the lower limb muscular appears to occur around 7.0 m/s as increases in running velocity below 7.0 m/s appear to be driven by increases in muscle force of the ankle and beyond 7.0 m/s is driven by increases in muscle force of the hip (Dorn et al., 2012). While this exemplifies the dynamic nature of neuromuscular control in sprinting, what remains unanswered is the role of muscles of the trunk and thorax body during sprinting. Particularly, the muscles that attach to the thoracolumbar fascia, as a strong theoretical foundation suggests these muscles play an in regulating the pendulum like action of the contralateral arm and leg during locomotion, this may be particularly important during higher velocities (Gracovetsky & Farfan, 1986; Vleeming et al., 1995).

Sprinting is a whole-body movement which requires the CNS to optimize the relationship between many joints and segments. Multi segmental coordination has been shown to have an influence a variety of factors including an individual's health and performance (Cazzola et al., 2016; Seay et al., 2011). In many cases a coach tries to influence an individual's coordination by leveraging a variety of coaching tools such as sport specific drills, cueing and other training intervention (i.e., weightlifting). However, due to the limitation in available biomechanical technology to track changes accurately and reliably in sprint technique, the impact of these interventions has largely been determined using subjective methods of appraisal. This can make it challenging to effectively understand the effect of an intervention. Fortunately, recent advancements in wearable technology such as wireless EMG and inertial measurement units (IMUs) have allowed for practitioners to accurately quantify kinematic and neuromuscular coordination (Beange et al., 2019). This has resulted in a growing demand on biomechanical researchers to understand the link between whole-body multi-segmental coordination and specific movement outcomes such as sprint velocity (Glazier, 2021).

Biomechanical data typically consists of high volumes of high dimensional data. The volume and high dimensionality of these data sets make it challenging to select key features for statistical analysis. Traditionally, biomechanists have selected a single data point at an extreme point in a movement (i.e., range of motion). However, this can result in non-trivial statistical biases as this often ignores other regions of a waveform which may also be significant modes of variation. Furthermore, by selecting a discrete data point to represent a movement this eliminates information containing the spatiotemporal coordinative dynamics, that define optimal sport technique. This creates a challenge in the translation of information of coaching practices, as coaches assess movement by inspecting the behaviour of the entire body, not a single joint at a

discrete point in time. Fortunately, biomechanists can borrow data reduction techniques traditionally used in machine learning to reduce the volume and dimensionality of a data set. This is possible because biomechanical data is largely redundant due to time-varying spatiotemporal correlations that exist (Riley & Turvey, 2002). This means that by applying algorithms such as principal component analysis (PCA), we can effectively reduce the volume and dimensionality of the data while still preserving the time-varying spatial temporal coordinative information that defines optimal sport technique. PCA works by identifying primary modes of variation in a data set and representing them as orthogonal vectors, these vectors are called PCs. The outputs of PCA, called principal components (PC) are particularly useful as they can be used as inputs into more advanced machine learning algorithms such as regression, classification and clustering algorithms.

In recent years, machine learning and artificial intelligence has developed rapidly particularly in the field of natural language processing and autonomous cars. A lesser-known application of machine learning is in the objective quantification of human movement. One of the early pioneers in this area was Nikolaus Troje, who adapted a PCA to model the effect of age, body mass index, biological sex and emotion has on human walking. This initial framework has been adapted to model differences in skiing technique and classify athletes as novice or advanced (Gløersen et al., 2018; Ross et al., 2018a). PCA-based movement pattern recognition techniques have been growing in popularity due to its ability to provide easily interpretable models using single component reconstruction (SCR) (Brandon et al., 2013). Using SCR, a full-body avatar can be reconstructed to provide athletes and coaches with an easy-to-use technique to communicate key technical differences between individuals and/or to provide longitudinal feedback to an athlete or coach.

The PCA based framework developed by Troje, and subsequently implemented by Ross et al., (2018) shows promise in the ability to identify coordinative differences between individuals. However, what remains unknown is whether a PCA-based framework can identify kinematic and neuromuscular features that are correlated with sprint velocity.

1.1.1 Purpose

The purpose of this work is to leverage recent advancements in wearable sensor technology and data-driven tools to objectively assess the kinematic and neuromuscular determinants of sprint velocity through the analysis of a large dataset of university-aged sprinters. This hypothesis-generating study will serve as the foundation for future work related to the development of customizable data-driven sprint coaching tools.

1.1.2 Hypothesis Statement

It was hypothesized that several distinct kinematic and neuromuscular features would be present as significant contributors to the prediction of sprint velocity. These included distinct differences in the coordinative strategy of the thorax and pelvis and the timing and activation of the muscles attached to the thoracolumbar fascia.

2.3 MATERIALS & METHODS

2.3.1 Participants

Forty participants (27 male, 13 females; mean ± standard deviation age: 21.8 ± 3.2 years; height: 176.8 ± 8.4 cm) from a variety of team sports and track and field events were recruited for this study. Demographic information is presented in Table 6. One participant was removed from the sample due to issues with data quality. Participants were required to be recreationally active at least twice a week in a sprint-based sport. Participants must not have reported any neurological, cardiovascular, or muscular disorders that may impact their sprint performance and have no known allergies to rubbing alcohol or adhesives. The current protocol was approved by the institutional research ethics board in accordance with the Canadian Tri-Council Policy Statement (TCPS 2) on the Ethical Conduct for Research Involving Humans (REB #20-364).

Table 6. Participant Demographics

Demographic	Sample size	Age	Male	Female	Height
Rugby	6	21 +/- 2.5	4	2	178 +/- 20.5
Sprinting	4	20 +/-1.8	3	1	175+/- 14.2
Soccer	15	21.9 +/- 3.7	10	5	174.6 +/- 3.7
Ice Hockey	7	22.3 +/- 3.0	3	4	178.0 +/- 9.4
Other	8	23 +/- 3.0	8	0	180.4 +/- 4.1

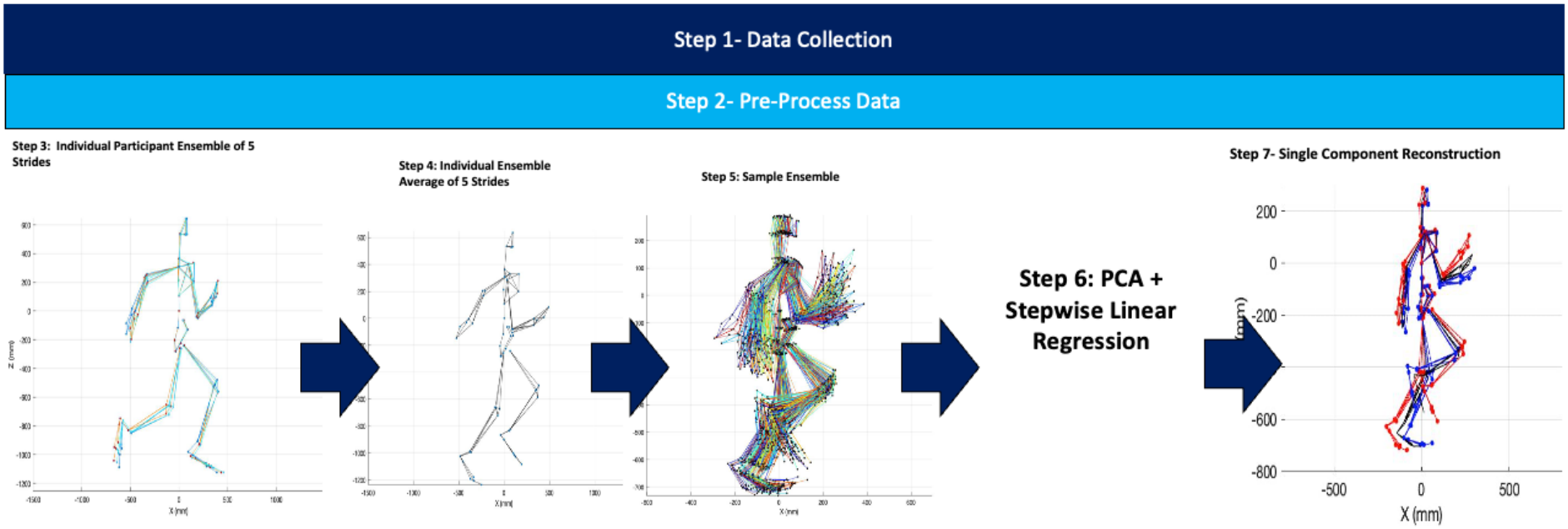

Figure 8. Summary of Experimental Workflow for both the kinematic and EMG data set. A similar process was completed for both data streams to create two different PCA frameworks

2.3.2 Experimental Protocol

An overview of the experimental design and data analysis protocol can be seen in Figure 8. Each participant completed a single experimental visit lasting approximately 2 hours. Following the completion of the informed consent form, all participants were instrumented with two types of wearable sensors. Full-body kinematics were collected using a 17-sensor IMU suit (XSens, Awinda). Specifically, IMU sensors were placed bilaterally on the feet, shank, thigh, upper arm, forearm, hands, and shoulders. A single sensor was placed on the sternum, pelvis, and head. All kinematic data was acquired at a frequency of 60 Hz. Muscle activation was recorded for nine muscles located from the lower body to upper body (need to include specific locations). Bipolar surface electrodes and sensors (Noraxon Ultium) were placed according to SENIAM guidelines on the right gastrocnemius (GAS), right bicep femoris (BF), right gluteus maximus (GMAX), right gluteus medius (GMED), right vastus lateralis (VLO), right rectus femoris (RF), left lumbar erector spinae (LES), left latissimus dorsi (LD), and left external obliques (EO). All EMG data was acquired at a frequency of 2000 Hz. For a complete review of specific landmarks for sensor attachments please refer to Table 8 and Figure 9.

Following instrumentation, the participant underwent a self-directed warm-up for 5 minutes. Once the participant completed the warmup, they then completed three 60 m over-ground sprints on synthetic track, each separated by a period of at least 5 minutes of passive rest to avoid any influence of neuromuscular fatigue. During these over-ground sprints, 3D whole-body kinematics and neuromuscular activity were recorded simultaneously. The trial with the fastest peak sprint velocity achieved was selected and used for further analysis.

Table 8. Summary of the location of each sensor

Location	Optimal position
Foot	Middle of the bridge of the foot
Lower leg	Medial surface of the tibia
Upper leg	Lateral side above knee
Pelvis	Flat on sacrum
Sternum	Flat in the middle of the chest
Shoulder	Scapula
Upper arm	Lateral side above the elbow
Forearm	Lateral and flat side of the wrist
Hand	Backside of hand
Head	Rear of head

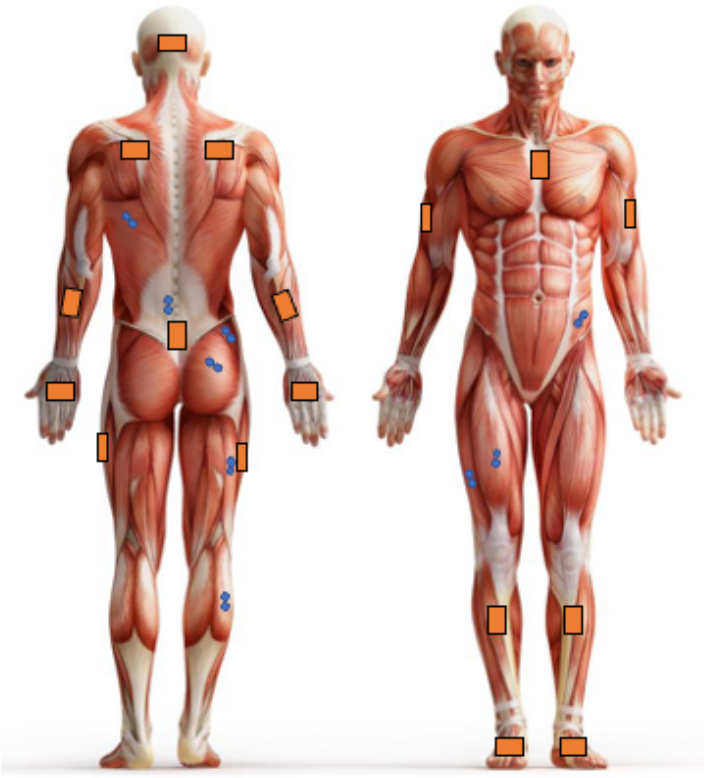

Figure 9. Bipolar electrode (blue circles) and IMU (orange squares) placement on the participant

2.3.3 Data Analysis

3D kinematic data were high definition (HD) reprocessed using XSens MVN Analyze software and a 64-marker data set was exported into a .c3d file. The .c3d file was imported into MATLAB (2021b) using Biomechanical Tool Kit 5 (Barre & Armand, 2014). The origin of the coordinate system for the imported data was reset so that the x, y, z positions of the right ankle at the beginning of the sprinting trial represented the origin. To correct positional drift during the sprinting trials we created a custom PCA framework to create a new global coordinate system (GCS) to ensure that all positional data were aligned for all sprints, and for all participants. Specifically, PCA was used to derive the three highest components of variation in the XYZ 64-marker dataset, across all timepoints, for each sprint. Next, 3D rotations were then computed between each 3D loading vector and the original global coordinates to derive a 3D rotational offset. Once obtained this rotational offset was applied to all markers such that the new x-axis corresponded to the axis of progression (i.e., PC1), the new y-axis corresponded to the mediolateral axis (i.e., PC2), and the new z-axis corresponded to the vertical axis (i.e., PC3) for each participant/sprint. This allowed for all participants and sprints to be registered to the same 3D coordinate axes prior to further analyses. Once all data were realigned all data were cropped only include 60 m of sprinting. This was done by determining the frame which the x-position of the T8 marker reached 60 m.

Sprint velocity during the 60 m sprint was calculated by first calculating the Euclidean norm of the thoracic marker and then calculating its first derivative. The magnitude and point of the maximal velocity was then identified, which was used to inform the selection of the five cycles used for our analysis. To facilitate the extraction of individual cycles, the local minima of the z-position of the right ankle maker was used. After five separate strides were partitioned,

they were then each time normalized to 101 frames using a polynomial spline function and subsequently de-biased by subtracting the location of the T12 marker (x, y, z) from all 64 markers in the dataset. This was done to ensure that there was no forward progression of the sprinter and thus none of this variability would be detected by the PCA.

After stride segmentation, the five strides about maximal velocity were then ensemble averaged, and subsequently scaled by dividing each participants height and reshaped to a 1 x 19392 (64 markers * 3 axes * 101 data points) vector. The 1 x 19392 vector for each participant (representing an average stride about peak velocity during the fastest sprinting trial) was then used to construct a PCA matrix, where each row represented a participant, and each column represented the time-varying series of the x, y and z position of each marker. The result was a 40 x 19392 data matrix (40 participants * 64 markers * 3 axes * 101 data points) which was used as an input for the PCA (Eq 1).

$$\begin{bmatrix} M1(x,y,z)_{\frac{1}{1}-101} & M2(x,y,z)_{\frac{1}{1}-101} & M3(x,y,z)_{\frac{1}{0}-101} & M4(x,y,z)_{\frac{1}{1}-101} & \dots & M64(x,y,z)_{\frac{1}{1}-101} \\ M1(x,y,z)_{\frac{2}{1}-101} & M2(x,y,z)_{\frac{2}{1}-101} & M3(x,y,z)_{\frac{2}{1}-101} & M4(x,y,z)_{\frac{2}{1}-101} & \dots & M64(x,y,z)_{\frac{2}{1}-101} \\ M1(x,y,z)_{\frac{n}{1}-101} & M2(x,y,z)_{\frac{n}{1}-101} & M3(x,y,z)_{\frac{n}{1}-101} & M4(x,y,z)_{\frac{n}{1}-101} & \dots & M64(x,y,z)_{\frac{n}{1}-101} \end{bmatrix} \quad (1)$$

Raw EMG data were imported into MATLAB (2021b). All EMG data were full wave rectified and low pass filtered using a dual pass 2nd order Butterworth filter with a cut-off of 250 Hz. The filter cut off was determined using a residual analysis (***See Appendix E***) (Winter, 2009). The filtered data were amplitude normalized by averaging the maximum of the three highest peaks in the first 20 m of the sprint. It has been suggested that this technique may be superior over MVIC normalization due to the EMG values being obtained in similar neural condition (i.e.,

dynamic sprinting) as MVICs fail to reflect the neural drive in dynamic high velocity contractions and can create challenges in interpretation (Ball & Scurr, 2012). Following normalization, the analyses of the EMG signals mirrored the approach taken for the kinematic data. Specifically, the normalized EMG data was then partitioned into five cycles and time normalized using a polynomial function to 2000 data points. These cycles were selected about the point of maximal velocity. The data was then reshaped to a 1 x 18000 vector (9 EMG channels * 2000 data points). Each participant's vector was then complied into a 40 x 18000 data matrix which was used as an input for the PCA (Eq 2).

$$\begin{bmatrix} EMG1_{\underline{1}}{}_{1-1000} & EMG2_{\underline{1}}{}_{1-1000} & EMG3_{\underline{1}}{}_{0-1000} & EMG4_{\underline{1}}{}_{1-1000} & \dots & EMG9_{\underline{1}}{}_{1-1000} \\ EMG1_{\underline{2}}{}_{1-1000} & EMG2_{\underline{2}}{}_{1-1000} & EMG3_{\underline{2}}{}_{1-1000} & EMG4_{\underline{2}}{}_{1-1000} & \dots & EMG9_{\underline{2}}{}_{1-1000} \\ EMG1_{\underline{n}}{}_{1-1000} & EMG2_{\underline{n}}{}_{1-1000} & EMG3_{\underline{n}}{}_{1-1000} & EMG4_{\underline{n}}{}_{1-1000} & \dots & EMG9_{\underline{n}}{}_{1-1000} \end{bmatrix} \quad (2)$$

2.3.4 Feature Selection and Regression Analysis

Following the application of the PCA to the kinematic and EMG data matrices, PCs that explain >95% of the variance in the dataset were retained for further analysis. Simple linear regression was performed on the PC scores and maximal sprint velocity (m/s). After it was determined that multiple PCs had moderate-to-weak correlations with sprint velocity, a multivariate linear regression was constructed using stepwise linear regression. Specifically, dependent variables into the kinematic and EMG stepwise regression models included age, sex, height, and the retained PCs. The stepwise linear regression function used both forward and backward stepwise search mode. The stepwise regression had a tolerance criterion of ($p > 0.10$). If the variable added had p-values that exceeded the exit tolerance, then the variable with the

largest p-value was removed. Any PC variables that were determined to be significant contributors to the kinematic and EMG stepwise linear regression model were subsequently reconstructed using multicomponent component reconstruction (MCR), SCR and interpreted using PCA spatial and temporal biplots.

SCR and multicomponent reconstruction (MCR) were used to reconstruct an upper and lower limit that provides insight into functional meaning of our model. SCR provide a functional interpretation of the biomechanical meaning of each PC by representing how each feature is scaled an individual PC (Eq 3 and 4). Following the completion of SCR, it appeared that multiple PCs had an interacting effect. To accommodate these potential interactions, MCR (Eq 5 and 6) to understand how all the PCs included in our stepwise linear regression scaled our features over the gait cycle. This provided us with a more holistic insight into the scaling of features that are represented in our stepwise linear regression models.

$$\hat{x}_U = \bar{x} + u_R * z_{95} \quad (3)$$

$$\hat{x}_L = \bar{x} + u_R * z_{05} \quad (4)$$

$$\hat{x}_U = \bar{x} + u_1 * z_{95} + u_2 * z_{95} + u_3 * z_{95} + \cdots u_n * z_{95} \quad (5)$$

$$\hat{x}_U = \bar{x} + u_1 * z_{95} + u_2 * z_{95} + u_3 * z_{95} + \cdots u_n * z_{95} \quad (6)$$

2.4 Results

The mean peak velocity during the 60 m sprint was 7.94 ± 0.69 m/s (Males = 8.13 ± 0.58, females = 7.24 ± 0.56) (**Figure 10A, 10B, 11A, and 11B**).

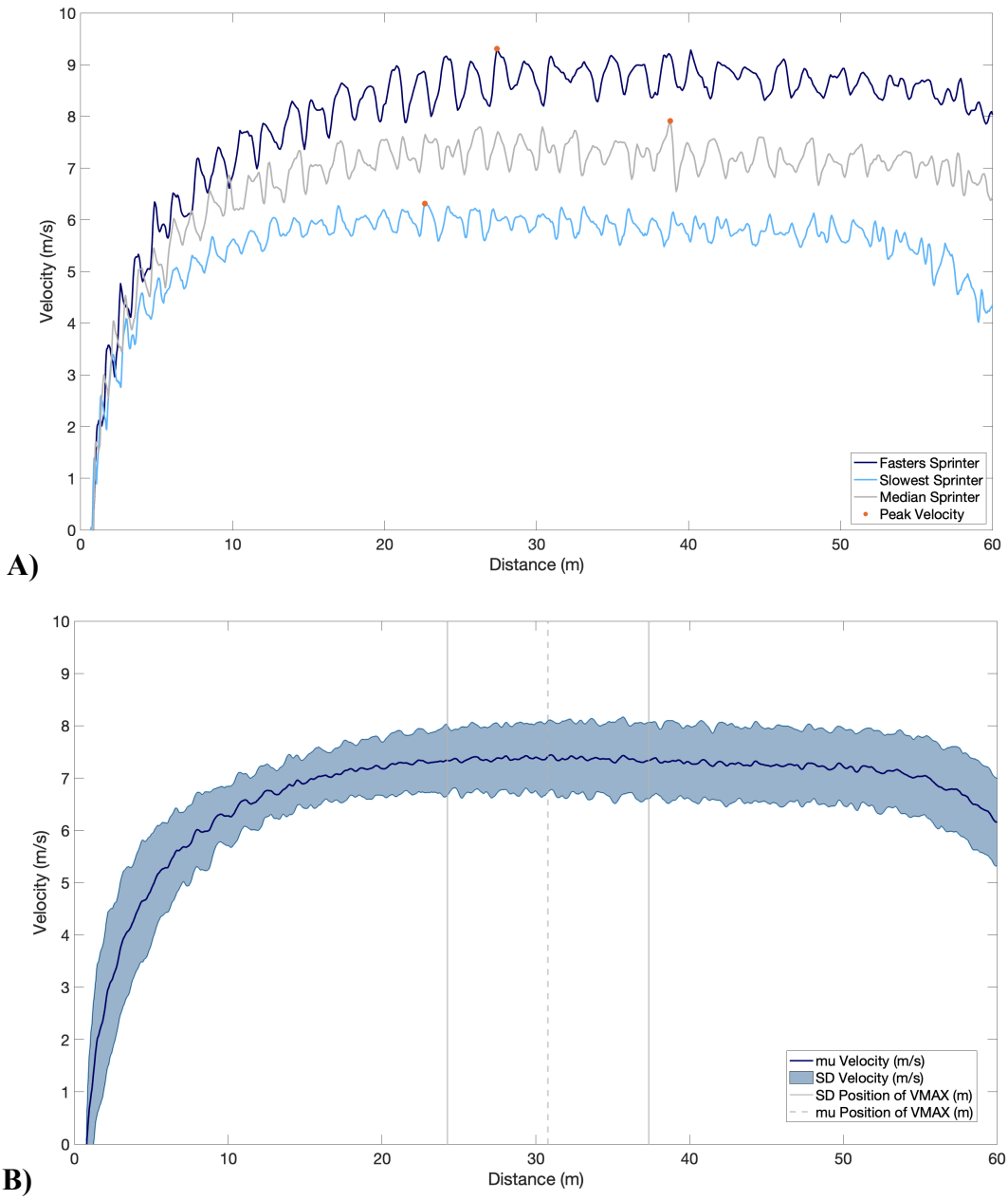

Figure 10. A) Displays the velocity profile of the fastest sprinter (Dark Blue), slowest sprinter (Light Blue) and median sprinter (Grey) for the entire 60 m. Peak velocity is represented by the orange dot on each velocity profile. **B)** Displays the mean and standard deviation velocity profile over the 60 m sprint and the mean and standard deviation of the position of the maximal velocity.

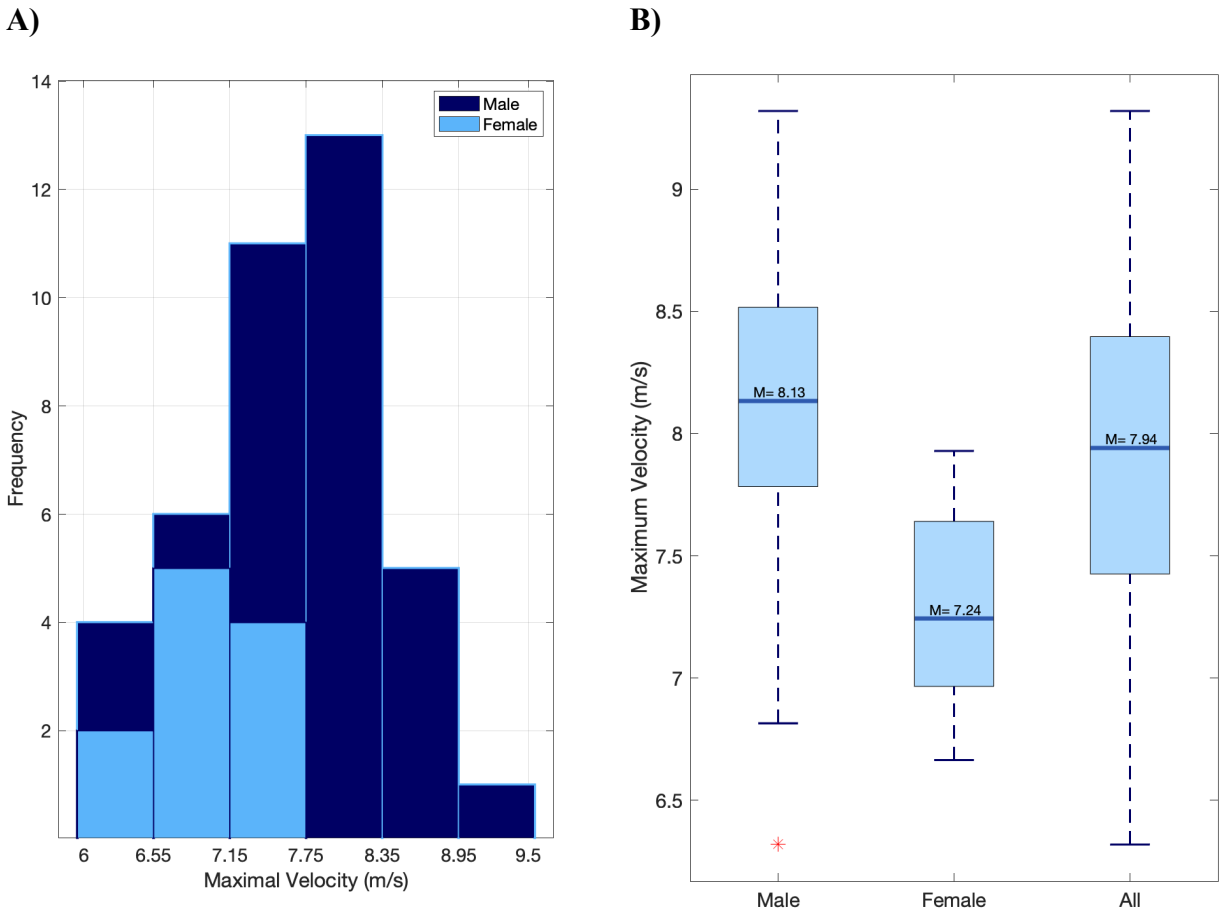

Figure 11. A) Displays the distribution of peak sprint velocities for both males and females. **B)** Displays the mean sprint velocity for male, female, and all participants.

2.4.1 Principal Component Analysis and Linear Regression (Kinematics)

In the assessment of the kinematic data, the first 21 PCs were retained, which explained a collective 95.4% of the total variance in our dataset (**Figure 12A**). Individually, these PCs displayed weak-moderate correlations with maximal sprint velocity (r = 0.02 – 0.55), this suggests that the relationship between movement coordination and sprint velocity may be impacted by a multitude of kinematic variables **(Appendix D**). Stepwise linear regression revealed that PC 1 (p = 0.0002), PC 3 (p = 0.0119), PC 9 (p = 0.0055), PC 11 (p = 0. 0066), PC 12 (p = 0.0772), PC 13 (p = 0.0130), PC 16 (p = 0.00004) and Sex (p =0.0255) were significant

contributors to a multivariate linear model capable of predicting sprint velocity. The linear regression model (Eq 3) displayed a $R^2 = 0.795$ with a root mean squared error (RMSE) = 0.351, P-value = 1.02e-08. A summary of the model can be found in Table 9.

$$Y = PC\ 1 + PC\ 3 + PC\ 9 + PC\ 11 + PC\ 12 + PC\ 13 + PC\ 16 + SEX \quad (3)$$

Table 9. Description of kinematic stepwise linear regression model

Feature	Estimate	SE	t Statistic	p Value
(Intercept)	7.6141	0.13203	57.6	4.1581e-33
PC 1	-0.0002	3.5833e-05	-4.23	0.0002
PC 3	-0.0001	-2.6740	-2.67	0.0119
PC 9	-0.0003	-2.9866	-2.99	0.0055
PC 11	-0.0003	-2.9122	-2.92	0.0066
PC 12	0.0002	0.0001	1.83	0.0772
PC 13	0.0003	0.0001	2.64	0.0130
PC 16	0.0007	0.0002	4.73	4.6579e-05
Sex	0.3877	0.16523	2.35	0.02551

2.4.2 Principal Component Analysis and Linear Regression (Electromyography)

In the assessment of the EMG data, the first 33 PCs were retained, which explained a cumulative 95.7 % of the variance in the EMG data set (**Figure 8B**). Individually, these PCs displayed a weak-moderate linear correlation with sprint velocity (r = 0.01-0.33), as with the kinematic data, this suggested that there are multiple neuromuscular factors that influence peak sprint velocity (**Appendix D**). Stepwise linear regression revealed that PC 1 (p = 0.011), PC 5 (p = 0.019), PC 21 (p=0.016), PC 22 (p=0.105) and Sex (p =0.0001) were significant contributors to predicting sprint velocity. The linear regression model displayed an $R^2 = 0.586$ with a RMSE = 0.444, P-value = 1.64e-05. A summary of this model is presented in **Table 10.**

$$Y = PC\ 1 + PC\ 5 + PC\ 21 + PC\ 22 + SEX \quad (4)$$

Table 10. Description of EMG stepwise linear regression model

Feature	Estimate	SE	t Statistic	p Value
(Intercept)	7.306	0.154	47.306	5.198 e-34
PC 1	-0.0008	0.0002	-3.105	0.0107
PC 5	-0.001	0.0004	-2.873	0.0189
PC 21	-0.0018	0.0007	-2.535	0.016
PC 22	0.002	0.0008	2.709	0.105
Sex	0.703	0.162	4.342	0.0001

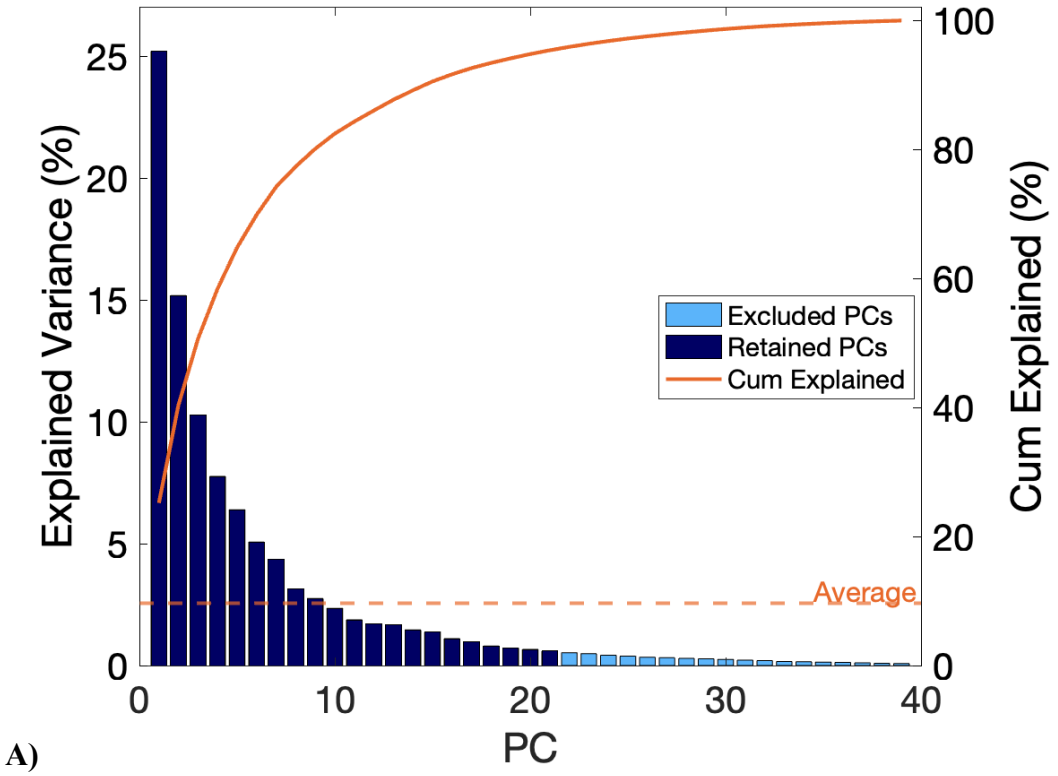

A)

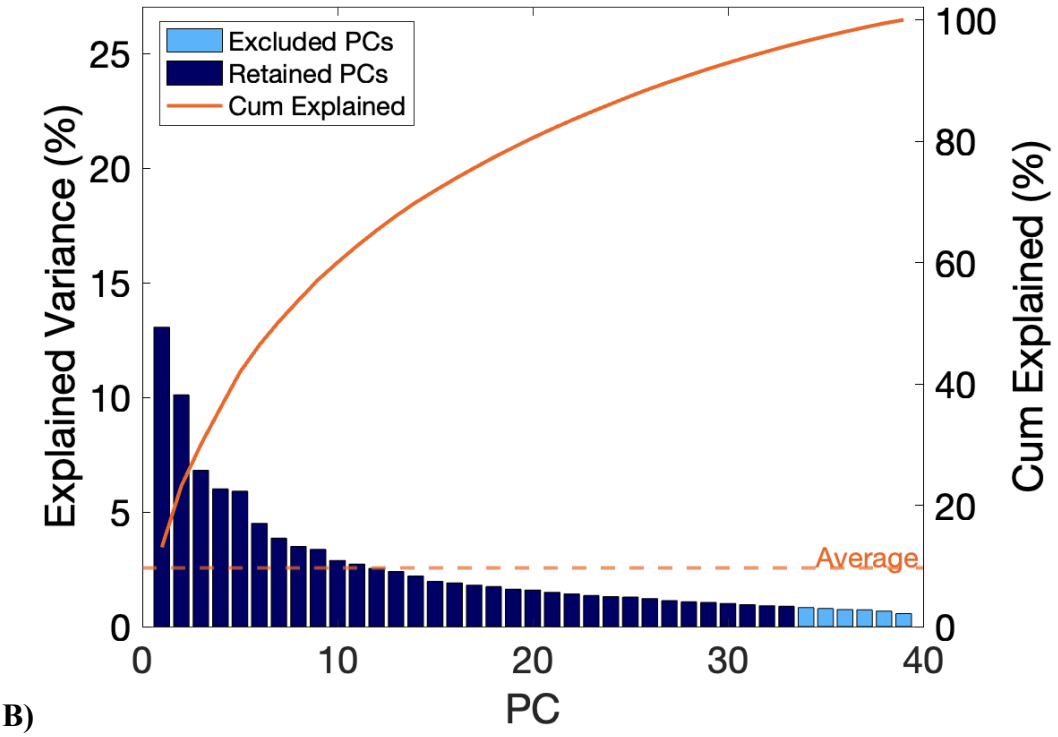

B)

Figure 12. A) Screen Plot for PCs from kinematic PCA, **B)** Scree Plot for PCs from EMG PCA

2.4.3 Functional Interpretation of Kinematic PCs

This section discusses the biomechanical meaning of each of the PC used in the kinematic stepwise linear regression model. Through visual inspection of the PCs using SCR the functional meaning of each PC was determined. Following, the competition of the SCR analysis, it was evident that multiple PCs represented the same kinematic feature (i.e., heel recovery). However, the directionality of the difference between the fast and slow sprinter contradicted one another. For example, PC 1 demonstrated that sprinters with faster sprint velocities were associated with higher heel recovery, but PC 9 demonstrated a lower heel recovery position was indicative of a faster sprint velocity. This suggested that there may be an interaction effect between PCs which influenced the timing and magnitude of the sprint postures. Thus, we used MCR to understand this effect and gain a better representation of our stepwise linear regression model. A summary of the biomechanical meaning each individual PC can be found in **Table 11**, and a detailed analysis can be seen in ***Appendix F***.

Table 11. Summary of PC explained variance and Biomechanical Interpretation

PC	Explained Variance (%)	Biomechanical Interpretation
1	**25.2**	Contra-lateral limb coordination and dynamic trunk extension related to COM projection
3	**10.3**	Lower limb stance leg kinematics associated with height of heel recovery and dynamic trunk extension
9	**2.7**	Transverse plane asymmetry of the lower limb during the swing phase
11	**1.7**	Trunk inclination across the entire gait cycle
12	**1.7**	Transverse plane asymmetry of the lower limb during the swing phase and dynamic trunk extension
16	**1.1**	Mid stance heel width

MCR was completed using PC 1, 3, 9, 11, 12 and 15, together these PCs represent 42.7% of the total variance in our data set **(Table 11).** MCR revealed that faster sprint velocities were generally associated with differences in the timing of the arm swing, a dynamic trunk extension strategy, a faster knee drive and a higher heel recovery **(Figure 13 A-C**). These amongst more subtle differences will be presented in the following section.

During the early stance phase MCR revealed that faster sprint velocity was associated with a higher heel recovery, less deviation in the posture of the head, a smaller stance distance relative to the COM. The joint kinematics of the stance side leg displayed less hip flexion, more dorsiflexion and more hip adduction were associated with faster sprint velocities. Additionally, differences appeared in the timing of the arm swing and onset of trunk rotation. Specifically, it appeared that avatar representing faster sprint velocities demonstrated a leading trunk rotation and arm swing strategy when compared to the slower sprint avatar.

During the mid-stance several different features were identifiable using MCR. The segmental kinematics revealed that a forward leaning shank on the stance side and a foot position in front of the COM were demonstrated by the sprint avatar representing faster sprint velocity. The joint kinematics revealed several differences in the joint angles of the lower and upper extremity. Specifically, the stance side leg demonstrated that a greater degree of plantar flexion, a less flexed knee and a less flexed elbow were present in the avatar that represented faster sprint velocities. Additionally, the faster sprint avatar had swing side kinematics that showed greater hip flexion and shoulder flexion relative to the slower sprint avatar. In addition to the segmental and joint kinematics variation existed in the dynamic behaviour of the trunk. Specifically, the faster sprint avatar begins extending its trunk, this trunk extension continues until the avatar reaches the early swing phase.

MCR reveled differences in the late-stance joint and segmental kinematics between the slow and fast sprint avatars. Notable segmental kinematic features included a more perpendicular shank ankle on the swing side, a more forward leaning shank angle on the stance side, a more upright trunk position, a hand position closer to the midline and greater separation between the right and left upper limb. The joint kinematics also revealed that the faster sprint avatar had stance side kinematics that displayed greater plantarflexion of the ankle, greater flexion of the shoulder and greater internal rotation of the shoulder. On the swing side a less flexed knee, a more flexed shoulder and a more extended elbow was demonstrated by the faster sprint avatar. In addition, distinct differences in the timing of the arm swing and trunk extension strategy can be seen between the faster and slower sprint avatar. Specifically, it appears that dynamic trunk extension and upper swing of the arm is timed to aid in the propulsion of the sprinter into the flight phase of the sprint.

During the early swing phase, it was revelated that several kinematic features varied between the slow and fast sprint avatar. Specifically, the segmental kinematics of the faster sprint avatar demonstrated a swing side foot position further in front of the COM, a more parallel shank segment on the stance side and a head more in line with the midline of the body. The joint kinematics of the faster sprint avatar showed that the stance side leg had greater knee flexion and a more externally rotated hip and on the wing side it had a less flexed knee and hip when compared to the slower sprint avatar.

MCR revelated that during the late wing phase the avatar that represented a faster sprint velocity demonstrated key differences in the segmental and joint kinematics. Specifically, the segmental kinematics revealed that the faster sprint avatar had a stance side foot position closer to the COM, a narrower stance width and a swing side shank angle more parallel to the ground.

The joint kinematics revealed that the faster sprint avatar demonstrated a more flexed knee on the swing side and a less flexed knee and more extended hip on the stance side leg.

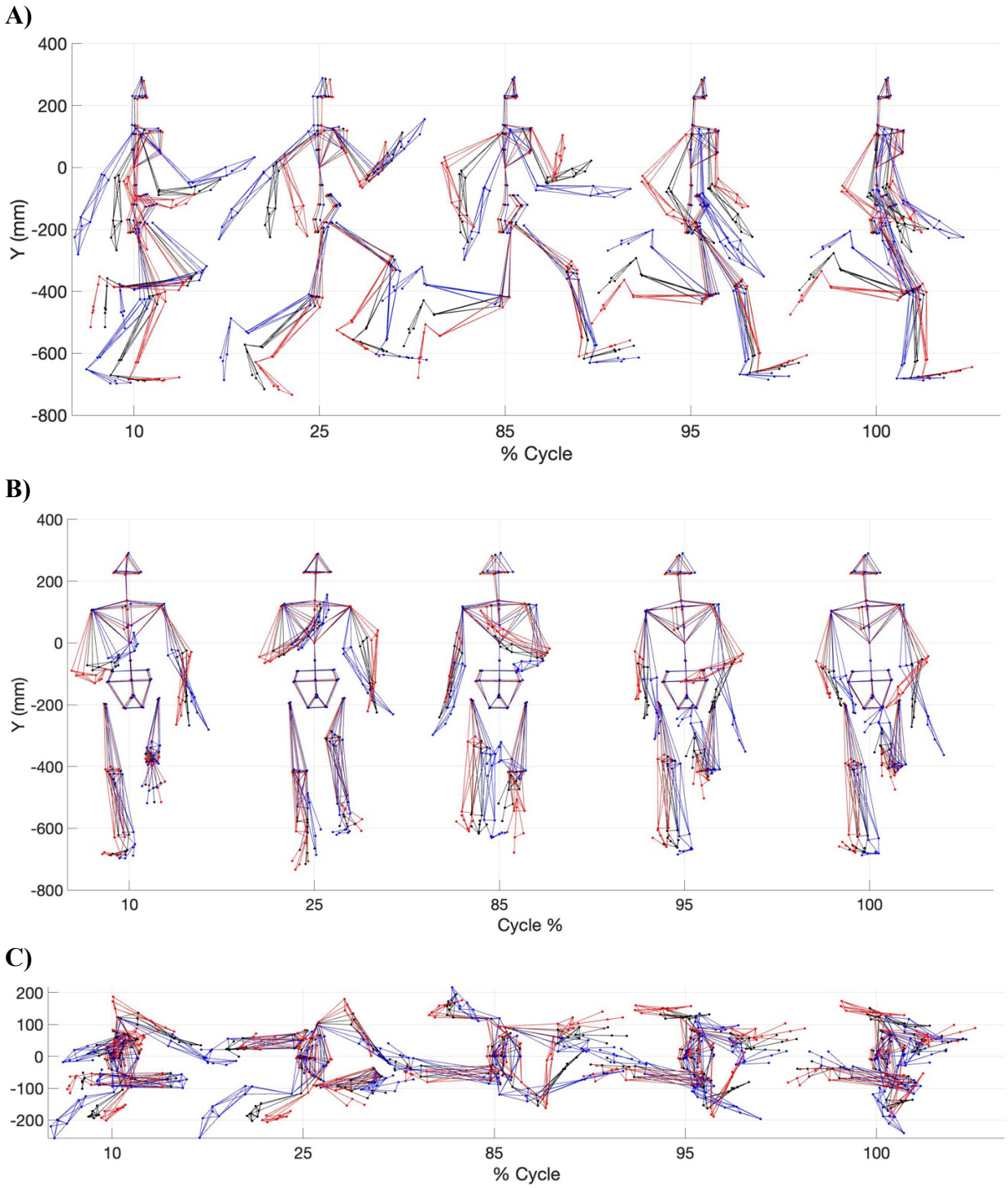

Figure 13. MCR for PC 1, 3, 9, 11, 12 and 6 **A**) Sagittal plane view **B)** Frontal plane view **C**) Transverse plane view. The red avatar represents the 5th percentile (slow), black represents the mean and blue represents the 95th percentile (fast)

2.4.4 Interpretation of Electromyography PCs

This section interprets the biomechanical meaning of each PC used in the EMG stepwise linear regression model. SCR and MCR was used to reconstruct the data from the PCA and interpret its biomechanical meaning. SCR was used to interpret the biomechanical meaning of each PC. However, like the kinematic data the directionality of the effect each PC had on the waveform contradicted each other. For example, the reconstruction of GMAX showed that faster sprint velocities were associated with less glute activation between 50-100% of the gait cycle however PC 5 demonstrated that more glute activation at the same point in the gait cycle was associated with faster sprint velocities. To understand the interaction of these PCs and better interpret our stepwise linear regression model we used MCR. A summary of the biomechanical meaning of each PC can be seen in **Table 12,** a detailed description can be seen in the ***Appendix G***.

Table 12. Summary of PC explained variance and Biomechanical Interpretation

PC	Explained Variance (%)	Biomechanical Interpretation
1	13.1	Phase shift feature for the musculature of the posterior chain. Magnitude scaler for EO Difference feature for VLO and RF
5	5.9%	Difference features for the GAS, GMED, LD, EO, VLO, RF and GMAX
21	1.5%	No biomechanical meaning
22	1.4%	No biomechanical meaning

MCR was completed using PC 1, 5, 21 and 22 together these PCs represented 21.9% of the total variance in our data set **(Table 12).** MCR revelated that PCs scaled the GAS, GMAX, LD, EO,

VLO and RF as a difference feature **(Figure 14)** While LES and BF displayed phase shift features and GMED displayed a magnitude scaler. GAS displayed greater magnitudes of activation prior to touch down and during stance. GMAX had greater activation during stance phase and less during stance phase. LD had less activation during the stance phase and greater activation during the stance phase. EO had greater activation throughout the entire gait cycle. VLO had less activation during the early stance phase and greater activation during the swing phase. RF had less activation during the early swing phase. LES operated in an anti-phase manor relative to the slow sprinter, with more activation during the stance phase and late swing phase. BF had more activation during the late stance and early swing phases. GMED had greater activation during the 20-100% of the gait cycle.

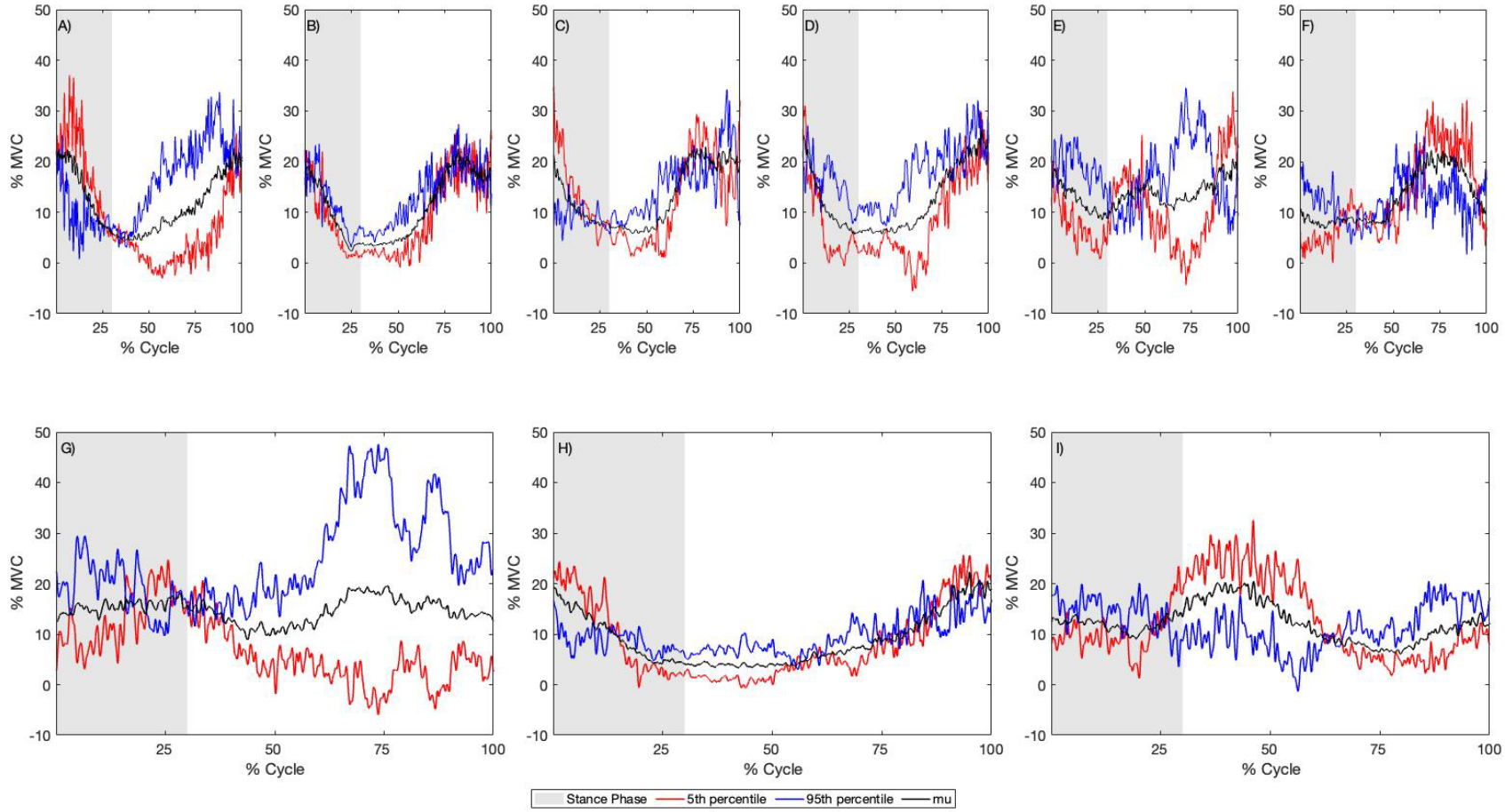

Figure 14. MCR for PC 1, 5, 21 and 22 for **A**) GAS, **B)** BF, **C)** GMAX, **D)** GMED, **E)** LES, **F)** LD, **G)** EO, **H)** VLO, **I)** RF. Blue represents the 95%tile sprinter (fast), Red represents the 5%tile sprinter (slow), and grey represents the stance phase.

2.5 Discussion

This study aimed to leverage advancements in wearable sensors and data science to identify key neuromuscular and kinematic determinants of peak sprint velocity in a large group of university aged athletes. After collecting full-body kinematics and 9 channels of EMG on a large non-homogenous group (n = 40) of sprint-based athletes, PCA was conducted on the kinematic and EMG data separately to identify key modes of variation associated with faster peak sprint velocities. Specifically, stepwise linear regression was used to find a correlation between the PCs, demographic variables including height, age and biological sex and peak sprint velocity obtained during the 60 m sprint. Significant multivariable regression models were generated for both kinematic and EMG features identified using PCA. In contrast to the kinematic data, the stochastic nature of EMG signal resulted in the inclusion of far more PCs to explain >95% of the variance in the data set. This partially contributed to the kinematic model outperforming model as the kinematic model displayed a higher R^2 value, and therefore a better ability to predict sprint performance from PCA-derived features. This suggests that the kinematic data set used in this thesis is a better predictor of sprint performance when compared to the EMG dataset.

The kinematic data set may have outperformed the EMG data set for several reasons. 1) the kinematic data set more information compared to the EMG dataset. For example, the kinematic dataset contained information regarding the whole-body, while the EMG data set only contained information regarding 9 muscles of the body. 2) Dynamic EMG has several limitations due to the biophysics of the signal. For instance, the sensor is attached to the muscle, which displays viscoelastic properties and during high velocity dynamic movements this can result in inconsistent signal pick up volumes and motion artifact. These methodological limitations can

induce non-physiologically significant variance which could make the EMG signal more stochastic, which may decrease the predictive power of the data set. 3) The human movement system is a complex system with many different subcomponents, EMG provides information on the neuromuscular activity of a muscle, however this is only one subsystem that influences sprint performance. Specifically, sEMG signals do not capture any potential contributions from passive tissues (i.e., thoracolumbar fascia) which may affect the performance of a sprinter. In contrast, kinematic data represent human movement on a macroscopic level, which allows for the behaviour of all sub-systems (i.e., passive, active, neural) to be analyzed. This may allow for kinematic data to be better predict sprint velocity since the data collected is the macroscopic behaviour of the system. Despite these limitations, the EMG model resulted in a significant model and can provide valuable information regarding the neuromuscular determinants of sprint velocity. Future work with this data should be focused on deriving more functional meaning from the EMG data set, such as calculating muscle synergy and co-contraction indices to better understand differences associated with faster sprint velocity.

A common challenge in the use of PCA, is identifying the biomechanical meaning of PCs. Previous work in this area has used SCR to infer the biomechanical meaning of a PC (Brandon et al., 2013; Ross et al., 2018a). For example, using SCR we're able to identify the variation in the behavior of the waveform by plotting the mean, 95 percentile and 5 percentile PC score. In our study, we constructed a movement avatar which allowed for us to understand that PC 1 represented inter-limb coordination associated with the projection of the COM. The challenge with this is we only identify the meaning of one PC. This is a large limitation in this type of analysis as it is thought that coordination of human movement is highly intricate and co-dependent in nature (Kelso, 1999). This means that orthogonal modes of variation represented in

a PC could contain information that influences the timing and magnitude of a feature when used in a multivariate model. When analyzing our SCR, it appeared that this in fact occurred in our data set, as PC 1 represented a higher heel recovery and PC 9 represented a lower heel recovery despite both being correlated with sprint velocity. As a result, we decided to utilize MCR which reconstructed the sprint avatar and EMG waveform using all PCs included in the stepwise linear regression. This allowed for us to interpret the meaning of the multivariate linear regression model, which is likely to more accurately represent the key kinematic and neuromuscular features associated with sprint velocity. From this we were able to identify a variety of kinematic and neuromuscular features that were associated with faster sprint velocities. Some of the kinematic features included a dynamic trunk extension strategy, higher heel recovery and differences in the coordination of the contralateral limbs. While the EMG features demonstrated that faster sprint velocities were associated with a later peak activation of the LES, greater BF and GAS activation during the swing phase. MCR appeared to perform well for the kinematic data set, however the several muscles from the EMG data set appeared to suffer from reconstruction artifact. For instance, the EO displays negative activation values, despite this being impossible from the prepressing steps taken prior to input of the sEMG signal into the PCA matrix. We believe that this is likely due to reconstructing a high-dimensional data set with such few PCs.

2.5.1 Kinematic Indicators of Sprint Performance

The kinematic model used seven PCs as significant contributors to the stepwise linear regression model. The PC selected showed that a variety of kinematic features had significant correlations with peak sprint velocities. Generally, these kinematic features resulted in differences in the timing and magnitude of movement expressed by the upper and lower body.

Many of these features have been identified previously in the literature as being associated with maximal sprint velocity. For example, previous segmental kinematics which have been associated with faster sprint velocities include (1) smaller horizontal distance between the knees at foot strike, (2) a more perpendicular stance side thigh during early stance (Yada et al., 2011), (3) a stance foot closer to the COM during mid-stance (Hunter et al., 2004, 2005; Yada et al., 2011) , and (4) a more upright trunk at midstance (Sides, 2015). Additionally, joint kinematics associated with faster sprint velocity include (1) less knee flexion during early to late stance in the stance side leg (Bushnell & Hunter, 2007; Yada et al., 2011) and (2) greater knee flexion of the swing side leg during mid-stance (Bushnell & Hunter, 2007). These findings were all supported by our MCR. This supports the utility of using a data driven approach to identify key kinematic features that are associated with faster sprint velocity. However, the distinct benefit of using a data driven approach is the ability to holistically evaluate sport technique. For instance, our data-driven technique identified several features that to our knowledge had not been previously reported in the literature. Specifically, we identified that differences in the contralateral limb coordination, trunk control strategy and arm swing were features present with the faster sprint avatar. This demonstrates the utility of a data-driven approach in reducing bias in the analysis of sprint technique as these features demonstrated in the upper body have largely been neglected in the previous 100 years of biomechanical analysis of sprint technique (Fenn, 1930).

An interesting finding in our study is the differences that occurred in the timing and sequencing of the arm swing. PC 1 and 3 represented differences in the timing and sequencing of the arm swing. Specifically, PC 1 appeared to represent variation in the timing of the arm swing that was associated with the contralateral lower limb, while PC 3 represented differences in the

range of motion of the arm swing. These differences in PC 1 and PC 3 also manifested themselves in the MCR. The MCR demonstrated showed that faster sprinters timed the upward swing of their arm closer to toe off. This may be beneficial in projecting the COM and generating greater flight time, which could impact stride length and ultimately sprint velocity. Although, the arm swing is not well understood, several studies have shown that the arm swing may be important in the generation greater vertical impulse (Hinrichs et al., 1987), stride length (Bhowmick & Bhattacharyya, 1988) and of horizontal velocity (Bhowmick & Bhattacharyya, 1988). Further, empirical evidence suggest that the arm-swing is important in generating sprint velocity as several studies have demonstrated a reduction in sprint velocity when the arm-swing motion is constrained (Grant et al., 2003; Wdowski & Gittoes, 2013). More work is required to better understand the impact of the arm-swing on sprint performance. Specifically, understanding how differences in the coordination between the lower limb and upper limb arm swing have on previously studied biomechanical variable such as stride length, stride rate, ground contact times, flight time and ground reaction force (GRF) in addition to sprint velocity.

Previous findings have found that a wider stance width associated with faster sprint velocities as it was shown to also be associated with greater propulsive impulses (Nagahara et al., 2017). However, in our study, it was seen that the faster sprint avatar had a narrower stance width. Interestingly, it appeared despite the narrower stance width the faster sprinter avatar had less range of motion of the hip in the frontal plane during the stance phase. This could be explained by the greater GMAX and GMED activation seen in our EMG results. The greater activation of this musculature could allow for the faster sprint avatar to maintain a relatively isometric frontal plane hip which could allow for greater force to be transferred in the anterior-posterior direction which could facilitate faster sprint velocities. While alternatively, the slower

sprint avatar may have greater range of motion in the frontal plane during ground contact due to weaker hip abductors relative the adductors which can result in the medial translation of the thigh segment (Kulmala et al., 2017). This could result in less force being available to transition in the anterior-posterior direction which could facilitate a slower sprint velocity. Further research is required to understand the importance of frontal plane kinematics and step width. Specifically, future work should aim to understand if different neuromuscular control strategies and anthropometrics influence the need for a wider stance width to achieve a faster sprint velocity.

PCs 9 and 12 represented postural asymmetries of the lower swing side lower limb during the mid and mid-late stance phases. While much uncertainty surrounds asymmetry in regards to its effect on injury risk and performance (Bishop et al., 2018). It is widely agreed that asymmetries do exist in sprinting; however, the functional significance of such asymmetries is still up for debate. Several studies have displayed that no correlation between lower limb asymmetries exist between injury and performance (Bissas et al., 2022; Haugen et al., 2018). Although some have suggest that perhaps they serve as a compensatory mechanism to anthropometric discrepancies (Vagenas & Hoshizaki, 1991), chronic strength weakness or imbalances in range of motion (Bezodis et al., 2018). Nevertheless, asymmetry was present in our model of sprint velocity in PCs 9 and 12, which collectively explained 4.4% of the variation in our dataset. Further exploration into the functionality of asymmetry in sprinting is needed determine whether these PCs are simply a by-product of the methodology and participant pool analyzed here, or if these phenomena have potential clinical or functional significance.

Several PCs represented variation of the coordination of the trunk. Specifically, PCs 1, 3 and 12 captured represented trunk extension during the transition from late stance to early swing. While lower limb kinematics are well studied in sprinting, those of the spine and trunk are poorly

understood. To our knowledge, only one study has explored the kinematics of the trunk during sprinting. The results of Nagahara and colleagues (2018) demonstrated that a smaller inclination of the thorax was associated with greater increase in running speed. Despite this, the methodologies used in this study limited the spatial-temporal resolution which limit their ability to identify coordinative features that varied over time. The findings derived from our data-driven analyses provide new understanding into the role the trunk may play in sprint performance. Specifically, it appears that a dynamic trunk extension strategy is associated with faster sprint velocity. From our interpretation of the data, it appears that the timing of this trunk extension is used to aid the sprinter in generating propulsive forces. Future work should aim to identify whether spatial-temporal coordination difference exist in slow vs fast sprinters and whether differences in the trunk kinematics result in any improvements in biomechanically relevant phenomenon such as increases in ground reaction force, step length, and flight time.

2.5.2 Electromyographic Indicators of Sprint Performance

Four PCs were used as significant contributors to the EMG stepwise linear regression model. However, two of these PCs (PCs 21 and 22) appeared to represent noise or some other non-physiological phenomenon.

PC 1 displayed a systematic phase shift feature in the posterior muscles that attach to the thoraco-lumbar fascia. This systematic shift in the activation of the posterior musculature to later in the gait cycle may serve to maximize the acceleration of the lower leg during touch-down. Previous, work by Clark and colleagues (2020) has shown that the angular kinematics of the thigh and ankle are closely related. This close relationship was proposed to be advantageous because the velocity gained from the hip was transferred to the shank at impact. This increase in the foots velocity at touch down can be advantageous as it has been shown to create a larger

vertical ground reaction force (Clark et al., 2020), which has been demonstrated to be differentiator between sprinters and non-sprinters (Weyand et al., 2000). To our knowledge, this is the first study to evaluate the impact the muscles that attach to the thoracolumbar fascia have on sprint performance. These preliminary findings along with a strong theoretical foundation warrant further exploration into the role the coordination of these muscles have on sprint performance. Specifically, future studies should aim to understand the significance of this pattern by these muscles through muscle force modelling, synergist analysis, and co-contraction indices in addition to the SCR and MCR analyses implemented here.

2.5.3 Development of a Data-Driven Training Tool using Multi-Component Reconstruction

One of the principal strengths of methodological approaches taken in this thesis is to use a data-driven approach to identify key performance indicators in sprint performance. To this point individual contributors (i.e., principal components) have been interpreted in isolation using methods of SCR and MCR (i.e., Brandon et al., 2013). Given the potentially interacting nature of the multiple features identified in each stepwise linear regression model it is possible that a MCR approach can be taken using all significant predictors to generate representative depictions of the kinematic and electromyographic data of those tending to have relatively faster or relatively slower peak sprint velocities. This approach has the capacity to create visual animations or avatars which can be used to depict strategies one may take to enhance sprint performance, and could be used in an enhanced, data-driven coaching framework. Examples of the MCR derived from the kinematic and EMG data are depicted in Figures 13 and 14 respectively.

Although the differences identified in the kinematic and EMG data set using a data-driven method appeared to be well represented in the biomechanical literature, several methodological concerns do exist. For instance, our primary concern with the method used in

this thesis is the presentation of negative muscle activation values for several muscles. This occurred despite all EMG waveforms having positive activation values prior to being input into the PCA. We have attributed this error as artifact from the reconstruction process. As such, future work should investigate various methodologies to reconstruct multiple PCs. This will be useful in the pursuit of a more objective understanding of human movement, as MCR greatly enhances the interpretability of PCA-based movement pattern recognition frameworks.

2.5.4 Limitations

Although the approaches taken with this research have some fundamental strengths, they also do have some limitations worth addressing. A key limitation is the use of wearable technology which does not provide gold-standard kinematic data. Although validation studies have shown good agreement between the XSENS Awinda IMU suit and optical motion capture systems (Schepers et al., 2018), the sensors used in this study are subject to factors such as ferromagnetic interference and drift. Our selection of wearable sensors was selected based on several reasons. For one, it allowed for use to assess whether the data provided from wearable sensors was sensitive to identify differences in skill levels. Second, we wanted to capture a large distance of overground sprinting so that we could evaluate a sprinters coordination near maximal velocity. This would have not been feasible using the optical motion capture system available to the research team. To accommodate errors derived from the use of wearable IMU sensors many technical steps were taken to correct our data (i.e., drift reduction); however, it is possible that these technical treatments of our data were insufficient, and instrumentation noise may still exist in our dataset.

A second limitation may include the feature selection strategy used for this analysis. Specifically, we decided to retain many PCs, so that we could capture a variety of modes of

variation that explained sprint performance. There is the possibility that by doing this we may have biased our stepwise linear regression towards PC features which represent biomechanically or physiologically irrelevant phenomena (i.e., noise). Future work in PCA should focus on more objective PC selection criteria based on heuristics and statistical based selection criteria to ensure greater certainty that the appropriate dimensionality of the data is selected.

Finally, due to the time and scope of this master's thesis the sample size was limited to 40 participants, 13 female and 27 males. This sampling approach yielded an imbalanced dataset of males and females, with the majority of females falling below the mean peak sprint velocity in our dataset. Additionally, the sample size of 40 limits our ability to apply more advanced machine learning algorithms to our data set which include unsupervised approaches such as clustering. As a result, we've constructed an "ideal" model of sprint velocity that provides a one-size fits all approach, while treating males and females equally in our statistical models. This is unlikely the most optimal technique for every sprinter to adapt as it is likely a wide variety of optimal technique exists based on differences in anthropometric, skill and internal physiology. This is an area for future work which would aim to identify fundamental sprinting phenotypes using clustering algorithms which would likely segment the strategies taken by males and females.

CHAPTER III – SUMMARY, CONCLUSION AND FUTURE DIRECTIONS

3.1 Summary of Thesis Findings

Sprint performance is a multifactorial skill that is dependent on a variety of kinematic, neuromuscular, and kinetic features. Sprinting is a well-studied area of the sport biomechanics literature. However, there has traditionally been a theoretical bias to understand the role the lower extremity plays in sprint performance, while neglecting the upper body. This despite strong theoretical evidence that the upper body may play an important role in sprinting. To supplement the previous research studies the goal of this thesis was to leverage advancements in data science and wearable technology to use a data-driven approach to objectively identify key coordinative features that were associated with sprint velocity.

To accomplish our goal, we recruited a large group of university aged athletes to complete three maximal 60 m sprints during which we concurrently collected full body kinematics and nine channels of EMG. Using a PCA based framework we produced two significant stepwise linear regression models (kinematic and EMG), with the kinematic model outperforming the EMG demonstrated by a higher r^2 value (0.795 vs 0.586). From these models we were able to identify several features that were associated with faster sprint velocity, not previously reported in the sprint biomechanics literature. These include differences in the contralateral coordination of the upper arm and lower leg, a dynamic trunk extension strategy, asymmetry between the legs during swing and differences in the arm swing mechanics. These findings suggest that the coordination between the upper and lower body may play a greater role in sprint performance than previous thought. As such, the lower body kinematics are not sufficient to explain differences in sprint velocity between individuals.

3.2 Conclusion and Future Direction

Data-science and wearable technology is an emerging area in biomechanics and sport performance. This study demonstrated the utility of a data-driven approach to identify key kinematic and EMG features in a large dataset which included whole-body kinematics and 9-channels of EMG. To our knowledge this is one of the few studies that directly linked a specific whole-body coordinative strategy to an objective performance outcome. This framework can serve as the foundation to bridge the gap between biomechanists and sport coaches. As we have successfully created an objective framework that can be used to inform adjustments in sport technique by a coach to improve a specific outcome of a movement (i.e., sprint velocity).

The work presented here is a promising step towards a more objective evaluation of sprint technique several key limitations do need to be addressed to increase the utility of this framework. We were successful in defining one "optimal" sprint technique to achieve higher sprint velocities, but it is likely that more than one sprint technique is associated with faster sprint velocities. Future work will look to identify different movement phenotypes that may have different ways of achieving faster peak sprint velocities. The end goal of this work will be to develop a data-driven coaching software which helps clinicians and coaches benchmark and address errors in neuromechanical coordination that limit an individual's performance. This will be the first application available on the market that truly provides objective information on an athlete's coordination. Which can have large implications on rehabilitation and performance training programs for athletes of all skill levels.

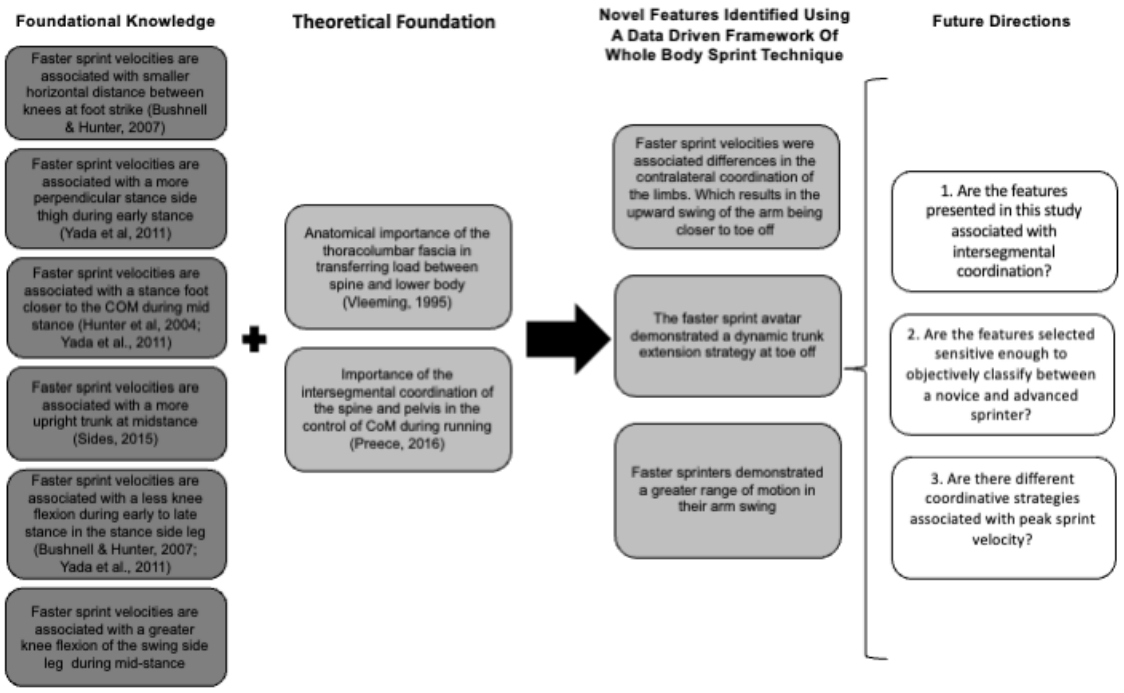

Figure 15. Extracted knowledge and future directions building the work presented in this thesis.

REFERENCES

Astephen, J. L., & Deluzio, K. J. (2004). A multivariate gait data analysis technique: Application to knee osteoarthritis. *Proceedings of the Institution of Mechanical Engineers. Part H, Journal of Engineering in Medicine*, *218*(4), 271–279. https://doi.org/10.1243/0954411041560983

Ball, N., & Scurr, J. (2012). Electromyography Normalization Methods for High-Velocity Muscle Actions: Review and Recommendations. *Journal of Applied Biomechanics*. https://doi.org/10.1123/jab.29.5.600

Barre, A., & Armand, S. (2014). Biomechanical ToolKit: Open-source framework to visualize and process biomechanical data. *Computer Methods and Programs in Biomedicine*, *114*(1), 80–87. https://doi.org/10.1016/j.cmpb.2014.01.012

Beange, K. H. E., Chan, A. D. C., Beaudette, S. M., & Graham, R. B. (2019). Concurrent validity of a wearable IMU for objective assessments of functional movement quality and control of the lumbar spine. *Journal of Biomechanics*, *97*, 109356. https://doi.org/10.1016/j.jbiomech.2019.109356

Bergamini, E., Picerno, P., Pillet, H., Natta, F., Thoreux, P., & Camomilla, V. (2012). Estimation of temporal parameters during sprint running using a trunk-mounted inertial measurement unit. *Journal of Biomechanics*, *45*(6), 1123–1126. https://doi.org/10.1016/j.jbiomech.2011.12.020

Bezodis, I. N., Kerwin, D. G., Cooper, S.-M., & Salo, A. I. T. (2018). Sprint Running Performance and Technique Changes in Athletes During Periodized Training: An Elite Training Group

Case Study. *International Journal of Sports Physiology and Performance*, *13*(6), 755–762. https://doi.org/10.1123/ijspp.2017-0378

Bhowmick, S., & Bhattacharyya, A. K. (1988). Kinematic analysis of arm movements in sprint start. *The Journal of Sports Medicine and Physical Fitness*, *28*(4), 315–323.

Bishop, C., Turner, A., & Read, P. (2018). Effects of inter-limb asymmetries on physical and sports performance: A systematic review. *Journal of Sports Sciences*, *36*(10), 1135–1144. https://doi.org/10.1080/02640414.2017.1361894

Bissas, A., Walker, J., Paradisis, G. P., Hanley, B., Tucker, C. B., Jongerius, N., Thomas, A., Merlino, S., Vazel, P.-J., & Girard, O. (2022). Asymmetry in sprinting: An insight into sub-10 and sub-11 s men and women sprinters. *Scandinavian Journal of Medicine & Science in Sports*, *32*(1), 69–82. https://doi.org/10.1111/sms.14068

Brandon, S. C. E., Graham, R. B., Almosnino, S., Sadler, E. M., Stevenson, J. M., & Deluzio, K. J. (2013). Interpreting principal components in biomechanics: Representative extremes and single component reconstruction. *Journal of Electromyography and Kinesiology*, *23*(6), 1304–1310. https://doi.org/10.1016/j.jelekin.2013.09.010

Bushnell, T., & Hunter, I. (2007). Differences in technique between sprinters and distance runners at equal and maximal speeds. *Sports Biomechanics*, *6*(3), 261–268. https://doi.org/10.1080/14763140701489728

Cazzola, D., Pavei, G., & Preatoni, E. (2016). Can coordination variability identify performance factors and skill level in competitive sport? The case of race walking. *Journal of Sport and Health Science*, *5*(1), 35–43. https://doi.org/10.1016/j.jshs.2015.11.005

Chumanov, E. S., Heiderscheit, B. C., & Thelen, D. G. (2007). The effect of speed and influence of individual muscles on hamstring mechanics during the swing phase of sprinting. *Journal of Biomechanics*, *40*(16), 3555–3562. https://doi.org/10.1016/j.jbiomech.2007.05.026

Clark, K. P., Meng, C. R., & Stearne, D. J. (2020). 'Whip from the hip': Thigh angular motion, ground contact mechanics, and running speed. *Biology Open*, *9*. https://doi.org/10.1242/bio.053546

Coh, M., Babic, V., & Maćkała, K. (2010). Biomechanical, Neuro-muscular and Methodical Aspects of Running Speed Development. *Journal of Human Kinetics*, *26*, 73–81. https://doi.org/10.2478/v10078-010-0051-0

de Ruiter, C. J., & van Dieën, J. H. (2019). Stride and Step Length Obtained with Inertial Measurement Units during Maximal Sprint Acceleration. *Sports*, *7*(9). https://doi.org/10.3390/sports7090202

Debaere, S., Delecluse, C., Aerenhouts, D., Hagman, F., & Jonkers, I. (2013). From block clearance to sprint running: Characteristics underlying an effective transition. *Journal of Sports Sciences*, *31*(2), 137–149. https://doi.org/10.1080/02640414.2012.722225

Debaere, S., Jonkers, I., & Delecluse, C. (2013). The Contribution of Step Characteristics to Sprint Running Performance in High-Level Male and Female Athletes: *Journal of Strength and Conditioning Research*, *27*(1), 116–124. https://doi.org/10.1519/JSC.0b013e31825183ef

Dorn, T. W., Schache, A. G., & Pandy, M. G. (2012). Muscular strategy shift in human running: Dependence of running speed on hip and ankle muscle performance. *Journal of Experimental Biology*, *215*(11), 1944–1956. https://doi.org/10.1242/jeb.064527

Federolf, P., Reid, R., Gilgien, M., Haugen, P., & Smith, G. (2014). The application of principal component analysis to quantify technique in sports. *Scandinavian Journal of Medicine & Science in Sports*, *24*(3), 491–499. https://doi.org/10.1111/j.1600-0838.2012.01455.x

Fenn, W. (1930). A cinematographic study of sprinters. *Sci.Monthly*, *93*, 433–462.

Glazier, P. S. (2021). Beyond animated skeletons: How can biomechanical feedback be used to enhance sports performance?11Animated skeletons—popularised by a proprietary general-purpose biomechanics modelling and analysis software package—have now largely superseded the humble stickman that has been integral to biomechanical feedback provision for the past few decades. Despite holding great appeal and captivating many an athlete and coach, these visualisations have limited utility in a feedback capacity, especially if presented in isolation, as is often the case. *Journal of Biomechanics*, *129*, 110686. https://doi.org/10.1016/j.jbiomech.2021.110686

Gløersen, Ø., Myklebust, H., Hallén, J., & Federolf, P. (2018). Technique analysis in elite athletes using principal component analysis. *Journal of Sports Sciences*, *36*(2), 229–237. https://doi.org/10.1080/02640414.2017.1298826

Golubitsky, M., Stewart, I., Buono, P. L., & Collins, J. J. (1999). Symmetry in locomotor central pattern generators and animal gaits. *Nature*, *401*(6754), 693–695. https://doi.org/10.1038/44416

Gracovetsky, S. (1985). An hypothesis for the role of the spine in human locomotion: A challenge to current thinking. *Journal of Biomedical Engineering*, *7*(3), 205–216. https://doi.org/10.1016/0141-5425(85)90021-4

Gracovetsky, S., & Farfan, H. (1986). The optimum spine. *Spine*, *11*(6), 543–573. https://doi.org/10.1097/00007632-198607000-00006

Grant, S., Oommen, G., McColl, G., Taylor, J., Watkins, L., Friel, N., Watt, I., & McLean, D. (2003). The effect of ball carrying method on sprint speed in rugby union football players. *Journal of Sports Sciences*, *21*(12), 1009–1015. https://doi.org/10.1080/0264041031000140671

Gurchiek, R. D., McGinnis, R. S., Needle, A. R., McBride, J. M., & van Werkhoven, H. (2018). An adaptive filtering algorithm to estimate sprint velocity using a single inertial sensor. *Sports Engineering*, *21*(4), 389–399. https://doi.org/10.1007/s12283-018-0285-y

Hamill, J., Palmer, C., & Van Emmerik, R. E. A. (2012). Coordinative variability and overuse injury. *Sports Medicine, Arthroscopy, Rehabilitation, Therapy & Technology: SMARTT*, *4*, 45. https://doi.org/10.1186/1758-2555-4-45

Haugen, T., Danielsen, J., McGhie, D., Sandbakk, Ø., & Ettema, G. (2018). Kinematic stride cycle asymmetry is not associated with sprint performance and injury prevalence in athletic sprinters. *Scandinavian Journal of Medicine & Science in Sports*, *28*, 1001–1008. https://doi.org/10.1111/sms.12953

Higashihara, A., Ono, T., Kubota, J., Okuwaki, T., & Fukubayashi, T. (2010). Functional differences in the activity of the hamstring muscles with increasing running speed. *Journal of Sports Sciences*, *28*(10), 1085–1092. https://doi.org/10.1080/02640414.2010.494308

Hinrichs, R. N., Cavanagh, P. R., & Williams, K. R. (1987). Upper Extremity Function in Running. I: Center of Mass and Propulsion Considerations. *Journal of Applied Biomechanics*, *3*(3), 222–241. https://doi.org/10.1123/ijsb.3.3.222

Hunter, J. P., Marshall, R. N., & McNair, P. J. (2004). Interaction of step length and step rate during sprint running. *Medicine and Science in Sports and Exercise*, *36*(2), 261–271. https://doi.org/10.1249/01.MSS.0000113664.15777.53

Hunter, J. P., Marshall, R. N., & McNair, P. J. (2005). Relationships between Ground Reaction Force Impulse and Kinematics of Sprint-Running Acceleration. *Journal of Applied Biomechanics*, *21*(1), 31–43. https://doi.org/10.1123/jab.21.1.31

Kandel, E. R., Schwartz, J., & Jessell, T. (2012). *Principles of Neural Science, 5th Edition*.

Kelso, J. A. S. (1997). *Dynamic Patterns: The Self-organization of Brain and Behavior*. MIT Press.

Kuitunen, S., Komi, P. V., & Kyröläinen, H. (2002). Knee and ankle joint stiffness in sprint running. *Medicine and Science in Sports and Exercise*, *34*(1), 166–173. https://doi.org/10.1097/00005768-200201000-00025

Kulmala, J.-P., Korhonen, M. T., Kuitunen, S., Suominen, H., Heinonen, A., Mikkola, A., & Avela, J. (2017). Whole body frontal plane mechanics across walking, running, and sprinting in young and older adults. *Scandinavian Journal of Medicine & Science in Sports*, *27*(9), 956–963. https://doi.org/10.1111/sms.12709

Kyröläinen, H., Avela, J., & Komi, P. V. (2005). Changes in muscle activity with increasing running speed. *Journal of Sports Sciences*, *23*(10), 1101–1109. https://doi.org/10.1080/02640410400021575

Lipsitz, L. A. (2002). Dynamics of StabilityThe Physiologic Basis of Functional Health and Frailty. *The Journals of Gerontology: Series A*, *57*(3), B115–B125. https://doi.org/10.1093/gerona/57.3.B115

MacWilliams, B. A., Rozumalski, A., Swanson, A. N., Wervey, R. A., Dykes, D. C., Novacheck, T. F., & Schwartz, M. H. (2013). Assessment of Three-Dimensional Lumbar Spine Vertebral Motion During Gait with Use of Indwelling Bone Pins: *The Journal of Bone & Joint Surgery*, *95*(23), e184. https://doi.org/10.2106/JBJS.L.01469

Mann, R., Moran, G., & Dougherty, S. (1986). Comparative electromyography of the lower extremity in jogging, running, and sprinting. *The American Journal of Sports Medicine*, *14*(6), 501–510. https://doi.org/10.1177/036354658601400614

Mattes, K., Wolff, S., & Alizadeh, S. (2021). Kinematic Stride Characteristics of Maximal Sprint Running of Elite Sprinters – Verification of the "Swing-Pull Technique." *Journal of Human Kinetics*, *77*. https://doi.org/10.2478/hukin-2021-0008

Mero, A., & Komi, P. V. (1987). Electromyographic activity in sprinting at speeds ranging from sub-maximal to supra-maximal. *Medicine and Science in Sports and Exercise*, *19*(3), 266–274.

Morin, J.-B., Bourdin, M., Edouard, P., Peyrot, N., Samozino, P., & Lacour, J.-R. (2012). Mechanical determinants of 100-m sprint running performance. *European Journal of Applied Physiology*, *112*(11), 3921–3930. https://doi.org/10.1007/s00421-012-2379-8

Nagahara, R., Matsubayashi, T., Matsuo, A., & Zushi, K. (2014). Kinematics of transition during human accelerated sprinting. *Biology Open*, *3*(8), 689–699. https://doi.org/10.1242/bio.20148284

Nagahara, R., Matsubayashi, T., Matsuo, A., & Zushi, K. (2018). Kinematics of the thorax and pelvis during accelerated sprinting. *The Journal of Sports Medicine and Physical Fitness*, *58*(9), 1253–1263. https://doi.org/10.23736/S0022-4707.17.07137-7

Nagahara, R., Mizutani, M., Matsuo, A., Kanehisa, H., & Fukunaga, T. (2017). Association of Step Width with Accelerated Sprinting Performance and Ground Reaction Force. *International Journal of Sports Medicine*, *38 7*, 534–540. https://doi.org/10.1055/s-0043-106191

Newell, K. M., & Vaillancourt, D. E. (2001). Dimensional change in motor learning. *Human Movement Science*, *20*(4–5), 695–715. https://doi.org/10.1016/s0167-9457(01)00073-2

Novacheck, T. F. (1998). The biomechanics of running. *Gait & Posture*, *7*(1), 77–95. https://doi.org/10.1016/S0966-6362(97)00038-6

Ohtaki, Y., Sagawa, K., & Inooka, H. (2001). A Method for Gait Analysis in a Daily Living Environment by Body-Mounted Instruments. *JSME International Journal Series C Mechanical Systems, Machine Elements and Manufacturing*, *44*(4), 1125–1132. https://doi.org/10.1299/jsmec.44.1125

Pataky, T. C., Robinson, M. A., & Vanrenterghem, J. (2013). Vector field statistical analysis of kinematic and force trajectories. *Journal of Biomechanics*, *46*(14), 2394–2401. https://doi.org/10.1016/j.jbiomech.2013.07.031

Pinniger, G. J., Steele, J. R., & Groeller, H. (2000). Does fatigue induced by repeated dynamic efforts affect hamstring muscle function? *Medicine and Science in Sports and Exercise*, *32*(3), 647–653. https://doi.org/10.1097/00005768-200003000-00015

Pinto, B. L., & McGill, S. M. (2020). *Voluntary Muscle Relaxation Can Mitigate Fatigue and Improve Countermovement Jump Performance*. 5.

Preece, S. J., Mason, D., & Bramah, C. (2016a). The coordinated movement of the spine and pelvis during running. *Human Movement Science*, *45*, 110–118. https://doi.org/10.1016/j.humov.2015.11.014

Preece, S. J., Mason, D., & Bramah, C. (2016b). The coordinated movement of the spine and pelvis during running. *Human Movement Science*, *45*, 110–118. https://doi.org/10.1016/j.humov.2015.11.014

Riley, M. A., & Turvey, M. T. (2002). Variability and Determinism in Motor Behavior. *Journal of Motor Behavior*, *34*(2), 99–125. https://doi.org/10.1080/00222890209601934

Ross, G. B., Dowling, B., Troje, N. F., Fischer, S. L., & Graham, R. B. (2018a). Objectively Differentiating Movement Patterns between Elite and Novice Athletes. *Medicine & Science in Sports & Exercise*, *50*(7), 1457–1464. https://doi.org/10.1249/MSS.0000000000001571

Ross, G. B., Dowling, B., Troje, N. F., Fischer, S. L., & Graham, R. B. (2018b). Objectively Differentiating Movement Patterns between Elite and Novice Athletes. [Miscellaneous Article]. *Medicine & Science in Sports & Exercise*, *50*(7), 1457–1464. https://doi.org/10.1249/MSS.0000000000001571

Salo, A. I. T., Bezodis, I. N., Batterham, A. M., & Kerwin, D. G. (2011). Elite Sprinting: Are Athletes Individually Step-Frequency or Step-Length Reliant? [Miscellaneous Article]. *Medicine & Science in Sports & Exercise*, *43*(6), 1055–1062. https://doi.org/10.1249/MSS.0b013e318201f6f8

Schache, A. G., Bennell, K. L., Blanch, P. D., & Wrigley, T. V. (1999). The coordinated movement of the lumbo–pelvic–hip complex during running: A literature review. *Gait & Posture*, *10*(1), 30–47. https://doi.org/10.1016/S0966-6362(99)00025-9

Schache, A. G., Blanch, P., Rath, D., Wrigley, T., & Bennell, K. (2002). Three-dimensional angular kinematics of the lumbar spine and pelvis during running. *Human Movement Science*, *21*(2), 273–293. https://doi.org/10.1016/S0167-9457(02)00080-5

Schepers, M., Giuberti, M., & Bellusci, G. (2018). *Xsens MVN: Consistent Tracking of Human Motion Using Inertial Sensing*. https://doi.org/10.13140/RG.2.2.22099.07205

Schmidt, M., Rheinländer, C., Nolte, K. F., Wille, S., Wehn, N., & Jaitner, T. (2016). IMU- based Determination of Stance Duration During Sprinting. *Procedia Engineering*, *147*, 747–752. https://doi.org/10.1016/j.proeng.2016.06.330

Seay, J. F., Van Emmerik, R. E. A., & Hamill, J. (2011). Low back pain status affects pelvis-trunk coordination and variability during walking and running. *Clinical Biomechanics*, *26*(6), 572–578. https://doi.org/10.1016/j.clinbiomech.2010.11.012

Seel, T., Raisch, J., & Schauer, T. (2014). IMU-Based Joint Angle Measurement for Gait Analysis. *Sensors*, *14*(4), 6891–6909. https://doi.org/10.3390/s140406891

Shin, J.-H., Wang, S., Yao, Q., Wood, K. B., & Li, G. (2013). Investigation of coupled bending of the lumbar spine during dynamic axial rotation of the body. *European Spine Journal: Official Publication of the European Spine Society, the European Spinal Deformity Society, and the European Section of the Cervical Spine Research Society*, *22*(12), 2671–2677. https://doi.org/10.1007/s00586-013-2777-6

Sides, D. L. (2015). *Kinematics and kinetics of maximal velocity sprinting and specificity of training in elite athletes* [Phd, University of Salford]. http://usir.salford.ac.uk/id/eprint/34332/

Slawinski, J., Millot, B., Houel, N., & Dinu, D. (2020). Use of an Inertial Measurement System to Calculate Maximal Power during Running Sprint Acceleration: Comparison with the Radar System. *Proceedings*, *49*(1), 23. https://doi.org/10.3390/proceedings2020049023

Sung, P. S., Park, W.-H., & Kim, Y. H. (2012). Three-dimensional kinematic lumbar spine motion analyses of trunk motion during axial rotation activities. *Journal of Spinal Disorders & Techniques*, *25*(3), E74-80. https://doi.org/10.1097/BSD.0b013e3182404b87

Thelen, D. G., Chumanov, E. S., Hoerth, D. M., Best, T. M., Swanson, S. C., Li, L., Young, M., & Heiderscheit, B. C. (2005). Hamstring muscle kinematics during treadmill sprinting. *Medicine and Science in Sports and Exercise*, *37*(1), 108–114. https://doi.org/10.1249/01.mss.0000150078.79120.c8

Troje, N. F. (2002). Decomposing biological motion: A framework for analysis and synthesis of human gait patterns. *Journal of Vision*, *2*(5), 2–2. https://doi.org/10.1167/2.5.2

Vagenas, G., & Hoshizaki, B. (1991). Functional Asymmetries and Lateral Dominance in the Lower Limbs of Distance Runners. *Journal of Applied Biomechanics*, *7*(4), 311–329. https://doi.org/10.1123/ijsb.7.4.311

Verkhoshansky, Y. V., & Siff, M. C. (2009). *Supertraining* (M. Yessis, Trans.).

Vleeming, A., Pool-Goudzwaard, A. L., Stoeckart, R., van Wingerden, J. P., & Snijders, C. J. (1995). The posterior layer of the thoracolumbar fascia. Its function in load transfer from spine to legs. *Spine*, *20*(7), 753–758.

Wdowski, M. M., & Gittoes, M. J. R. (2013). Kinematic adaptations in sprint acceleration performances without and with the constraint of holding a field hockey stick. *Sports Biomechanics*, *12*(2), 143–153. https://doi.org/10.1080/14763141.2012.749507

Weyand, P. G., & Davis, J. A. (2005). Running performance has a structural basis. *Journal of Experimental Biology*, *208*(14), 2625–2631. https://doi.org/10.1242/jeb.01609

Weyand, P. G., Sternlight, D. B., Bellizzi, M. J., & Wright, S. (2000). Faster top running speeds are achieved with greater ground forces not more rapid leg movements. *Journal of Applied Physiology (Bethesda, Md.: 1985)*, *89*(5), 1991–1999. https://doi.org/10.1152/jappl.2000.89.5.1991

Weygers, I., Kok, M., Konings, M., Hallez, H., De Vroey, H., & Claeys, K. (2020). Inertial Sensor-Based Lower Limb Joint Kinematics: A Methodological Systematic Review. *Sensors (Basel, Switzerland)*, *20*(3). https://doi.org/10.3390/s20030673

Winter, D. A. (2009). *Biomechanics and Motor Control of Human Movement*. John Wiley & Sons.

Yada, K., Ae, M., Tanigawa, S., Ito, A., Fukuda, K., & Kijima, K. (2011). STANDARD MOTION OF SPRINT RUNNING FOR MALE ELITE AND STUDENT SPRINTERS. *ISBS - Conference Proceedings Archive*. https://ojs.ub.uni-konstanz.de/cpa/article/view/4902

Yu, B., Queen, R. M., Abbey, A. N., Liu, Y., Moorman, C. T., & Garrett, W. E. (2008). Hamstring muscle kinematics and activation during overground sprinting. *Journal of Biomechanics*, *41*(15), 3121–3126. https://doi.org/10.1016/j.jbiomech.2008.09.005

APPENDIX A: ORIGIN AND INSERTION OF STUDY RELATED MUSCULATURE

Muscle	Origin	Insertion	
Erector Spinae	Arises by a broad tendon from posterior part of iliac crest, posterior surface of sacrum, sacroiliac ligaments, sacral and inferior lumbar spinous processes and supraspinous ligament	Iliocostalis	Lumborum, thoracis, cervices; fibres run superiorly to angles of lower ribs and cervical transverse processes
		Longissimus	Thoracis, cervicis, capitis; fibers run superiorly to ribs between tubercles and angles to transverse processes in thoracic and cervical regions and to mastoid process of temporal bone
		Spinalis	Thoracis, cervicis, capitis; fibers run superiorly to spinous processes in the upper thoracic region and to cranium
External Obliques	External surfaces of 5^{th}-12^{th} ribs	Linea alba, pubic tubercle and anterior half of iliac crest	
Latissimus Dorsi	Spinous processes of inferior 6 thoracic vertebrae; thoracolumbar fascia, iliac crest and inferior 3 or 4 ribs	Floor of intertubercular sulcus of humerus	
Gluteus Maximus	Ilium posterior to posterior gluteal line; dorsal surface of sacrum and coccyx; sacrotuberous ligaments	Most fibers end in iliotibial tract, which inserts inro lateral condyle of tibia; some fibers insert on gluteal tuberosity	
Gluteus Medius	External surface of ilium between anterior and posterior gluteal lines	Lateral surface of greater trochanter of femur	
Bicep Femoris	Long head: ischial tuberosity Short head: linea aspera and lateral supracondylar line of femur	Lateral side of head of fibula; tendon is split at the site by fibular collateral ligament of knee	

*Retrieved from *Moore et al 2022*

APPENDIX B: GENERAL HEALTH QUESTIONNAIRE

SPINE BIOMECHANICS
& NEUROMUSCULAR CONTROL LABORATORY

Generic Health History Form

Age: Sex: Height:

1. Have you experienced pain in any region of your body such as the ankle, upper thigh or lower back that has caused you to miss school, work or any regular activity?

   □Yes (If Yes, please describe) □No
   Date:

2. Have you experienced an injury to the ankle, upper thigh or lower back within the last three months that you have sought medical treatment (physician, chiropractor, physiotherapist)?

   □Yes (If Yes, please describe) □No
   Date:

3. Have you ever experienced skin sensitivity or an allergic reaction to adhesives such as medical tape or medical electrodes?

   □Yes (If Yes, please describe) □No

4. Have you ever sought medical treatment relating to a skin condition in the region of the lower back or upper thigh?

   □Yes (If Yes, please describe) □No
   Date:

5. Do you regularly engage in any type of physical activity?

   □Yes (If Yes, please describe) □No

6. Have you ever been classified as having a musculoskeletal (e.g. Parkinson's Disease or Cerebral Palsy) or Neurological (e.g. Diabetic Neuropathy or concussion) disorder which may affect your balance?

   □Yes (If Yes, please describe) □No

   Date:

7. Have you ever been classified as having an auditory (e.g., inner ear disorder, vertigo, upper respiratory infection, etc.) disorder which may affect your balance?

   □ Yes (If Yes, please describe) □No

   Date:

8. What is currently your main sport?

9. How long have you completed at your current main sport?

10. Current Performance Level
    a) Olympic/World Championship
    b) National
    c) International
    d) Provincial
    e) Club
    f) Other: _____

11. Are you currently employed or studying?
    a) Employed and studying
    b) Employed
    c) Studying
    d) Other: _____

12. How many months a year do you train?

13. How many hours a week do you currently train?

14. On a scale of 1-10 how intense is your average training session? (i.e. 1= very easy, 10 extremely challenging)

    □ 1 □ 2 □ 3 □4 □ 5 □ 6 □ 7 □ 8 □ 9 □ 10

15. How often do you compete in a year?
    a) Once a week b) Once a month c) Once every several months d) Once a year
    e) Other

APPENDIX C: Brock University REB Application

Brock University
Office of Research Ethics
Tel: 905-688-5550 ext. 3035
Email: reb@brocku.ca

Health Science Research Ethics Board

Certificate of Ethics Clearance for Human Participant Research

DATE: 8/9/2021

PRINCIPAL INVESTIGATOR: BEAUDETTE, Shawn - Kinesiology

FILE: 20-364 - BEAUDETTE

TYPE: Masters Thesis/Project STUDENT: Chris Vellucci
SUPERVISOR: Shawn Beaudette

TITLE: A data driven approach to identifying key biomechanical features that differentiate novice and advanced sprinters

ETHICS CLEARANCE GRANTED

Type of Clearance: NEW Expiry Date: 8/1/2022

The Brock University Health Science Research Ethics Board has reviewed the above named research proposal and considers the procedures, as described by the applicant, to conform to the University's ethical standards and the Tri-Council Policy Statement. Clearance granted from **8/9/2021** to **8/1/2022**.

The Tri-Council Policy Statement requires that ongoing research be monitored by, at a minimum, an annual report. Should your project extend beyond the expiry date, you are required to submit a Renewal form before 8/1/2022. Continued clearance is contingent on timely submission of reports.

To comply with the Tri-Council Policy Statement, you must also submit a final report upon completion of your project. All report forms can be found on the Office of Research Ethics web page at https://brocku.ca/research-at-brock/office-of-research-services/research-ethics-office/#application-forms

In addition, throughout your research, you must report promptly to the REB:

a) Changes increasing the risk to the participant(s) and/or affecting significantly the conduct of the study;
b) All adverse and/or unanticipated experiences or events that may have real or potential unfavourable implications for participants;
c) New information that may adversely affect the safety of the participants or the conduct of the study;
d) Any changes in your source of funding or new funding to a previously unfunded project.

We wish you success with your research.

Approved:

Craig Tokuno, Chair
Health Science Research Ethics Board

Note: Brock University is accountable for the research carried out in its own jurisdiction or under its auspices and may refuse certain research even though the REB has found it ethically acceptable.

If research participants are in the care of a health facility, at a school, or other institution or community organization, it is the responsibility of the Principal Investigator to ensure that the ethical guidelines and clearance of those facilities or institutions are obtained and filed with the REB prior to the initiation of research at that site.

APPENDIX D: CORRELATION PLOTS BETWEEN MAXIMAL VELOCITY AND PCs

Appendix D.1- Correlation between Maximal Velocity and Kinematic PCs

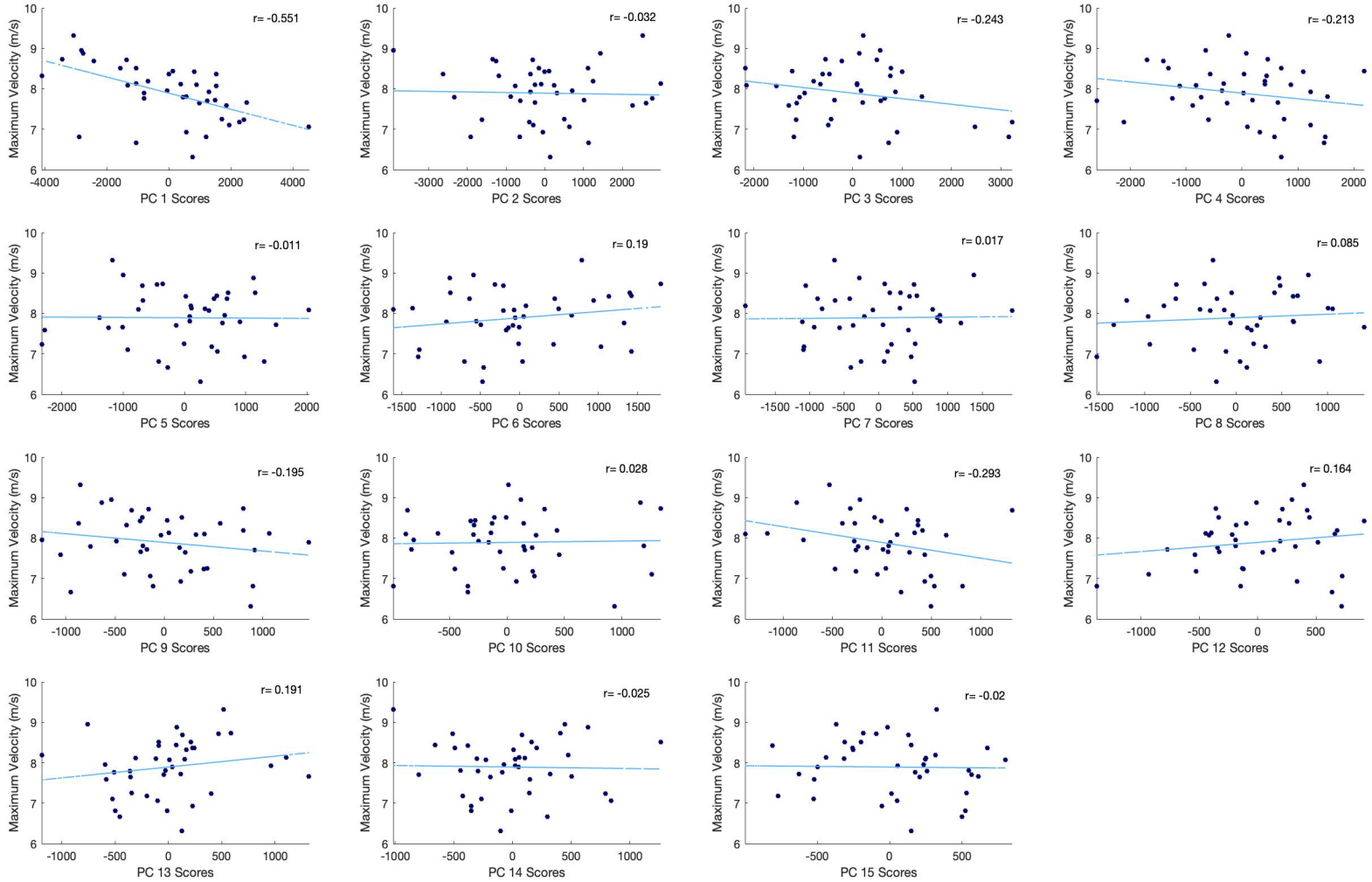

Appendix D.2- Correlation between Maximal Velocity and EMG PC

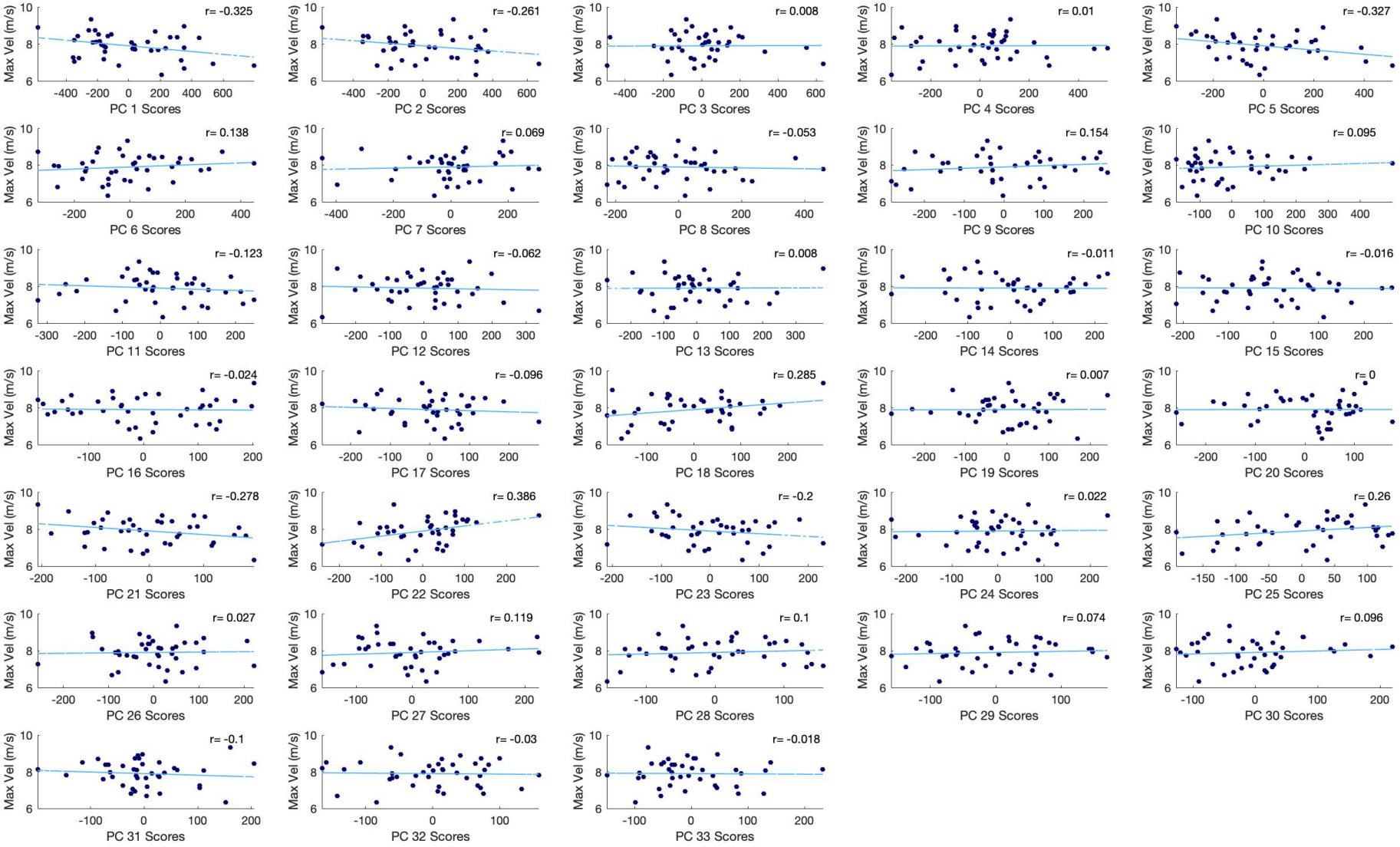

APPENDIX F: SINGLE COMPONENT RECONSTRUCTION OF KINEMATIC PCS

Appendix F.1- Single Component Reconstruction PC 1

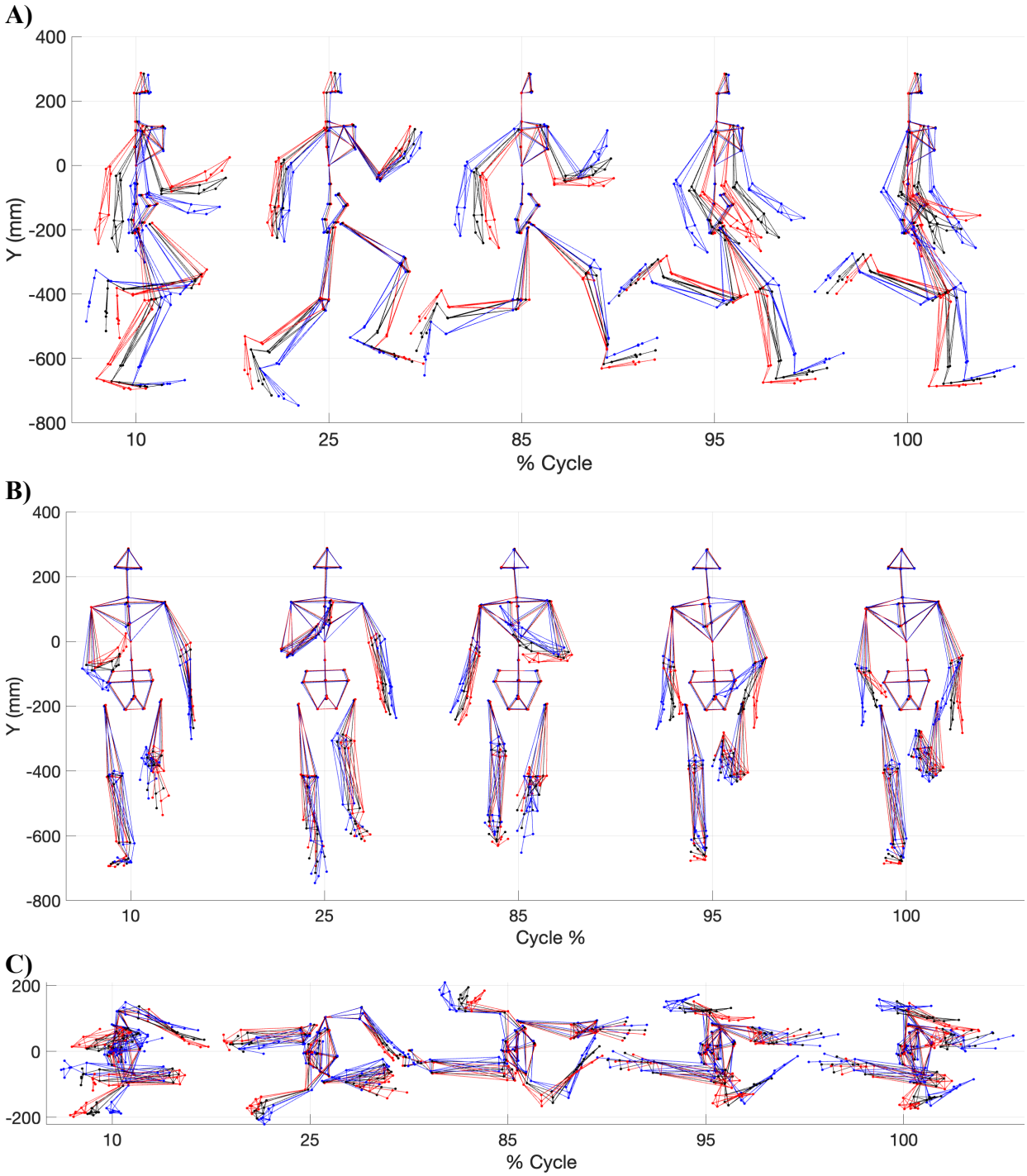

SCR for PC 1 **A**) Sagittal plane view **B)** Frontal plane view **C**) Transverse plane view. The blue avatar represents the 5th percentile (slow), black represents the mean and red represents the 95th percentile (fast)

Appendix F.2- Single Component Reconstruction PC 3

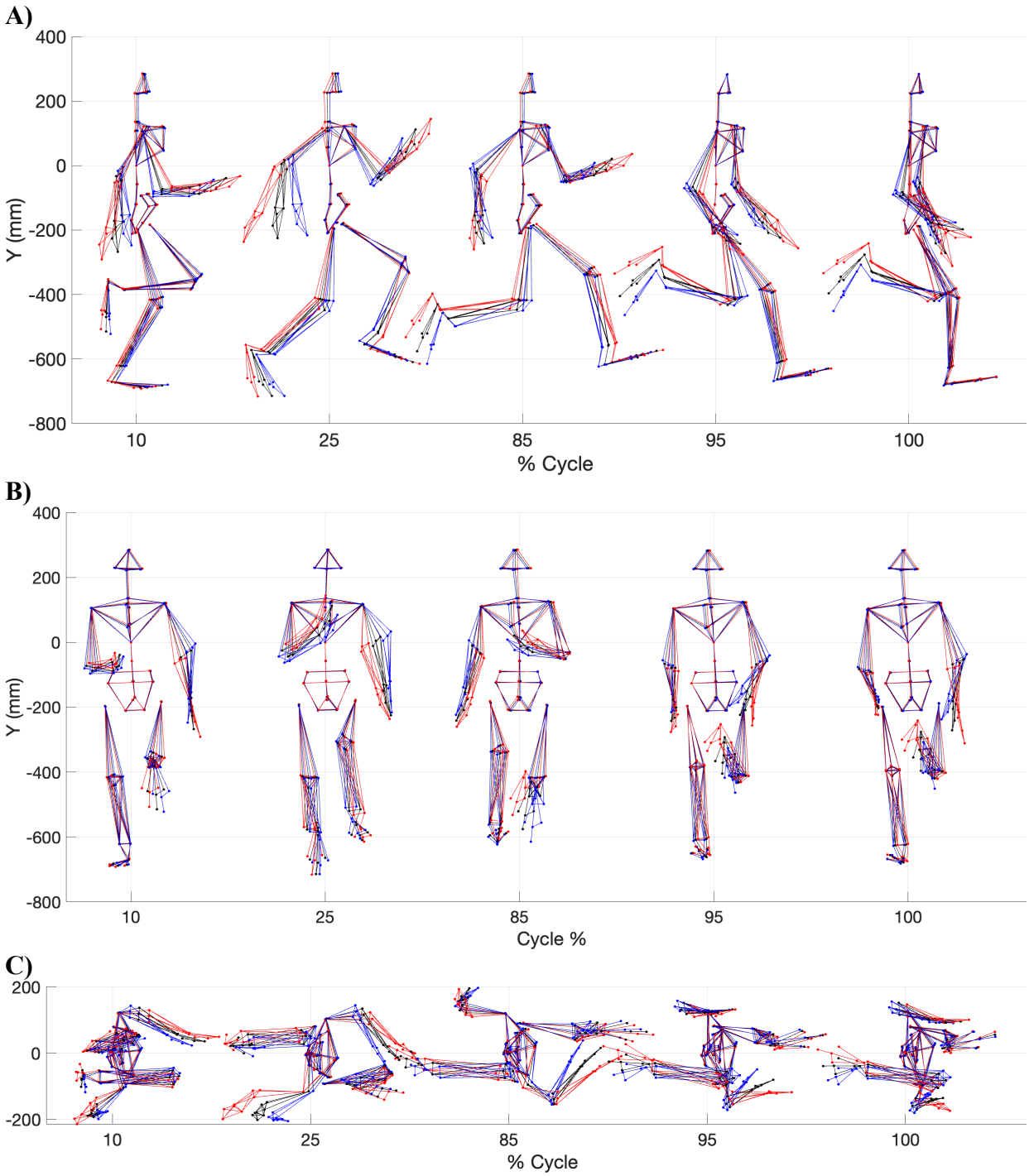

SCR for PC 3 **A**) Sagittal plane view **B)** Frontal plane view **C**) Transverse plane view. The blue avatar represents the 5th percentile (slow), black represents the mean and red represents the 95th percentile (fast)

Appendix F.3- Single Component Reconstruction PC 9

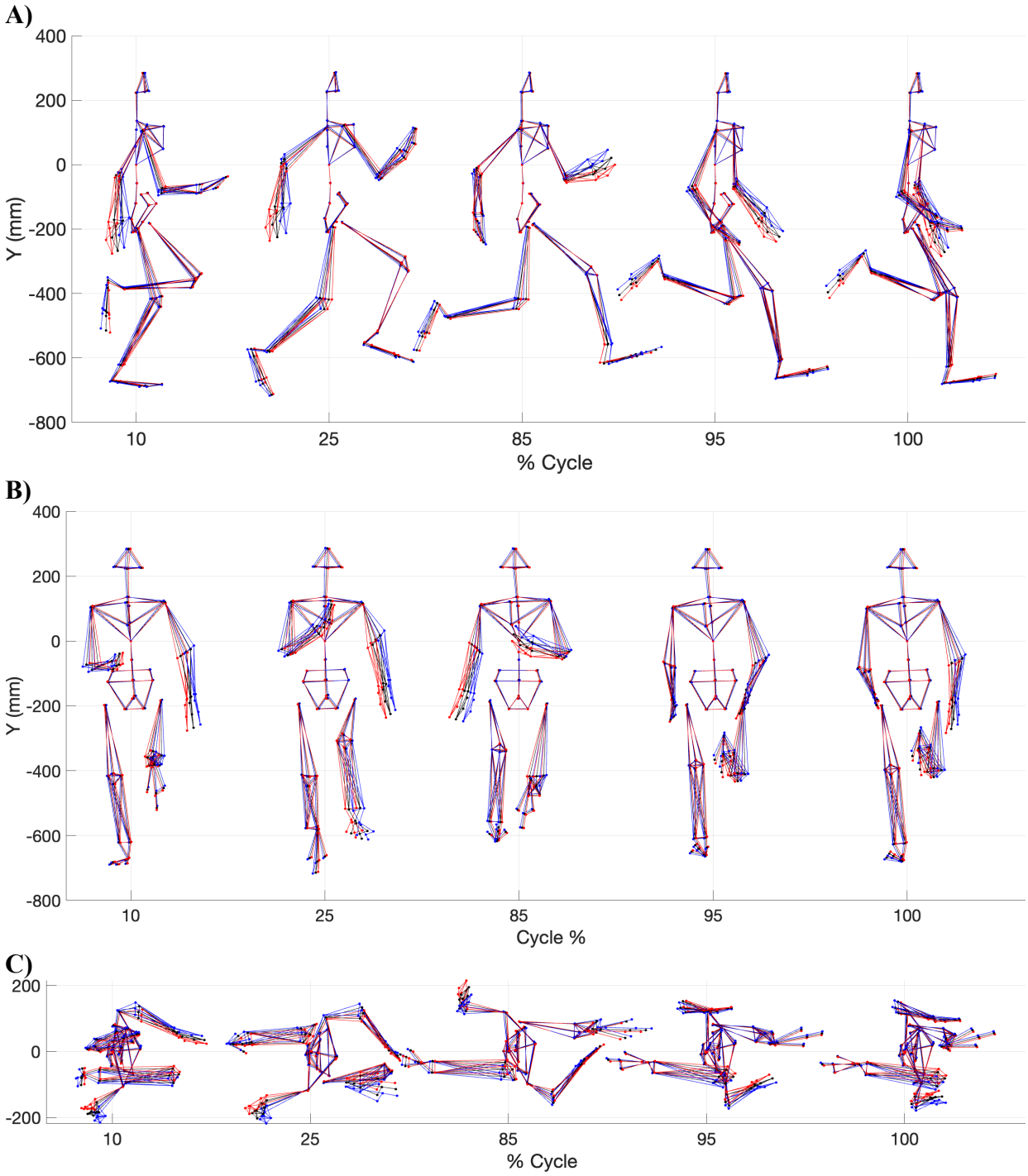

SCR for PC 9 **A**) Sagittal plane view **B)** Frontal plane view **C**) Transverse plane view. The blue avatar represents the 5th percentile (slow), black represents the mean and red represents the 95th percentile (fast)

Appendix F.4- Single Component Reconstruction PC 11

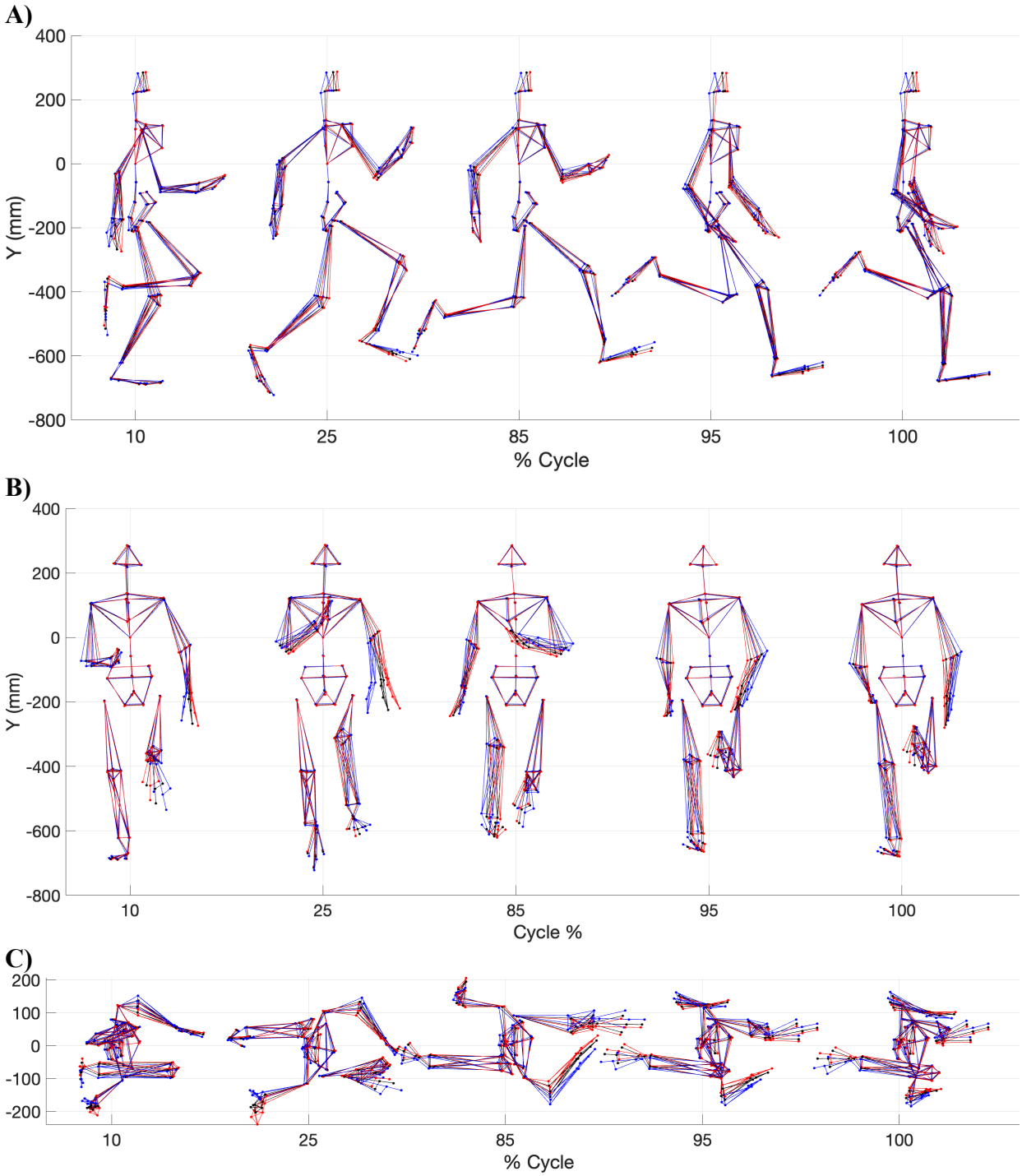

SCR for PC 11 **A**) Sagittal plane view **B)** Frontal plane view **C**) Transverse plane view. The blue avatar represents the 5th percentile (slow), black represents the mean and red represents the 95th percentile (fast)

Appendix F.5- Single Component Reconstruction PC 12

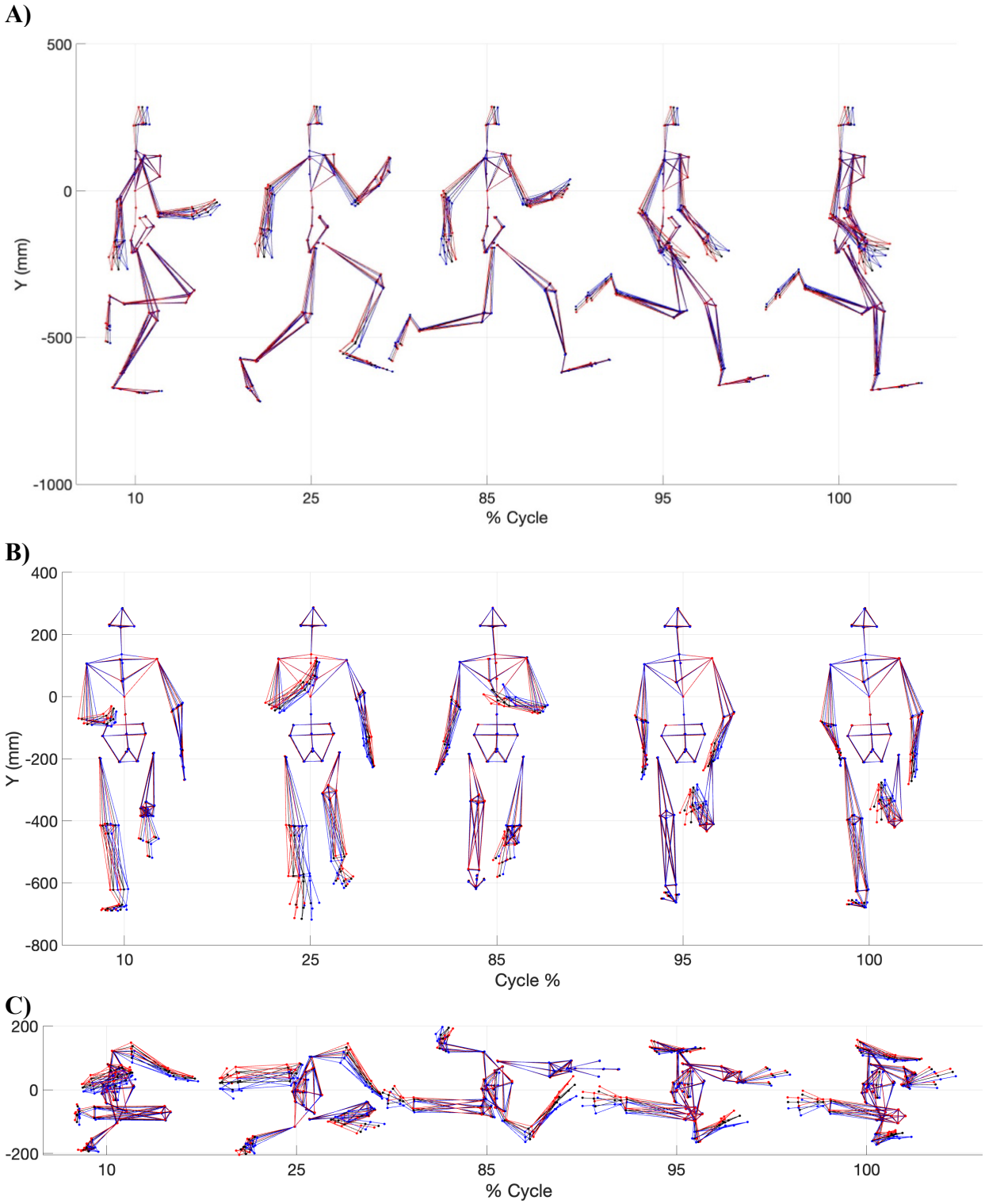

SCR for PC 12 **A**) Sagittal plane view **B)** Frontal plane view **C**) Transverse plane view. The blue avatar represents the 5th percentile (slow), black represents the mean and red represents the 95th percentile (fast)

Appendix F.6- Single Component Reconstruction PC 13

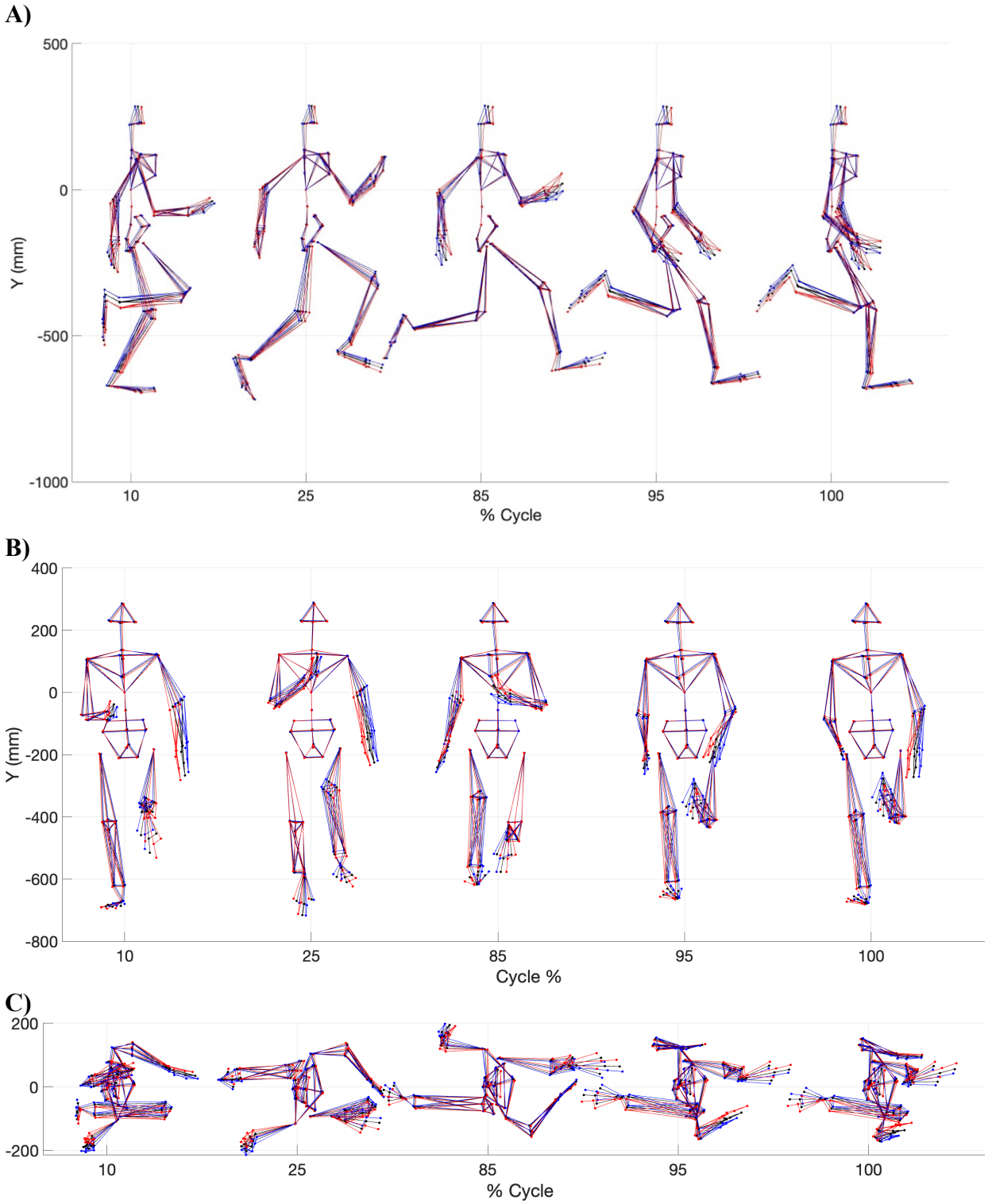

SCR for PC 13 **A**) Sagittal plane view **B)** Frontal plane view **C**) Transverse plane view. The blue avatar represents the 5th percentile (slow), black represents the mean and red represents the 95th percentile (fast)

APPENDIX G: SINGLE COMPONENT RECONSTRUCTION OF EMG

Appendix G.1- PC 1 SCR

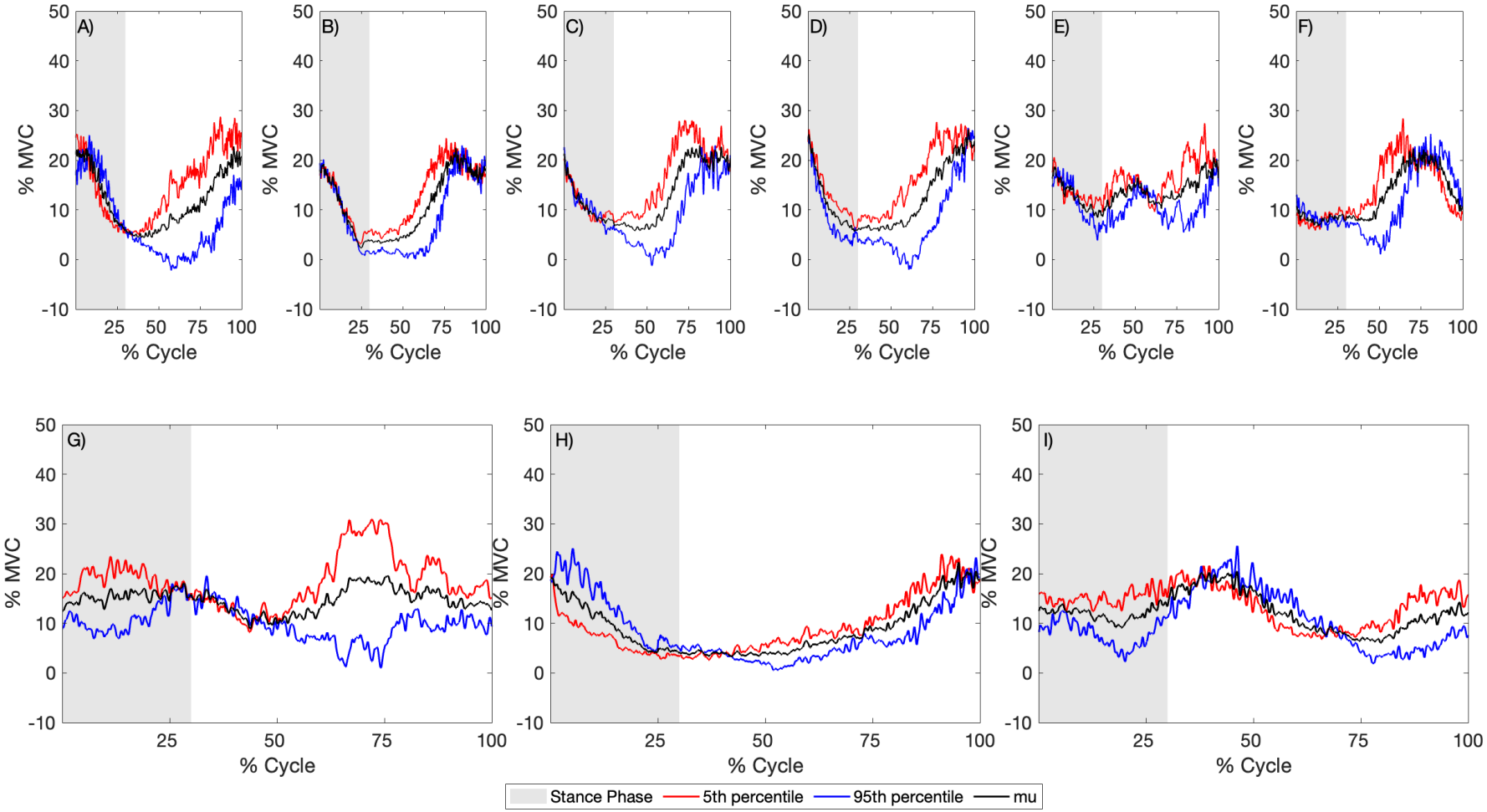

SCR for PC 1 the blue line represents a muscle activation pattern associated with faster sprint velocities, a red line is associated with slower sprint velocities, and black represents the mean

Appendix G.2- PC 5 SCR

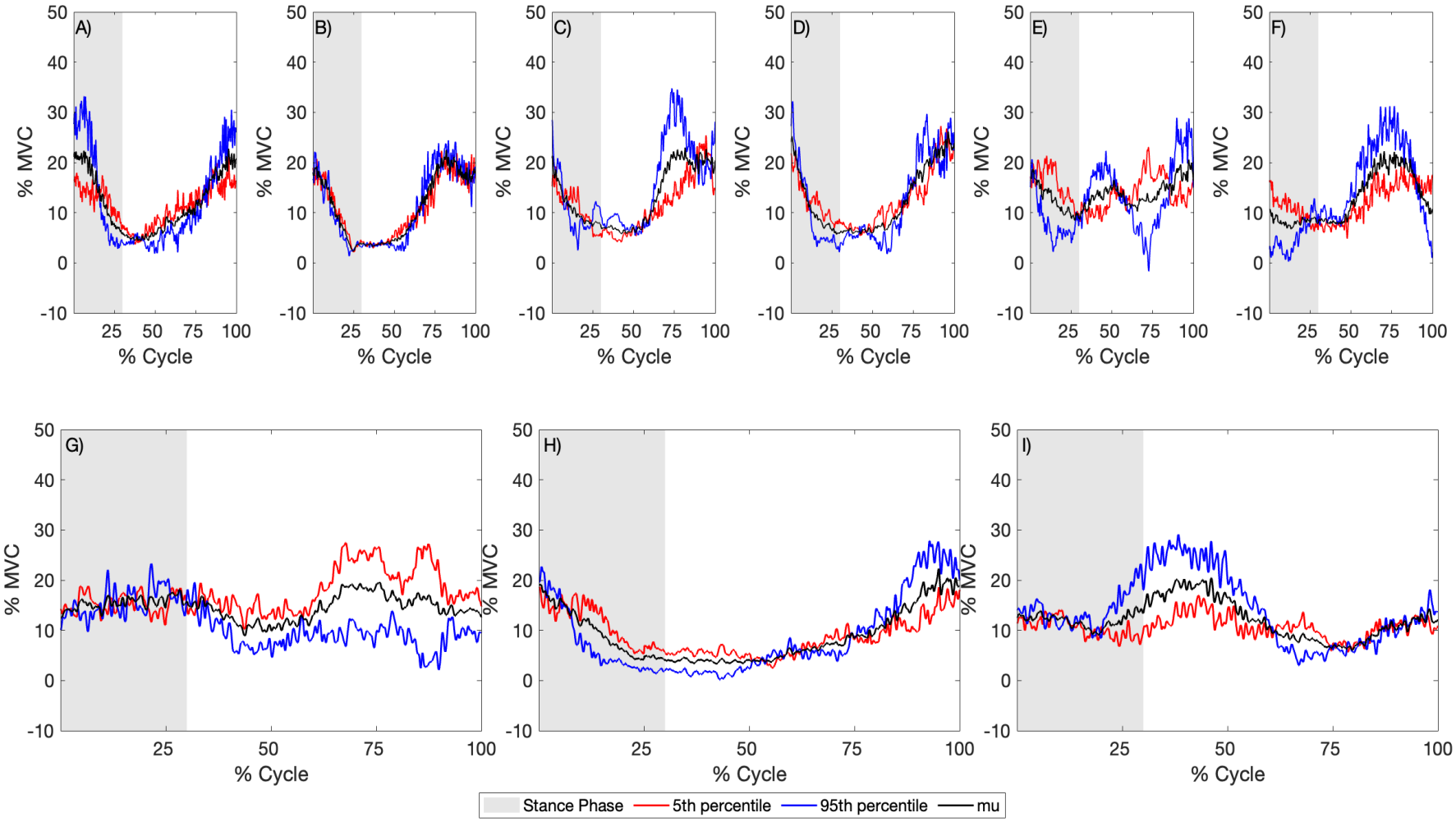

SCR for PC 5 the blue line represents a muscle activation pattern associated with faster sprint velocities, a red line is associated with slower sprint velocities, and black represents the mean

Appendix G.3- PC 21 SCR

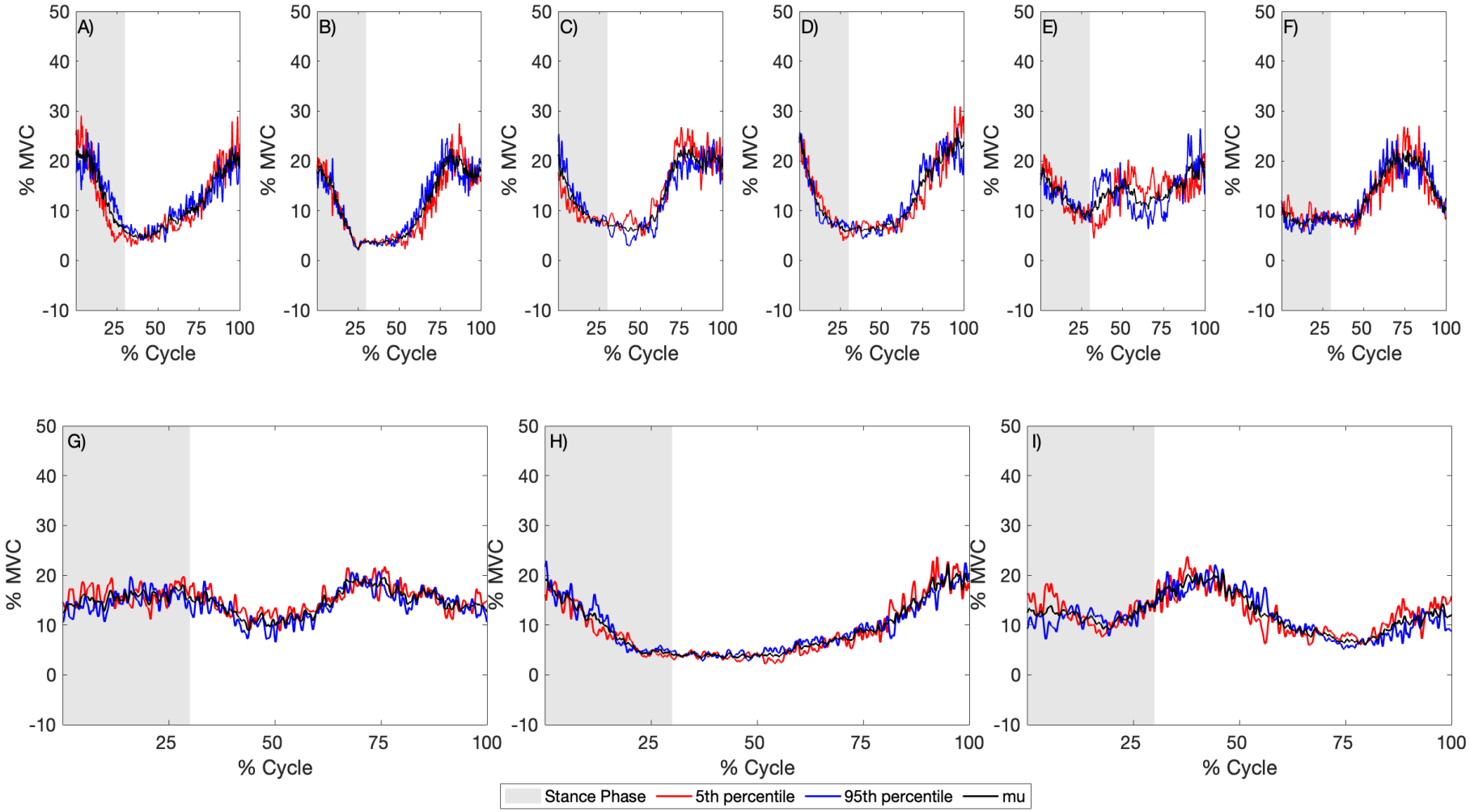

SCR for PC 21 the blue line represents a muscle activation pattern associated with faster sprint velocities, a red line is associated with slower sprint velocities, and black represents the mean

Appendix G.4- PC 22 SCR

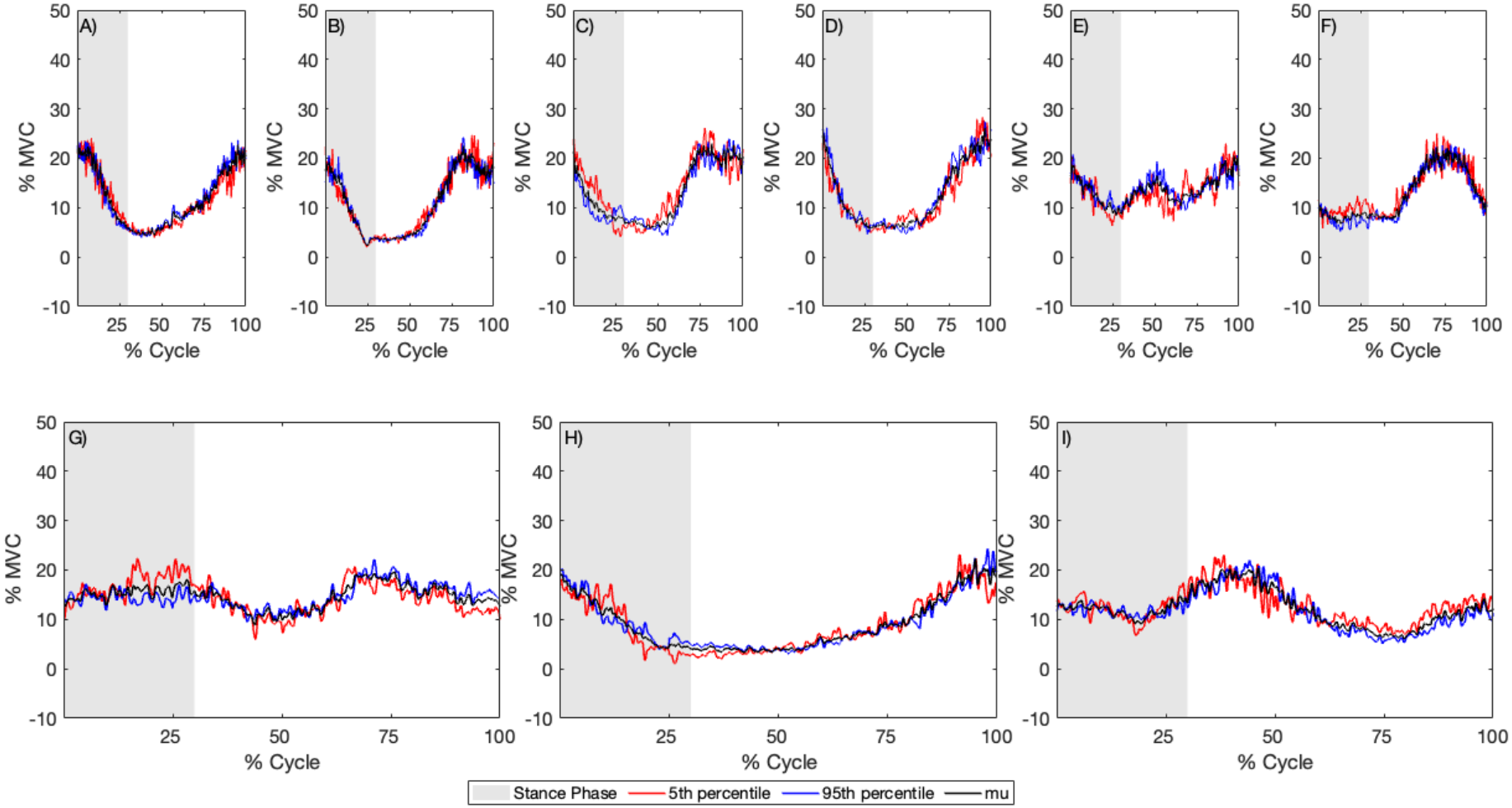

SCR for PC 22 the blue line represents a muscle activation pattern associated with faster sprint velocities, a red line is associated with slower sprint velocities, and black represents the mean

APPENDIX H: RESULTS FROM RESIDUAL ANALYSIS

Appendix H.1 – Summary of Residual Analysis Results

Participant	Trial	VLO (Hz)	LUM (Hz)	OBL (Hz)	MED (Hz)	BIC (Hz)	MAX (Hz)	REC (Hz)	LAT (Hz)	GAS (Hz)	MCUTOFF (Hz)
P001	1	196	184	255	213	403	180	241	297	285	**251**
P004	3	203	178	265	222	354	169	188	190	313	**231**
P005	1	201	282	220	282	364	203	271	434	282	**282**
P006	1	286	229	292	203	296	197	214	243	349	**257**
P019	2	273	192	301	254	235	235	271	248	341	**261**
P015	3	294	303	201	305	375	201	201	265	269	**268**

Appendix H.2 – Example of Residual Analysis- P014, LES

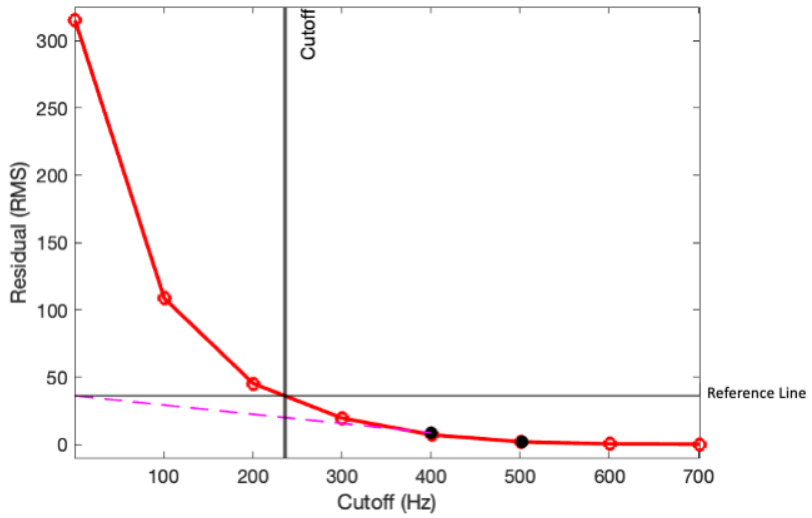

APPENDIX I: XSENS Marker Set

Appendix I.1- Locations of each marker on the anthropometric model

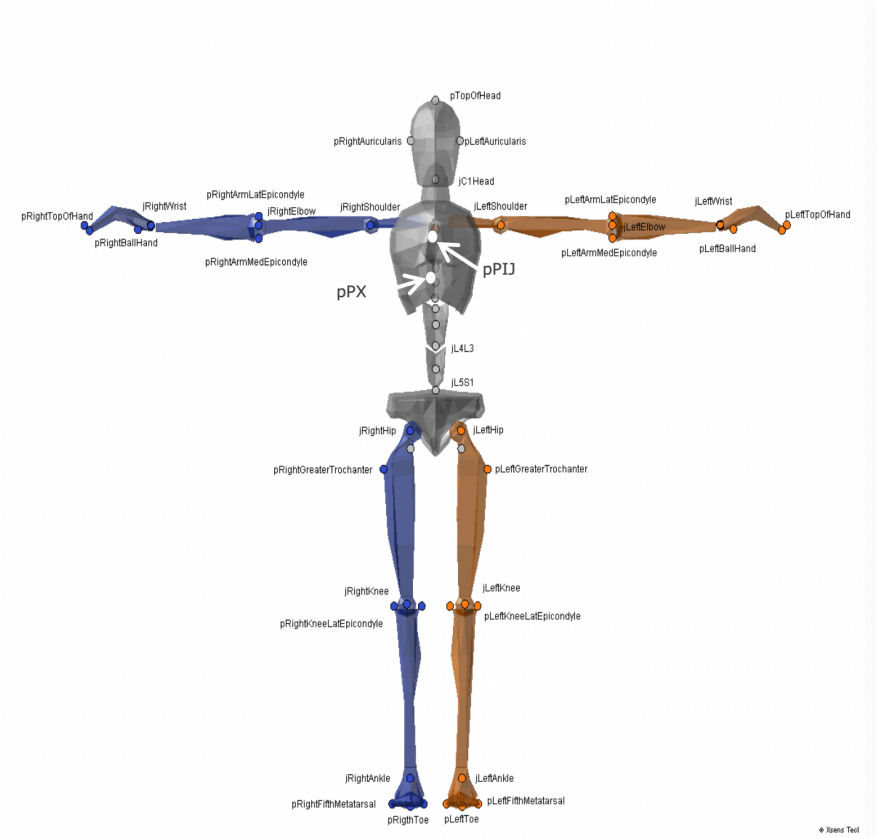

15.2.1Points exported in C3D Exporter

For an illustration of the location of the points, see Figure 93.

#	points	#	points
1	pHipOrigin	33	pRightTopOfHand
2	pRightASI	34	pRightPinky
3	pLeftASI	35	pRightBallHand
4	pRightCSI	36	pLeftTopOfHand
5	pLeftCSI	37	pLeftPinky
6	pRightIschialTub	38	pLeftBallHand
7	pLeftIschialTub	39	pRightGreaterTrochanter
8	pSacrum	40	pRightKneeLatEpicondyle
9	pL5SpinalProcess	41	pRightKneeMedEpicondyle
10	pL3SpinalProcess	42	pRightMiddleKneeCap (or pRightPatella)
11	pT12SpinalProcess	43	pLeftGreaterTrochanter
12	pPX	44	pLeftKneeLatEpicondyle
13	pIJ	45	pLeftKneeMedEpicondyle
14	pT4SpinalProcess	46	pLeftMiddleKneeCap (or pLeftPatella)
15	pT8SpinalProcess	47	pRightLatMalleolus
16	pC7SpinalProcess	48	pRightMedMalleolus
17	pTopOfHead	49	pRightTibialTub
18	pRightAuricularis	50	pLeftLatMalleolus
19	pLeftAuricularis	51	pLeftMedMalleolus
20	pBackOfHead	52	pLeftTibialTub
21	pRightAcromion	53	pRightHeelFoot
22	pLeftAcromion	54	pRightFirstMetatarsal
23	pRightArmLatEpicondyle	55	pRightFifthMetatarsal
24	pRightArmMedEpicondyle	56	pRightPivotFoot
25	pLeftArmLatEpicondyle	57	pRightHeelCenter
26	pLeftArmMedEpicondyle	58	pRightToe
27	pRightUlnarStyloid	59	pLeftHeelFoot
28	pRightRadialStyloid	60	pLeftFirstMetatarsal
29	pRightOlecranon	61	pLeftFifthMetatarsal
30	pLeftUlnarStyloid	62	pLeftPivotFoot
31	pLeftRadialStyloid	63	pLeftHeelCenter
32	pLeftOlecranon	64	pLeftToe